Fig. 1

2H7scFv-Ig cDNA and predicted amino acid sequence:

HindIII NcoI 2H7 V_L Leader Peptide→

```
                    M  D  F  Q  V  Q  I  F  S  F  L  L  I  S  A  S
1   AAGCTTGCCG CCATGGATTT TCAAGTGCAG ATTTTCAGCT TCCTGCTAAT CAGTGCTTCA

                                        2H7 VL→
    V  I  I  A  R  G  Q  I  V  L  S  Q  S  P  A  I  L  S  A  S
61  GTCATAATTG CCAGAGGACA AATTGTTCTC TCCCAGTCTC CAGCAATCCT GTCTGCATCT

    P  G  E  K  V  T  M  T  C  R  A  S  S  S  V  S  Y  M  H  W
121 CCAGGGGAGA AGGTCACAAT GACTTGCAGG GCCAGCTCAA GTGTAAGTTA CATGCACTGG

                BamHI
                ~~~~~~~
    Y  Q  Q  K  P  G  S  S  P  K  P  W  I  Y  A  P  S  N  L  A
181 TACCAGCAGA AGCCAGGATC CTCCCCCAAA CCCTGGATTT ATGCCCCATC CAACCTGGCT

    S  G  V  P  A  R  F  S  G  S  G  S  G  T  S  Y  S  L  T  I
241 TCTGGAGTCC CTGCTCGCTT CAGTGGCAGT GGGTCTGGGA CCTCTTACTC TCTCACAATC

    S  R  V  E  A  E  D  A  A  T  Y  Y  C  Q  Q  W  S  F  N  P
301 AGCAGAGTGG AGGCTGAAGA TGCTGCCACT TATTACTGCC AGCAGTGGAG TTTTAACCCA

(Gly4Ser)3 Linker
    P  T  F  G  A  G  T  K  L  E  L  K  G  G  G  G  S  G  G  G
361 CCCACGTTCG GTGCTGGGAC CAAGCTGGAG CTGAAAGGTG GCGGTGGCTC GGGCGGTGGT

                                                2H7 VH →
    G  S  G  G  G  G  S  S  Q  A  Y  L  Q  Q  S  G  A  E  L  V
421 GGATCTGGAG GAGGTGGGAG CTCTCAGGCT TATCTACAGC AGTCTGGGGC TGAGCTGGTG

    R  P  G  A  S  V  K  M  S  C  K  A  S  G  Y  T  F  T  S  Y
481 AGGCCTGGGG CCTCAGTGAA GATGTCCTGC AAGGCTTCTG GCTACACATT TACCAGTTAC

    N  M  H  W  V  K  Q  T  P  R  Q  G  L  E  W  I  G  A  I  Y
541 AATATGCACT GGGTAAAGCA GACACCTAGA CAGGGCCTGG AATGGATTGG AGCTATTTAT

    P  G  N  G  D  T  S  Y  N  Q  K  F  K  G  K  A  T  L  T  V
601 CCAGGAAATG GTGATACTTC CTACAATCAG AAGTTCAAGG GCAAGGCCAC ACTGACTGTA

    D  K  S  S  S  T  A  Y  M  Q  L  S  S  L  T  S  E  D  S  A
661 GACAAATCCT CCAGCACAGC CTACATGCAG CTCAGCAGCC TGACATCTGA AGACTCTGCG

    V  Y  F  C  A  R  V  V  Y  Y  S  N  S  Y  W  Y  F  D  V  W
721 GTCTATTTCT GTGCAAGAGT GGTGTACTAT AGTAACTCTT ACTGGTACTT CGATGTCTGG
```

Fig. 1 (continued)

```
                                        BclI
                                        ~~~~~~~human IgG1 Fc domain →
          G  T  G  T  T  V  T  V  S  D  Q  E  P  K  S  C  D  K  T  H
781   GGCACAGGGA CCACGGTCAC CGTCTCTGAT CAGGAGCCCA AATCTTGTGA CAAAACTCAC

          T  C  P  P  C  P  A  P  E  L  L  G  G  P  S  V  F  L  F  P
841   ACATGCCCAC CGTGCCCAGC ACCTGAACTC CTGGGGGGAC CGTCAGTCTT CCTCTTCCCC

          P  K  P  K  D  T  L  M  I  S  R  T  P  E  V  T  C  V  V  V
901   CCAAAACCCA AGGACACCCT CATGATCTCC CGGACCCCTG AGGTCACATG CGTGGTGGTG

          D  V  S  H  E  D  P  E  V  K  F  N  W  Y  V  D  G  V  E  V
961   GACGTGAGCC ACGAAGACCC TGAGGTCAAG TTCAACTGGT ACGTGGACGG CGTGGAGGTG

          H  N  A  K  T  K  P  R  E  E  Q  Y  N  S  T  Y  R  V  V  S
1021  CATAATGCCA AGACAAAGCC GCGGGAGGAG CAGTACAACA GCACGTACCG TGTGGTCAGC

          V  L  T  V  L  H  Q  D  W  L  N  G  K  E  Y  K  C  K  V  S
1081  GTCCTCACCG TCCTGCACCA GGACTGGCTG AATGGCAAGG AGTACAAGTG CAAGGTCTCC

          N  K  A  L  P  A  P  I  E  K  T  I  S  K  A  K  G  Q  P  R
1141  AACAAAGCCC TCCCAGCCCC CATCGAGAAA ACAATCTCCA AAGCCAAAGG GCAGCCCCGA

          E  P  Q  V  Y  T  L  P  P  S  R  D  E  L  T  K  N  Q  V  S
1201  GAACCACAGG TGTACACCCT GCCCCCATCC CGGGATGAGC TGACCAAGAA CCAGGTCAGC

          L  T  C  L  V  K  G  F  Y  P  S  D  I  A  V  E  W  E  S  N
1261  CTGACCTGCC TGGTCAAAGG CTTCTATCCC AGCGACATCG CCGTGGAGTG GGAGAGCAAT

          G  Q  P  E  N  N  Y  K  T  T  P  P  V  L  D  S  D  G  S  F
1321  GGGCAGCCGG AGAACAACTA CAAGACCACG CCTCCCGTGC TGGACTCCGA CGGCTCCTTC

          F  L  Y  S  K  L  T  V  D  K  S  R  W  Q  Q  G  N  V  F  S
1381  TTCCTCTACA GCAAGCTCAC CGTGGACAAG AGCAGGTGGC AGCAGGGGAA CGTCTTCTCA

          C  S  V  M  H  E  A  L  H  N  H  Y  T  Q  K  S  L  S  L  S
1441  TGCTCCGTGA TGCATGAGGC TCTGCACAAC CACTACACGC AGAAGAGCCT CTCCCTGTCT

                        XbaI
                        ~~~~~
          P  G  K  *  S  R
1501  CCGGGTAAAT GATCTAGA
```

Fig. 2

Production Levels of 2H7 scFvIgG1 (SSS-S)H WCH2 WCH3 by Stable CHO Lines

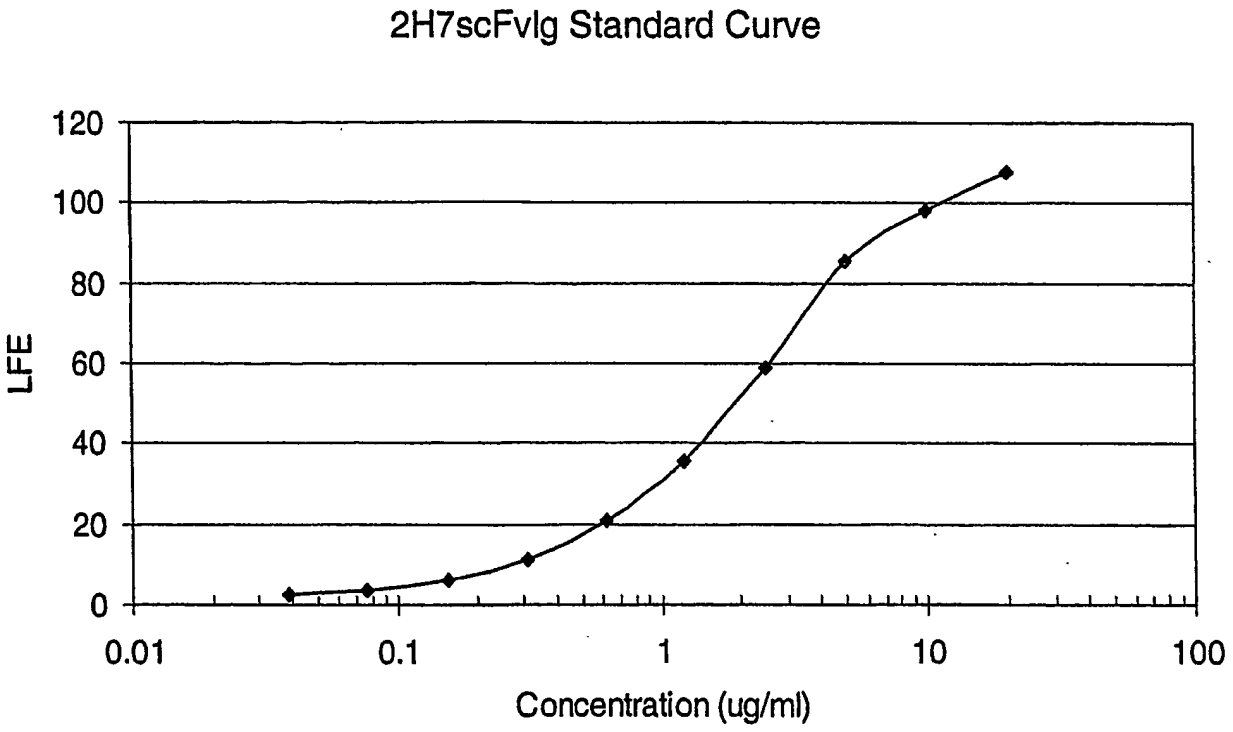

Clone	LFE @ 1:50 Estimated Concentration (µg/ml)
D2	26.156
IIIC6	25.755
IVA3	28.661
Spent bulk	29.664

Fig. 3

SDS-PAGE Analysis of
2H7 scFvIgG1 (SSS-S)H WCH2 WCH3 Protein.

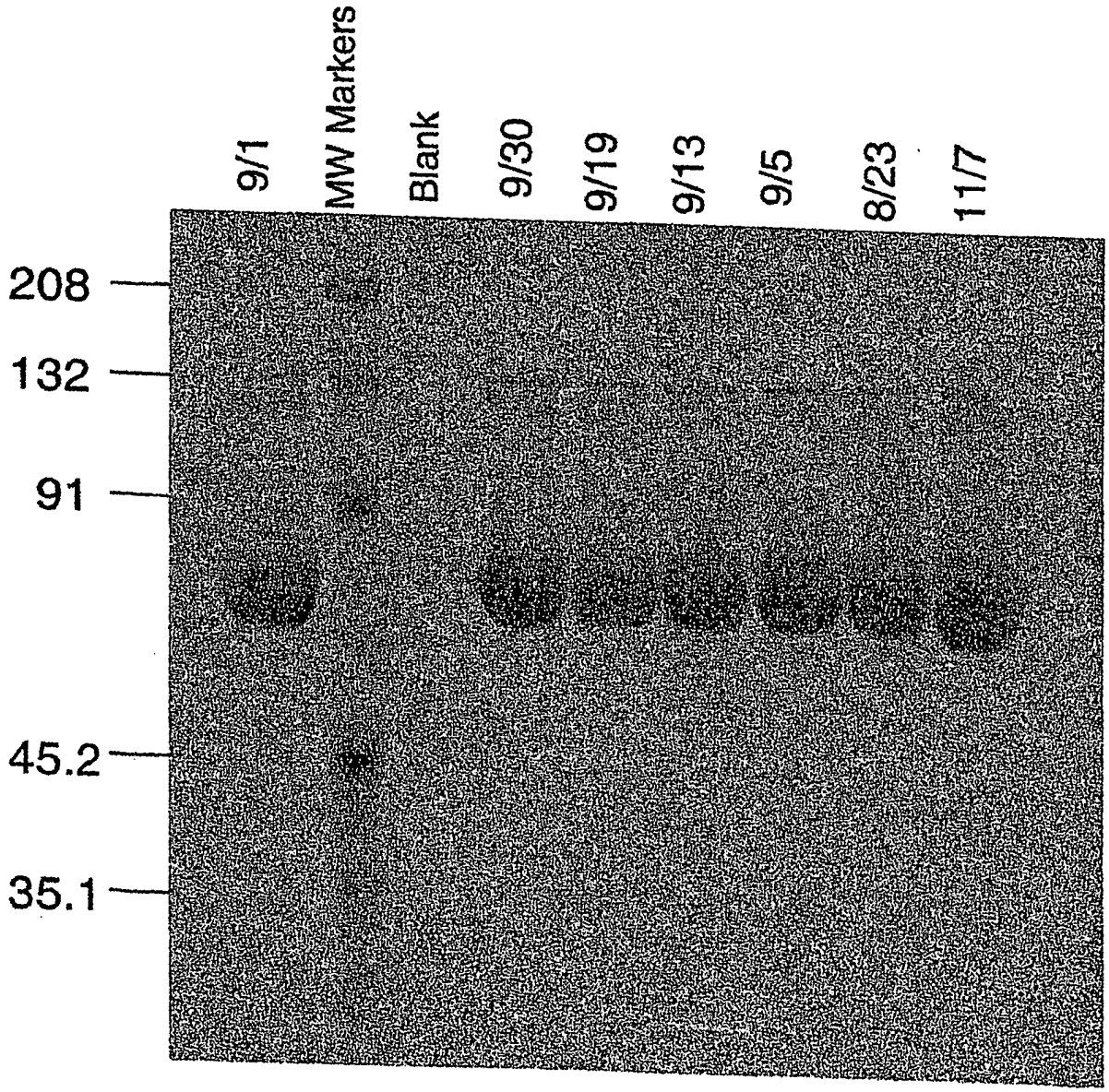

Fig. 4A

Complement Mediated B Cell Killing After Binding of CD20-targeted 2H7 scFvIgG1 (SSS-S)H WCH2 WCH3:

2H7scFv-Ig Concentration	RAMOS # live cells/total cells		BJAB # live cells/total cells	
20 μg/ml + complement	-	0.16	-	0.07
5 μg/ml + complement	-	0.2	-	N.D.
1.25 μg/ml + complement	-	0.32	-	0.1
Complement alone	-	0.98	-	0.94

*Viability was determined by trypan blue exclusion and is tabulated as the fraction of viable cells out of the total number of cells counted.

**N.D. (not determined).

Fig. 4B

Antibody-dependent cellular cytotoxicity (ADCC) mediated by 2H7scFv-IgG1 (SSS-S)H WCH2 WCH3:

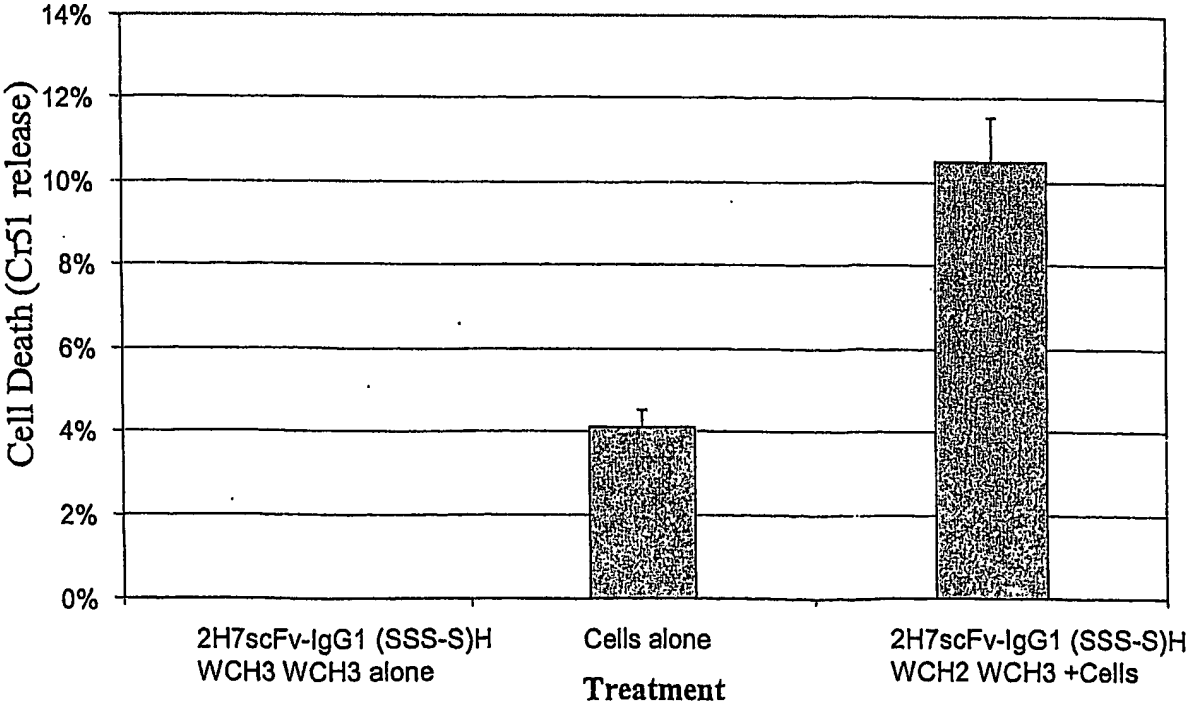

Fig. 5

Effects of Crosslinking of CD20 and CD40 Cell Surface Receptors on B Cell Proliferation:

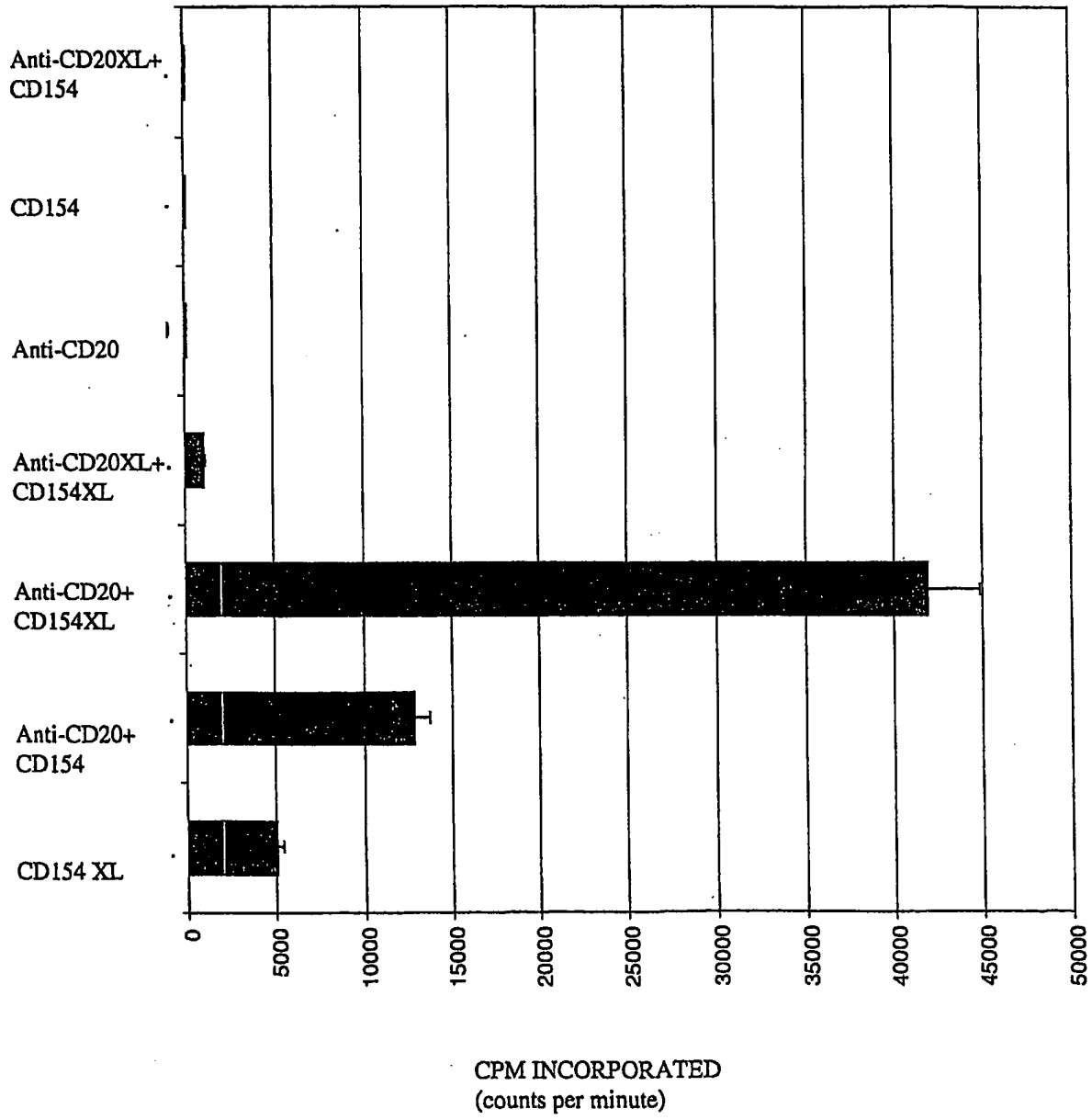

Fig. 6

Effect of Simultaneous ligation of CD20 and CD40 on CD95 and apoptosis.

Fig. 6A.

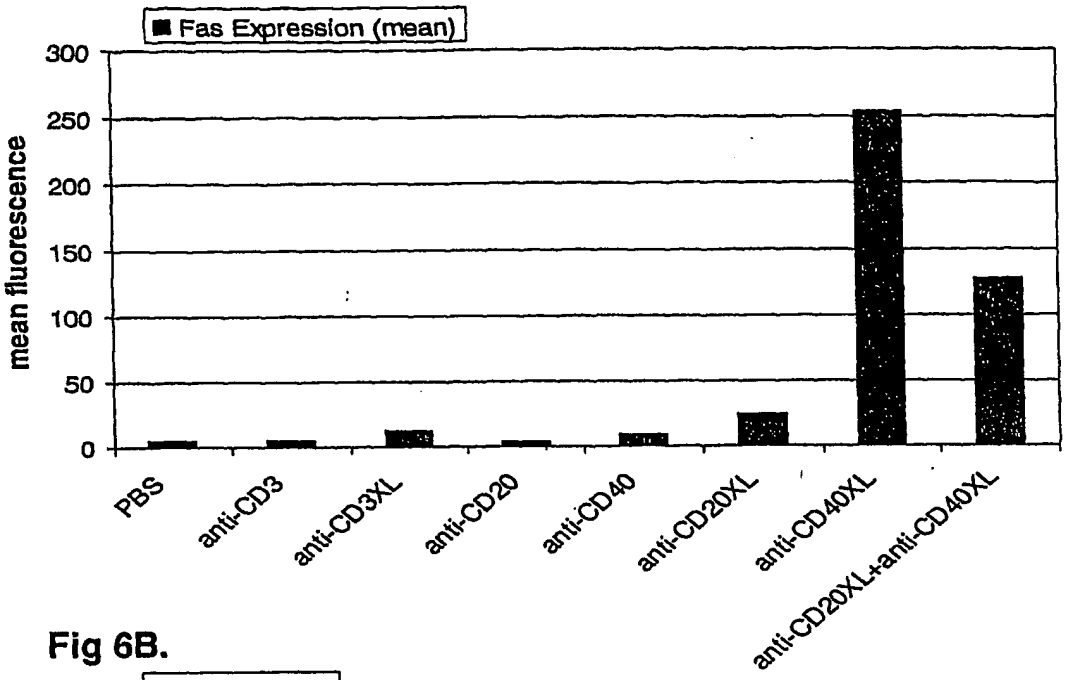

Fig 6B.

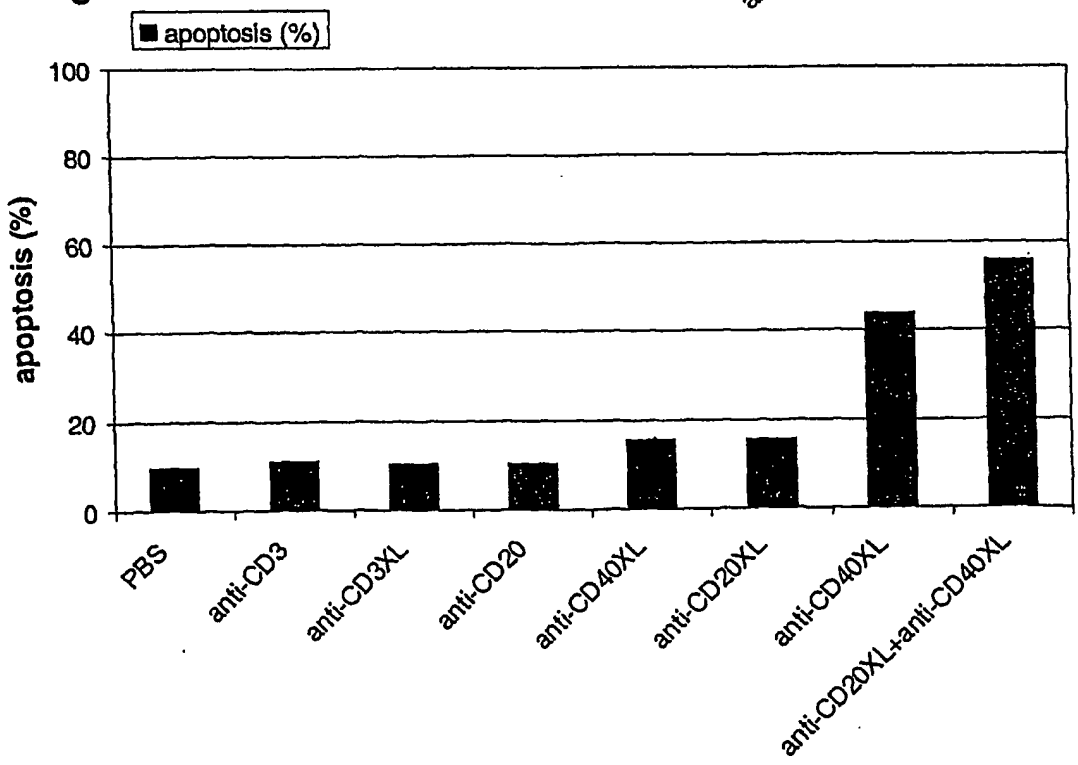

Fig. 7A

2H7-CD154 L2 cDNA and predicted amino acid sequence:

HindIII NcoI 2H7 V_L Leader Peptide →

```
                        M  D  F  Q  V  Q  I  F  S  F  L  L  I  S  A  S
1       AAGCTTGCCG CC   ATGGATTT TCAAGTGCAG ATTTTCAGCT TCCTGCTAAT CAGTGCTTCA

                                        2H7 VL →
        V  I  I  A  R  G  Q  I  V  L  S  Q  S  P  A  I  L  S  A  S
61      GTCATAATTG CCAGAGGACA AATTGTTCTC TCCCAGTCTC CAGCAATCCT GTCTGCATCT

        P  G  E  K  V  T  M  T  C  R  A  S  S  S  V  S  Y  M  H  W
121     CCAGGGGAGA AGGTCACAAT GACTTGCAGG GCCAGCTCAA GTGTAAGTTA CATGCACTGG

                        BamHI
                        ~~~~~~~
        Y  Q  Q  K  P  G  S  S  P  K  P  W  I  Y  A  P  S  N  L  A
181     TACCAGCAGA AGCCAGGATC CTCCCCCAAA CCCTGGATTT ATGCCCCATC CAACCTGGCT

        S  G  V  P  A  R  F  S  G  S  G  S  G  T  S  Y  S  L  T  I
241     TCTGGAGTCC CTGCTCGCTT CAGTGGCAGT GGGTCTGGGA CCTCTTACTC TCTCACAATC

        S  R  V  E  A  E  D  A  A  T  Y  Y  C  Q  Q  W  S  F  N  P
301     AGCAGAGTGG AGGCTGAAGA TGCTGCCACT TATTACTGCC AGCAGTGGAG TTTTAACCCA
```

(Gly$_4$Ser)$_3$ Linker →

```
        P  T  F  G  A  G  T  K  L  E  L  K  G  G  G  G  S  G  G  G
361     CCCACGTTCG GTGCTGGGAC CAAGCTGGAG CTGAAAGGTG GCGGTGGCTC GGGCGGTGGT

                                                    2H7 VH →
        G  S  G  G  G  G  S  S  Q  A  Y  L  Q  Q  S  G  A  E  L  V
421     GGATCTGGAG GAGGTGGGAG CTCTCAGGCT TATCTACAGC AGTCTGGGGC TGAGCTGGTG

        R  P  G  A  S  V  K  M  S  C  K  A  S  G  Y  T  F  T  S  Y
481     AGGCCTGGGG CCTCAGTGAA GATGTCCTGC AAGGCTTCTG GCTACACATT TACCAGTTAC

        N  M  H  W  V  K  Q  T  P  R  Q  G  L  E  W  I  G  A  I  Y
541     AATATGCACT GGGTAAAGCA GACACCTAGA CAGGGCCTGG AATGGATTGG AGCTATTTAT

        P  G  N  G  D  T  S  Y  N  Q  K  F  K  G  K  A  T  L  T  V
601     CCAGGAAATG GTGATACTTC CTACAATCAG AAGTTCAAGG GCAAGGCCAC ACTGACTGTA

        D  K  S  S  S  T  A  Y  M  Q  L  S  S  L  T  S  E  D  S  A
661     GACAAATCCT CCAGCACAGC CTACATGCAG CTCAGCAGCC TGACATCTGA AGACTCTGCG

        V  Y  F  C  A  R  V  V  Y  Y  S  N  S  Y  W  Y  F  D  V  W
721     GTCTATTTCT GTGCAAGAGT GGTGTACTAT AGTAACTCTT ACTGGTACTT CGATGTCTGG
```

Fig. 7A (continued)

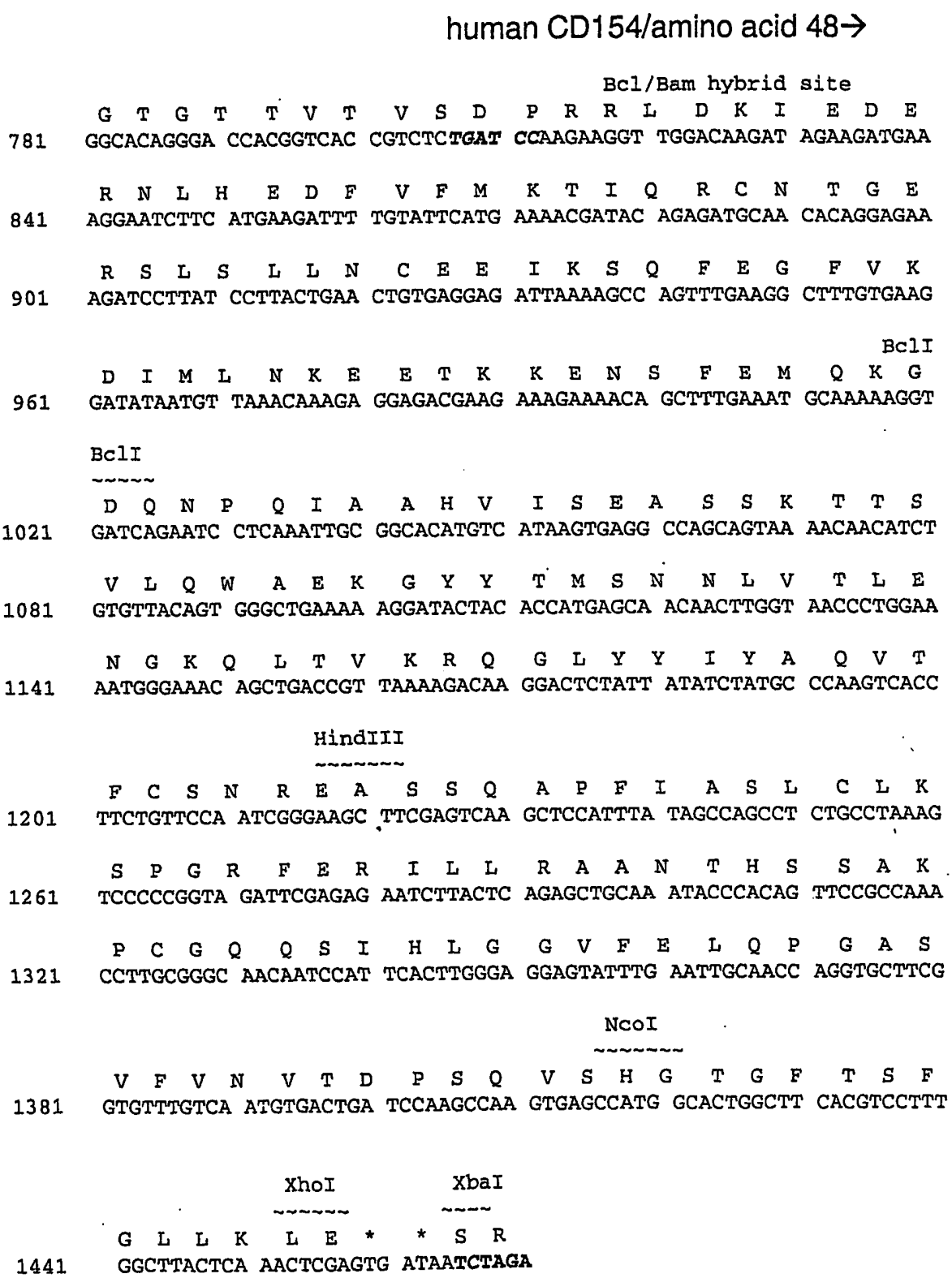

Fig. 7B.

2H7scFv-CD154 S4 cDNA and predicted amino acid sequence:

HindIII NcoI
~~~~~~ ~~~~~~2H7 V_L Leader Peptide→

```
                    M  D  F  Q  V  Q  I  F  S  F  L  L  I  S  A  S
1   AAGCTTGCCG CC   ATGGATTT TCAAGTGCAG ATTTTCAGCT TCCTGCTAAT CAGTGCTTCA
```

2H7 V_L →

```
     V  I  I  A  R  G  Q  I  V  L  S  Q  S  P  A  I  L  S  A  S
61  GTCATAATTG CCAGAGGACA AATTGTTCTC TCCCAGTCTC CAGCAATCCT GTCTGCATCT

     P  G  E  K  V  T  M  T  C  R  A  S  S  S  V  S  Y  M  H  W
121 CCAGGGGAGA AGGTCACAAT GACTTGCAGG GCCAGCTCAA GTGTAAGTTA CATGCACTGG
```

BamHI
~~~~~~~

```
     Y  Q  Q  K  P  G  S  S  P  K  P  W  I  Y  A  P  S  N  L  A
181 TACCAGCAGA AGCCAGGATC CTCCCCCAAA CCCTGGATTT ATGCCCCATC CAACCTGGCT

     S  G  V  P  A  R  F  S  G  S  G  S  G  T  S  Y  S  L  T  I
241 TCTGGAGTCC CTGCTCGCTT CAGTGGCAGT GGGTCTGGGA CCTCTTACTC TCTCACAATC

     S  R  V  E  A  E  D  A  A  T  Y  Y  C  Q  Q  W  S  F  N  P
301 AGCAGAGTGG AGGCTGAAGA TGCTGCCACT TATTACTGCC AGCAGTGGAG TTTTAACCCA
```

(Gly$_4$Ser)$_3$ Linker →

```
     P  T  F  G  A  G  T  K  L  E  L  K  G  G  G  G  S  G  G  G
361 CCCACGTTCG GTGCTGGGAC CAAGCTGGAG CTGAAAGGTG GCGGTGGCTC GGGCGGTGGT
```

2H7 V_H →

```
     G  S  G  G  G  G  S  S  Q  A  Y  L  Q  Q  S  G  A  E  L  V
421 GGATCTGGAG GAGGTGGGAG CTCTCAGGCT TATCTACAGC AGTCTGGGGC TGAGCTGGTG

     R  P  G  A  S  V  K  M  S  C  K  A  S  G  Y  T  F  T  S  Y
481 AGGCCTGGGG CCTCAGTGAA GATGTCCTGC AAGGCTTCTG GCTACACATT TACCAGTTAC

     N  M  H  W  V  K  Q  T  P  R  Q  G  L  E  W  I  G  A  I  Y
541 AATATGCACT GGGTAAAGCA GACACCTAGA CAGGGCCTGG AATGGATTGG AGCTATTTAT

     P  G  N  G  D  T  S  Y  N  Q  K  F  K  G  K  A  T  L  T  V
601 CCAGGAAATG GTGATACTTC CTACAATCAG AAGTTCAAGG GCAAGGCCAC ACTGACTGTA

     D  K  S  S  S  T  A  Y  M  Q  L  S  S  L  T  S  E  D  S  A
661 GACAAATCCT CCAGCACAGC CTACATGCAG CTCAGCAGCC TGACATCTGA AGACTCTGCG

     V  Y  F  C  A  R  V  V  Y  Y  S  N  S  Y  W  Y  F  D  V  W
721 GTCTATTTCT GTGCAAGAGT GGTGTACTAT AGTAACTCTT ACTGGTACTT CGATGTCTGG
```

Fig. 7B

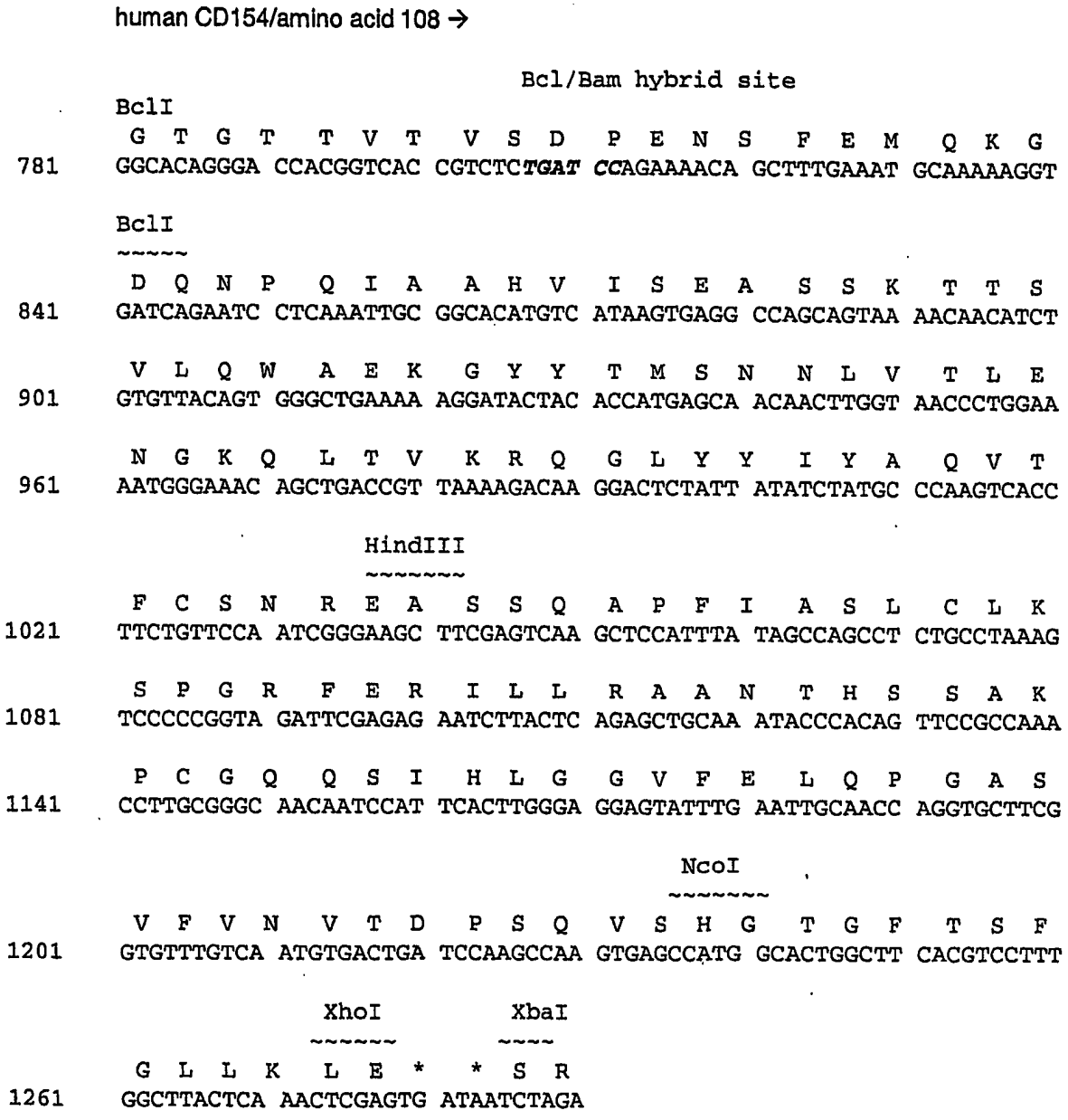
human CD154/amino acid 108 →
Bcl/Bam hybrid site
BclI
G T G T T V T V S D P E N S F E M Q K G
781 GGCACAGGGA CCACGGTCAC CGTCTCTGAT CCAGAAAACA GCTTTGAAAT GCAAAAAGGT
BclI
D Q N P Q I A A H V I S E A S S K T T S
841 GATCAGAATC CTCAAATTGC GGCACATGTC ATAAGTGAGG CCAGCAGTAA AACAACATCT
V L Q W A E K G Y Y T M S N N L V T L E
901 GTGTTACAGT GGGCTGAAAA AGGATACTAC ACCATGAGCA ACAACTTGGT AACCCTGGAA
N G K Q L T V K R Q G L Y Y I Y A Q V T
961 AATGGGAAAC AGCTGACCGT TAAAAGACAA GGACTCTATT ATATCTATGC CCAAGTCACC
HindIII
F C S N R E A S S Q A P F I A S L C L K
1021 TTCTGTTCCA ATCGGGAAGC TTCGAGTCAA GCTCCATTTA TAGCCAGCCT CTGCCTAAAG
S P G R F E R I L L R A A N T H S S A K
1081 TCCCCCGGTA GATTCGAGAG AATCTTACTC AGAGCTGCAA ATACCCACAG TTCCGCCAAA
P C G Q Q S I H L G G V F E L Q P G A S
1141 CCTTGCGGGC AACAATCCAT TCACTTGGGA GGAGTATTTG AATTGCAACC AGGTGCTTCG
NcoI
V F V N V T D P S Q V S H G T G F T S F
1201 GTGTTTGTCA ATGTGACTGA TCCAAGCCAA GTGAGCCATG GCACTGGCTT CACGTCCTTT
XhoI XbaI
G L L K L E * * S R
1261 GGCTTACTCA AACTCGAGTG ATAATCTAGA

Fig. 8

Simultaneous Binding of 2H7scFv-CD154 Fusion Proteins to CD20 and CD40

2H7scFv-CD154
Construct S4

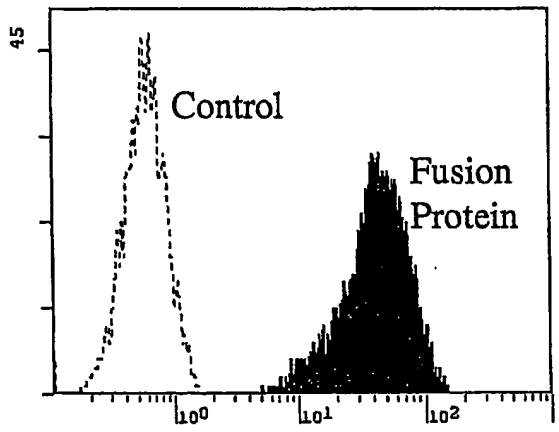

2H7scFv-CD154
Construct L2

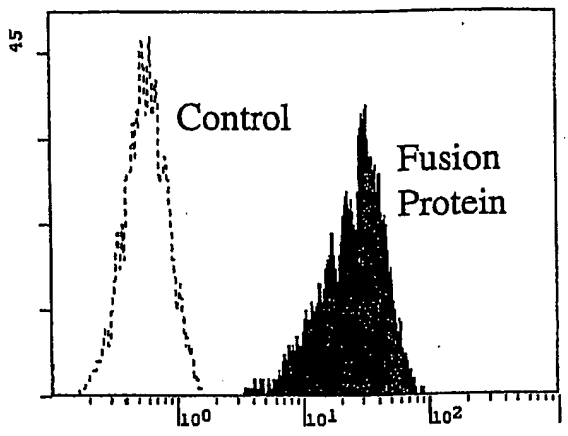

CD20 CHO cell targets + (control or fusion protein)
+ Biotin-CD40Ig + PE-SA

Fig. 9

Induction of Apoptosis Measured by Binding of Annexin V after incubation with 2H7scFv-CD154

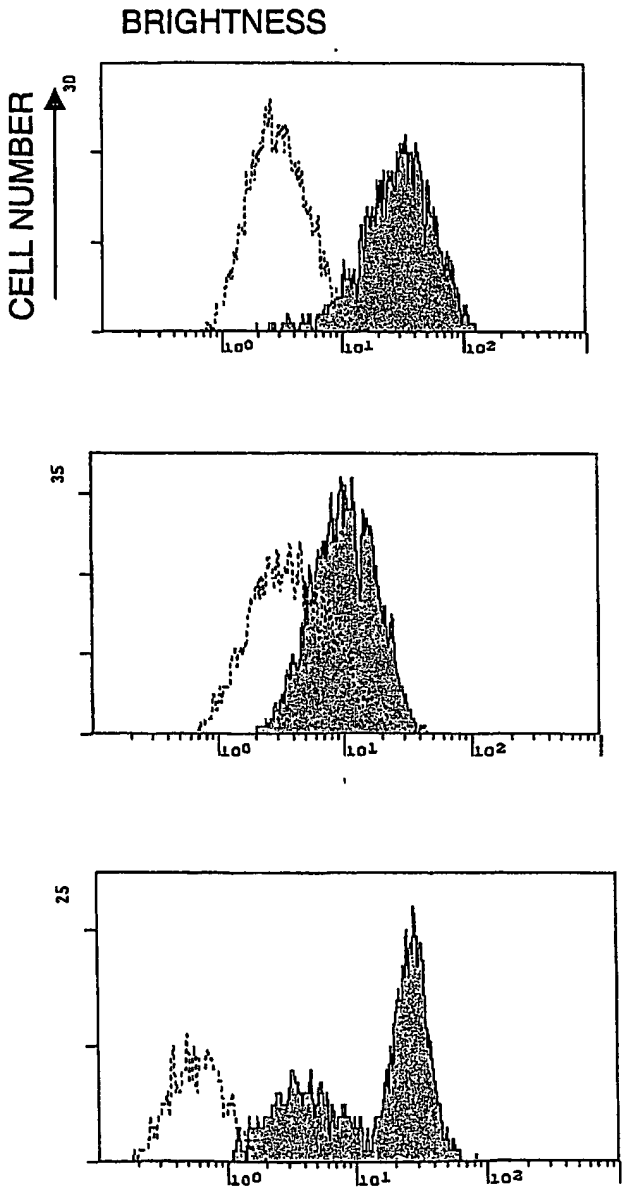

.....control supernatant ___2H7scFv-CD154 supernatant

Fig. 10

Proliferation of T51 B Cell Line After Incubation with 2H7 scFv-CD154 S4 or 2H7 scFv-CD154 L2 Constructs

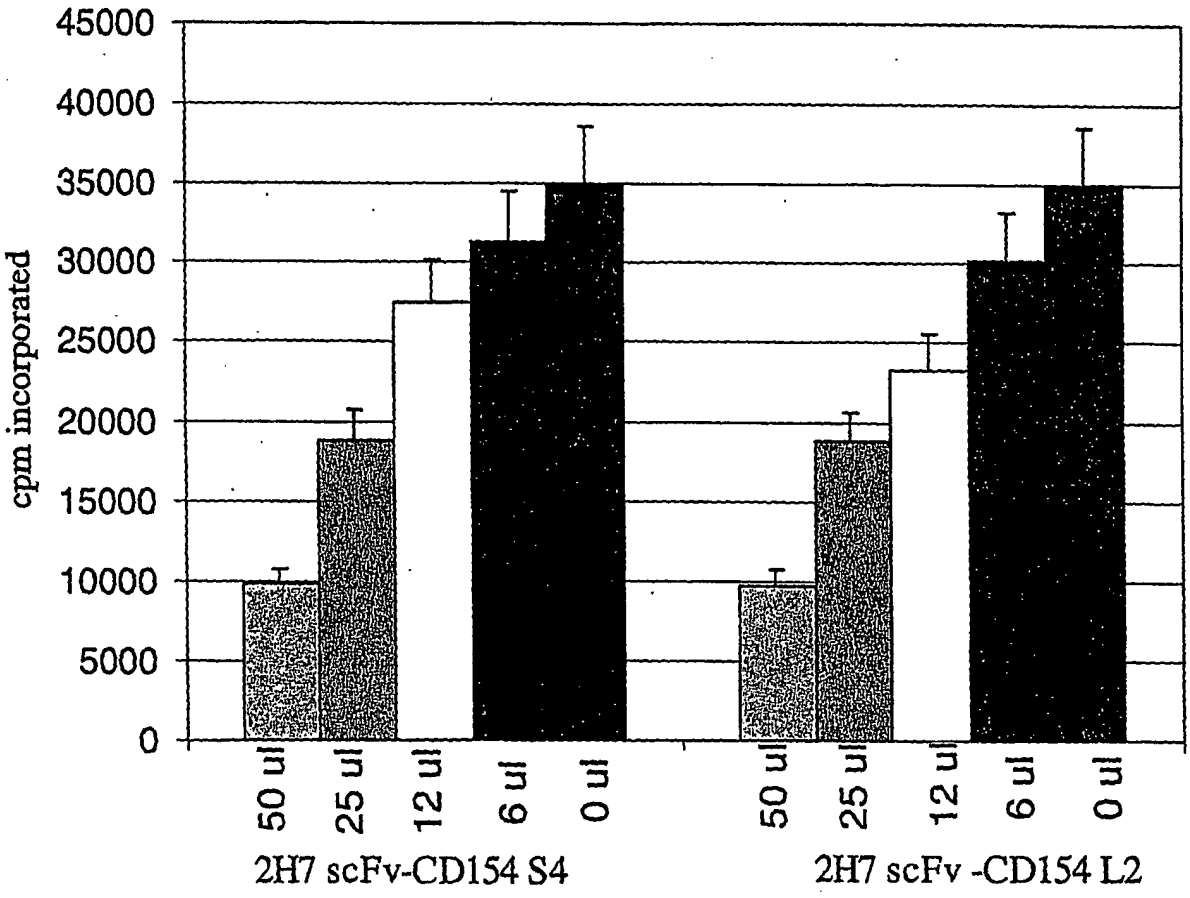

Fig. 11

Schematic Representation of 2H7 scFvIg Constructs

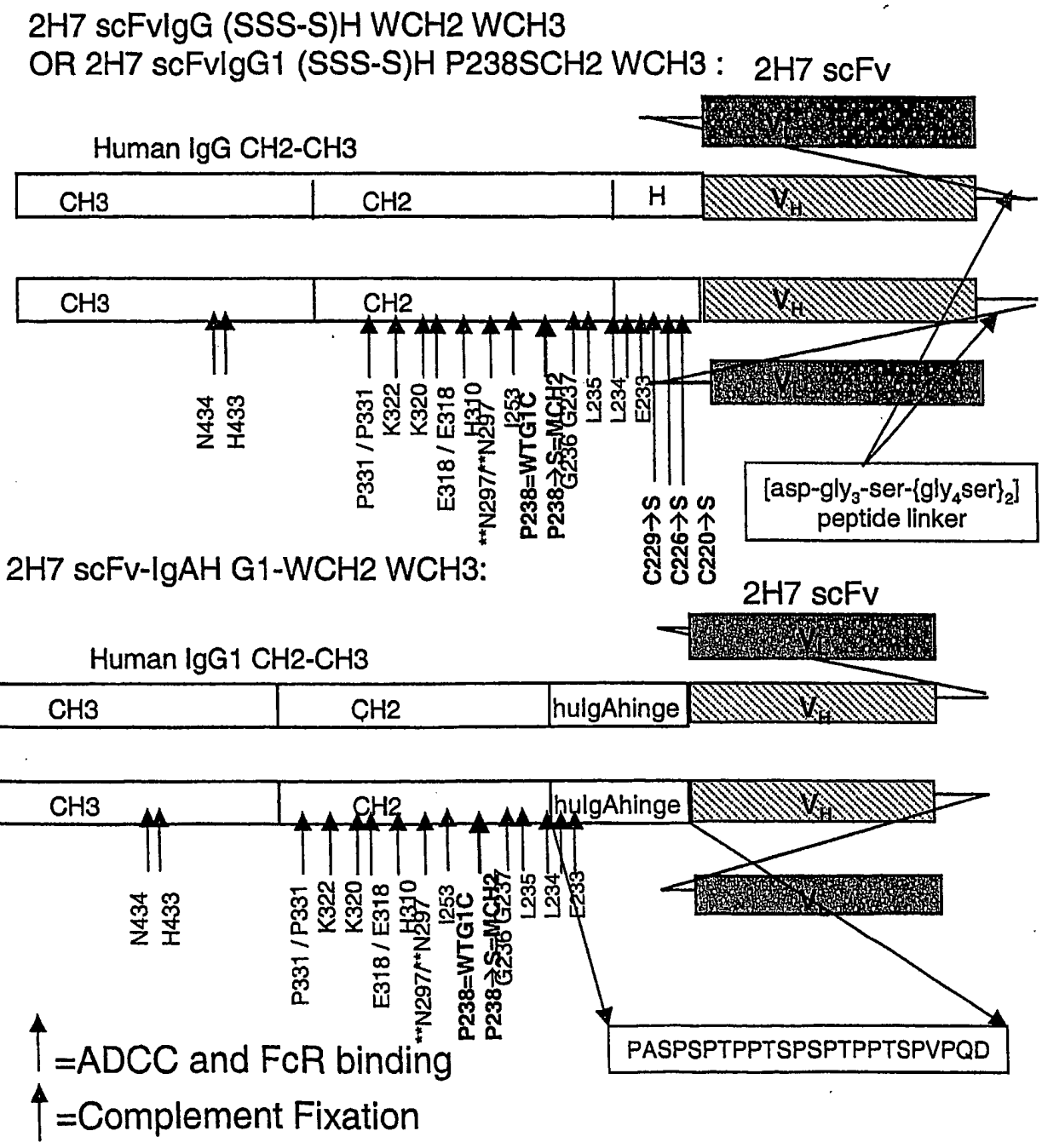

Fig. 12

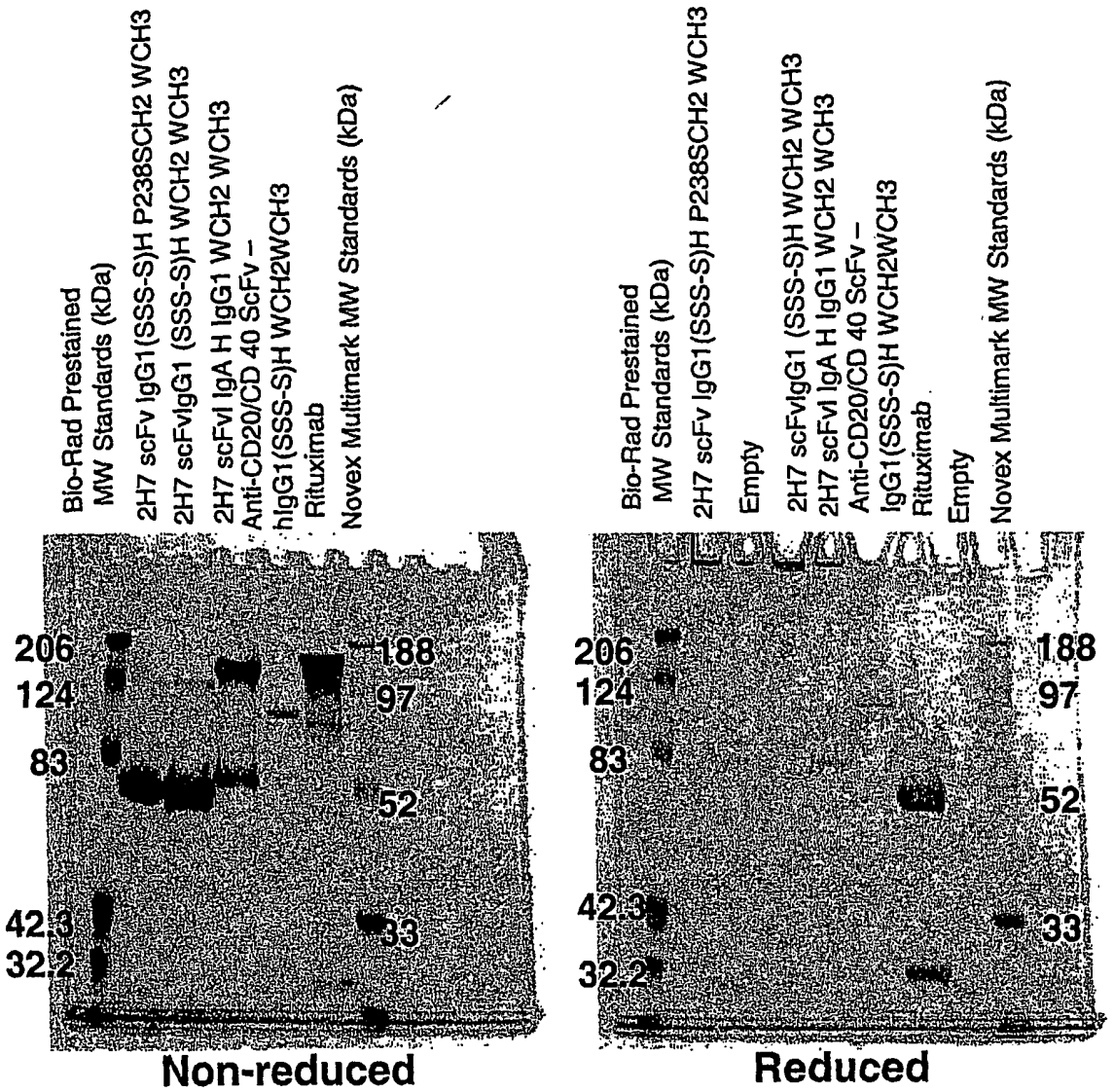

Figure 12: SDS-PAGE Analysis of CytoxB Derivatives. Purified fusion protein derivatives of CytoxB-scFvIg molecules and Rituximab were resuspended SDS sample buffer, boiled, loaded onto 10% Novex Tris-Bis gels (Invitrogen, San Diego, CA) and subjected to nonreducing (left panel) or reducing (right panel) SDS-PAGE electrophoresis at 175 volts. Two different molecular weight markers, BioRad prestained markers, and Novex Multimark molecular weight markers were also loaded onto each gel and the approximate size in kDa of each marker band is indicated along each side of the photographed gels. Gels were stained in Coomassie Blue stain and photographed with a SONY Mavica Digital camera. The mutant hinge forms of 2H7 scFvIgG1 migrate at approximately 70 kDa under both nonreducing and reducing conditions, indicating that these molecules are monomeric rather than dimeric in structure. The IgA hinge form of 2H7scFvIg migrates at approximately 75 kDa under reducing conditions, but migrates predominately as a dimer of 140 kDa with a fraction of the protein migrating at 75 kDa under nonreducing conditions. Under nonreducing conditions, rituximab migrates as a diffuse band of between 150 and 200 kDa. The heavy and light chains resolve into separate bands of approximately 32 and 50 kDa when rituximab is reduced and subjected to SDS-PAGE.

Fig. 13

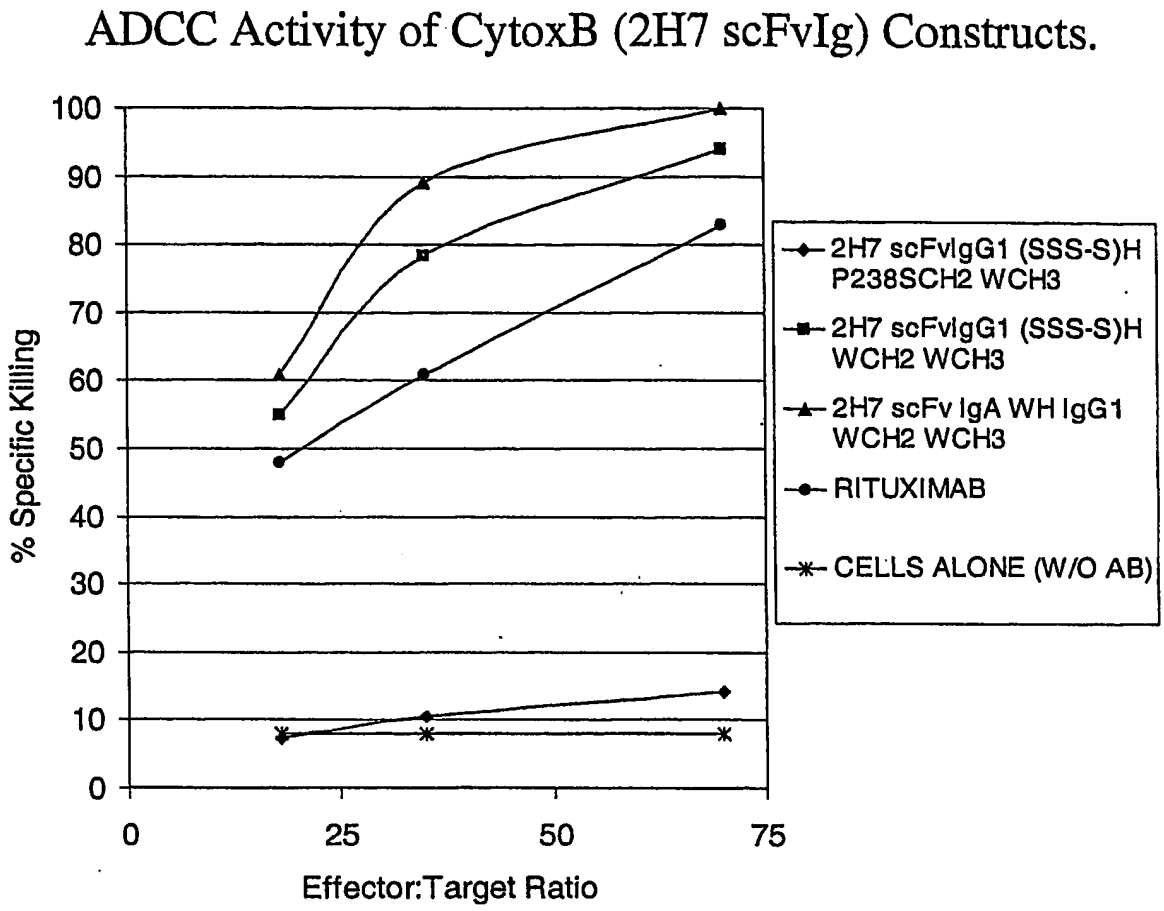

Figure 13: ADCC Activity of CytoxB Derivatives Compared to Rituximab. ADCC activity of CytoxB Derivatives or Rituximab was measured *in vitro* against BJAB B lymphoma cell line as target and using fresh human PBMC as effector cells. Effector to target ratios were varied as follows: 70:1, 35:1, and 18:1, with the number of BJAB cells per well remaining constant but varying the number of PBMC. Bjab cells were labeled for 2 hours with ^{51}Cr and aliquoted at a cell density of $5x10^4$ cells/well to each well of flat-bottom 96 well plates. Purified fusion proteins or rituximab were added at a concentration of 10 mg/ml, and PBMC were added at $9x10^5$ cells /well (18:1), $1.8x10^6$ cells/well (35:1), or $3.6x10^6$ cells/well (70:1), in a final volume of 200 µl. Spontaneous release was measured without addition of PBMC or fusion protein, and maximal release was measured by the addition of detergent (1% NP-40) to the appropriate wells.. Reactions were incubated for 4 hours, and 100 ml culture supernatant harvested to a Lumaplate (Packard Instruments) and allowed to dry overnight prior to counting cpm released on a Packard Top Count NXT Microplate Scintillation Counter.

Fig. 14

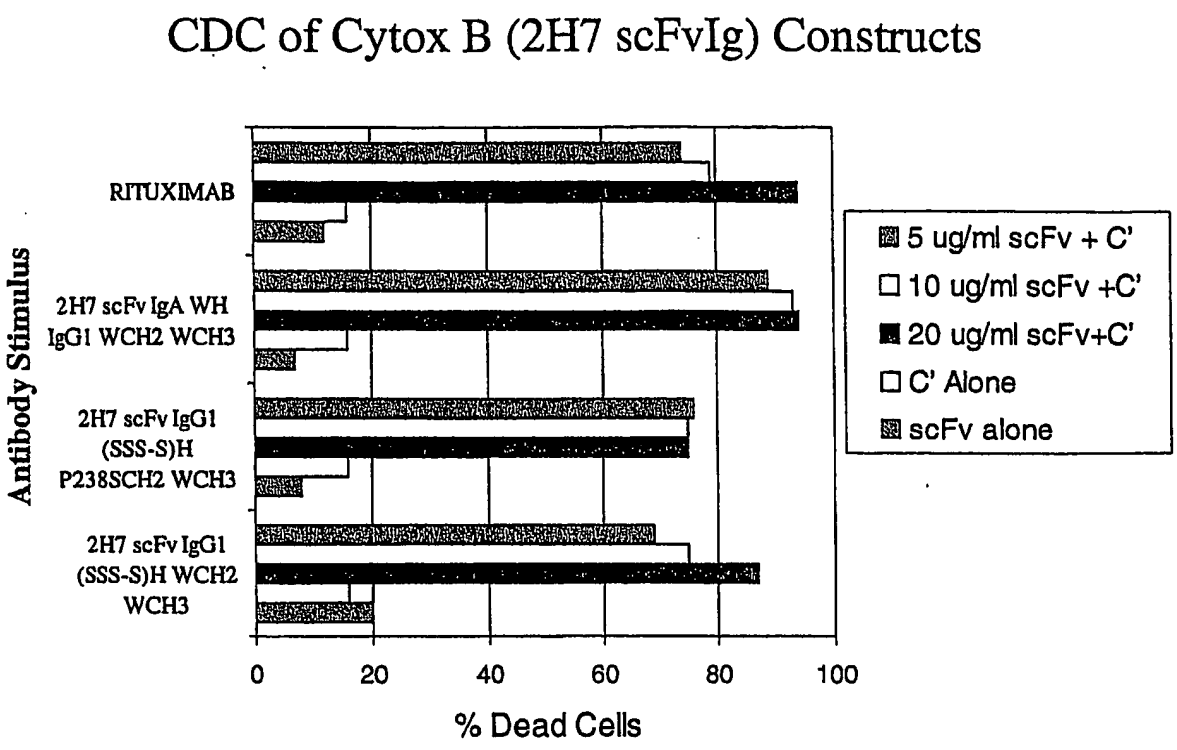

Figure 14: Complement Dependent Cytoxicity (CDC) Activity of CytoxB Derivatives Compared to Rituximab. 2H7 scFvIgG1 (SSS-S)H WCH2 WCH3, 2H7 scFvIgG1 (SSS-S)H WCH2 WCH3, and 2H7scFv IgA WH IgG1 WCH2 WCH3 derivatives and Rituximab were compared for their ability to mediate complement dependent cytoxicity. Rabbit complement (Pel-Freez) was diluted 1:10 and added to BJAB cells along with dilutions of each antibody derivative (20 μg/ml, 10 μg/ml, and 5 μg/ml). Controls were also included without addition of complement (C') or scFv derivative. Reactions were allowed to continue for 1 hour, and cells from each well were then stained with trypan blue and the cell viability counted using a hemacytometer. Data is graphed as % of dead cells/total cells counted for each condition assayed.

Fig. 15

2H7 (anti-CD20) scFv IgG1 (SSS-S)H WCH2 WCH3 In Vivo Half Life

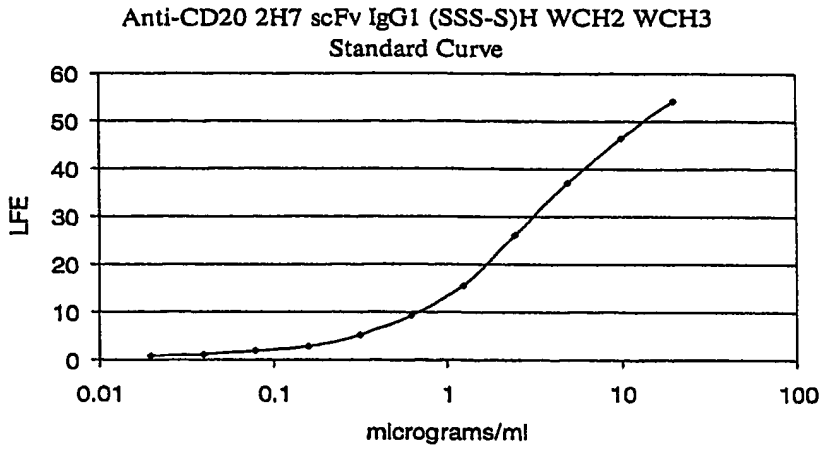

Macaque A99314

	Day	Binding intensity (LFE) @1:50 dilution of serum	estimated concentration (µg/ml)
	–7	0.213	<0.1
Injection #1 →	0	0.227	<0.1
	1	7.79	25.1
	3	5.51	15.6
Injection #2 →	7	3.37	9.4
	8	11.33	41.7
	10	5.45	15.4
	14	0.27	<0.1

Macaque F98081

	Day	Binding intensity (LFE) @ 1:50 dilution of serum	estimated concentration (µg/ml)
	–7	0.208	<0.1
Injection #1 →	0	0.219	<0.1
	1	6.73	21.9
	3	6.14	19.3
Injection #2 →	7	3.04	8.7
	8	9.83	33.8
	10	4.77	14.4
	14	0.231	<0.1

Fig. 16

B Cell Depletion in macaques mediated by Cytox B20 (2H7 scFv IgG1 (SSS-S)H WCH2 WCH3) Construct

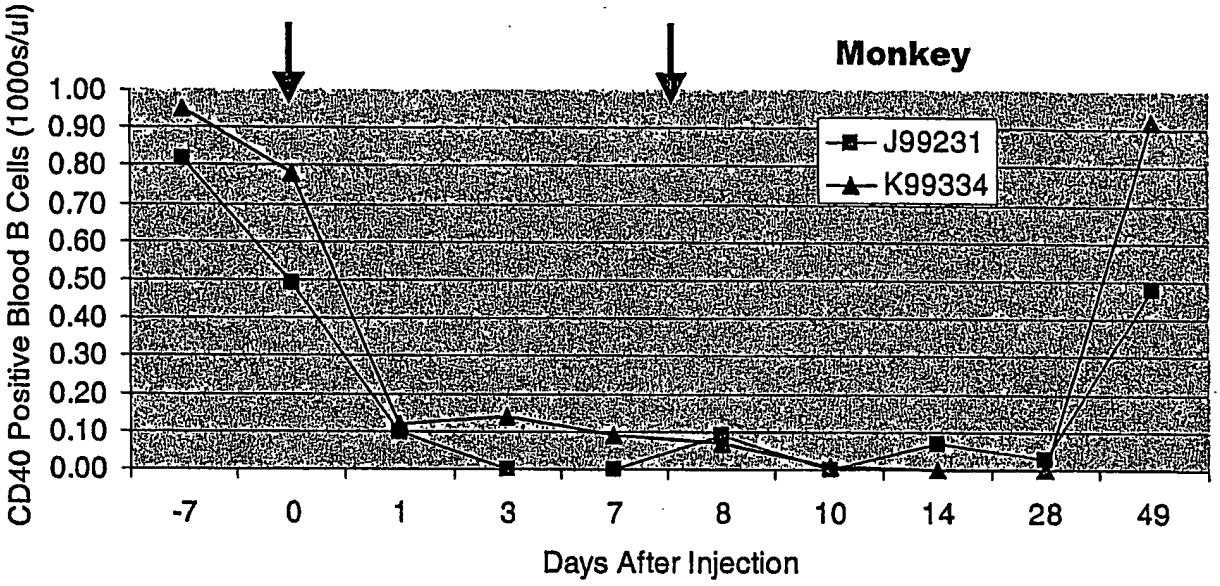

- **CytoxB20 injections of 6mg/kg yields 3 week B-cell depletion**
- **3-4 day half-life *in vivo***
- **CD20 saturation in lymph node B-cells at d14**
- **No first dose effects**
- **No anti-chimeric antibody development**

Fig. 17

Production Levels of HD37 scFvIg Constructs by CHO Cell Lines

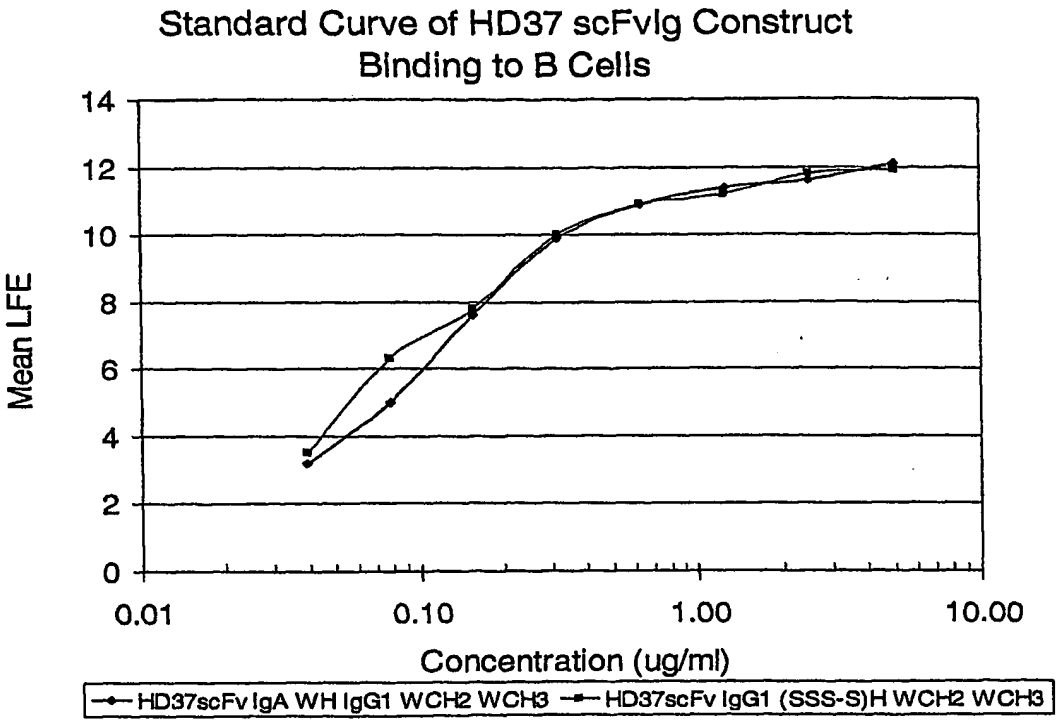

Clone/Isolate	Mean LFE at 1:100	Estimated Concentration
Bulk HD37 scFv		
IgA WH IgG1 WCH2 WCH3	11.2	> 60 ug/ml
1B2	10.4	>50 ug/ml
6C5	10.5	>50 ug/ml
4B1	8.6	>40 ug/ml
Bulk HD37 scFv		
IgG1 (SSS-S)H WCH2 WCH3	10.9	> 50 ug/ml
2G8	10.6	> 50 ug/ml
3F3	8.3	>40 ug/ml
3D9	11.1	> 60 ug/ml

Fig. 18

Production of L6 scFvIg constructs by CHO Cells

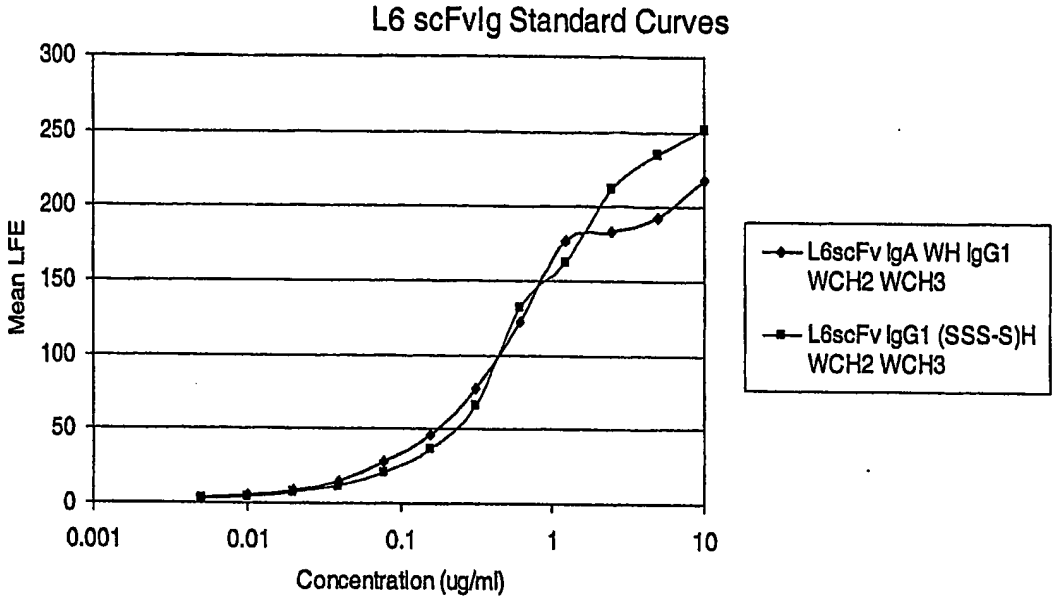

Construct	Mean LFE 1:20	Estimated Concentration
L6scFv IgA WH IgG1 WCH2 WCH3 unamplified CHO sup	51.1	6.25 ug/ml
L6scFv IgG1(SSS-S)H WCH2 WCH3 unamplified CHO sup	23.0	3.2ug/ml

Fig. 19

ADCC Activity of 2H7 scFvIg, G28-1 scFvIg, and HD37 scFvIg Constructs

ADCC Activity of scFvs Targeted to B Cell Antigens

A. 2H7 (anti-CD20) scFv constructs

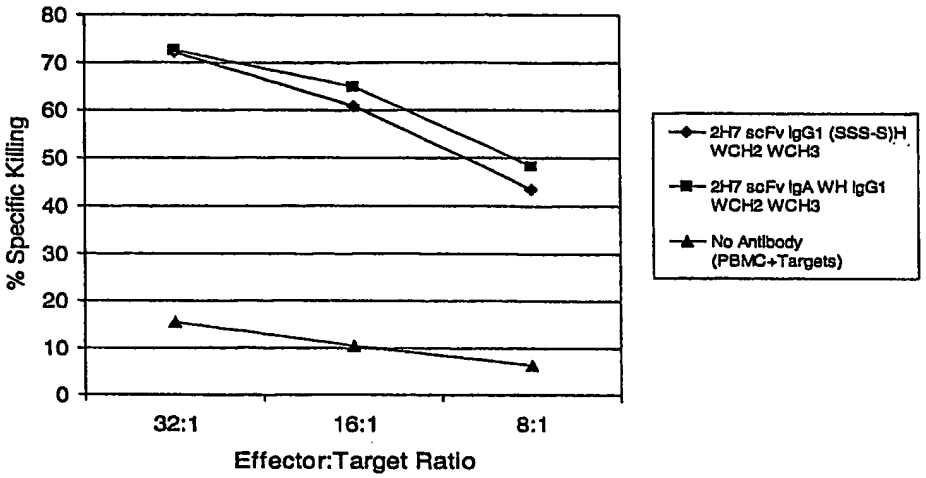

B. G28-1 (anti-CD37) scFv constructs

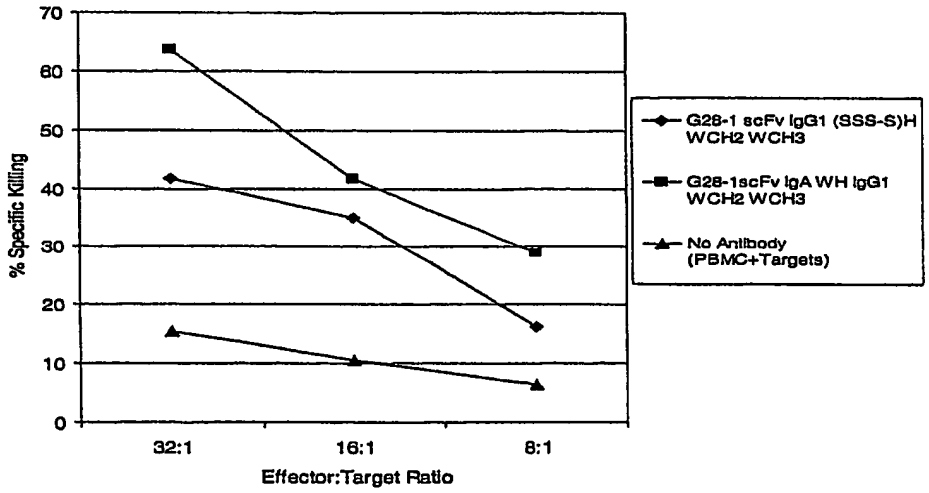

C. HD37 (anti-CD19) scFv constructs

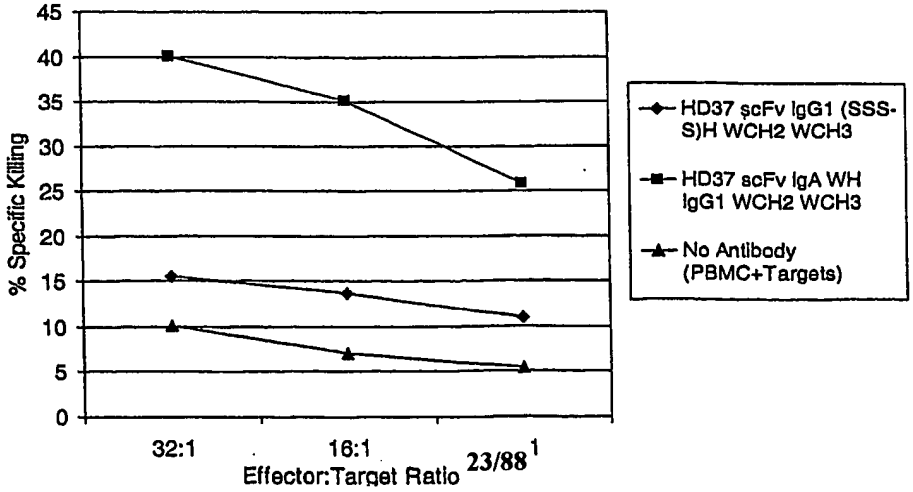

Fig. 20

ADCC Activity of L6 scFvIg Constructs

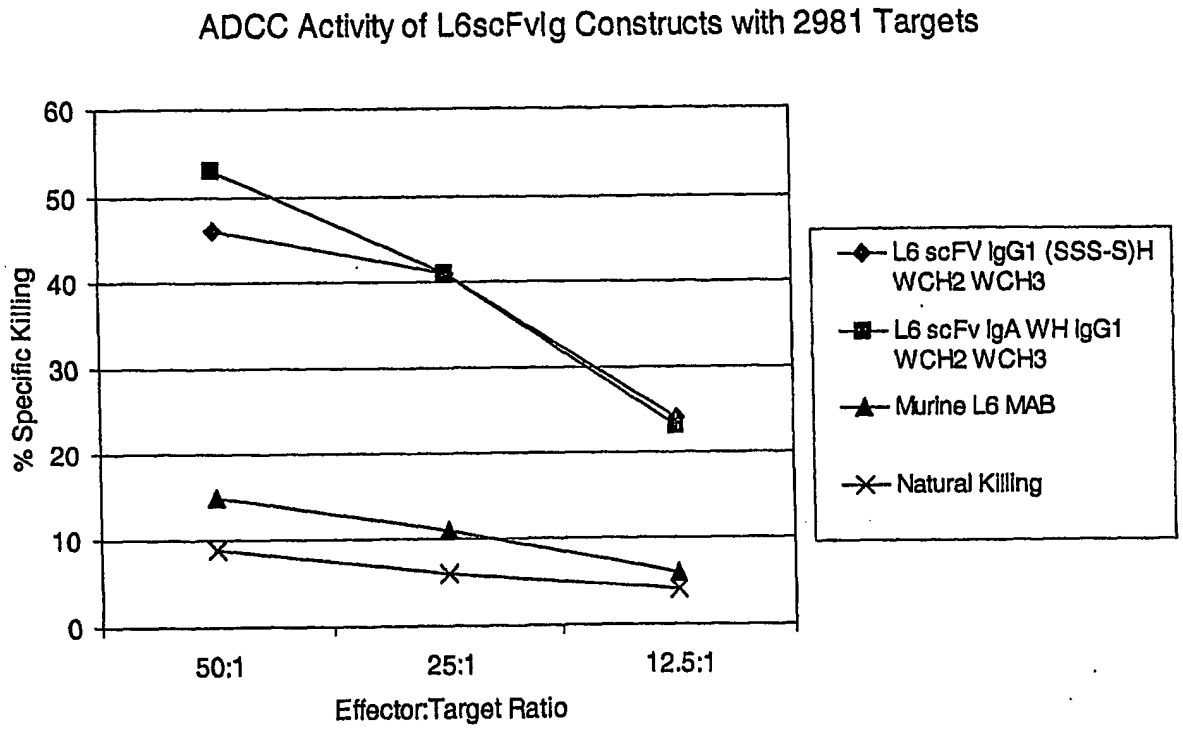

Fig. 21

SDS-PAGE Analysis of L6 and 2H7 scFvIg Fusion Proteins.

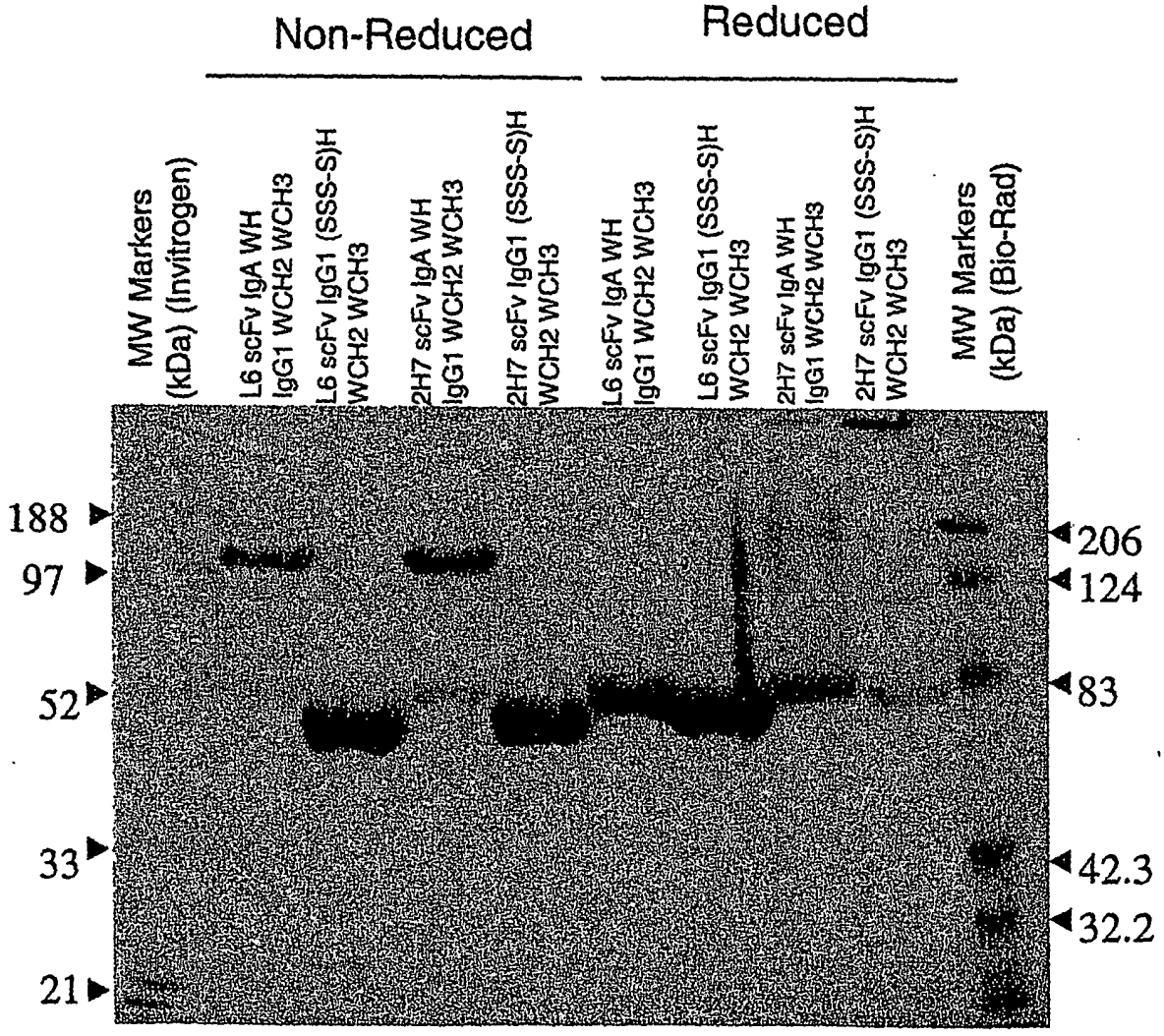

Fig. 22

SDS-PAGE Analysis of G28-1 and HD37 scFvIg Constructs.

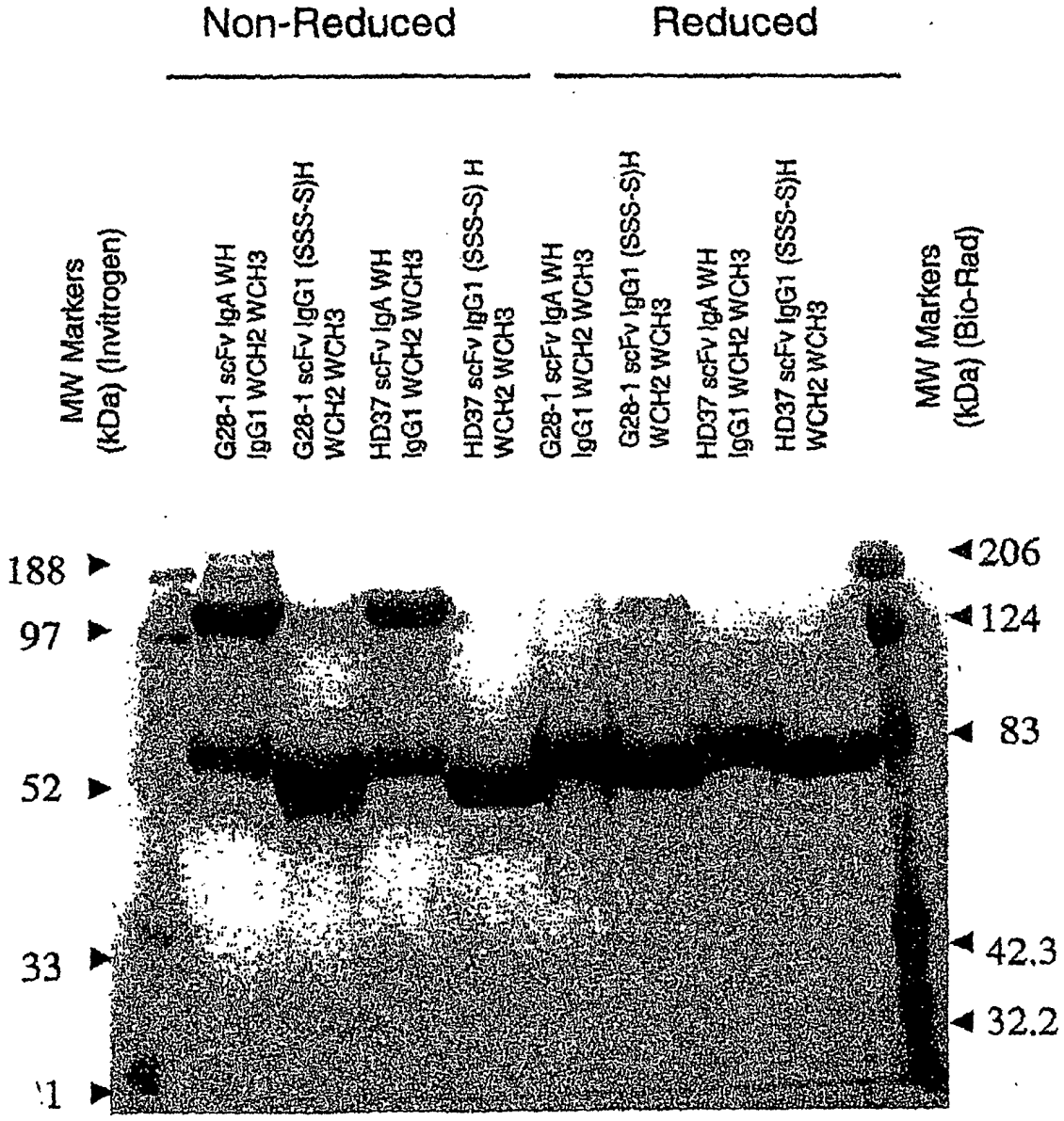

Fig. 23

Sequence alignment of human and llama Fc regions.

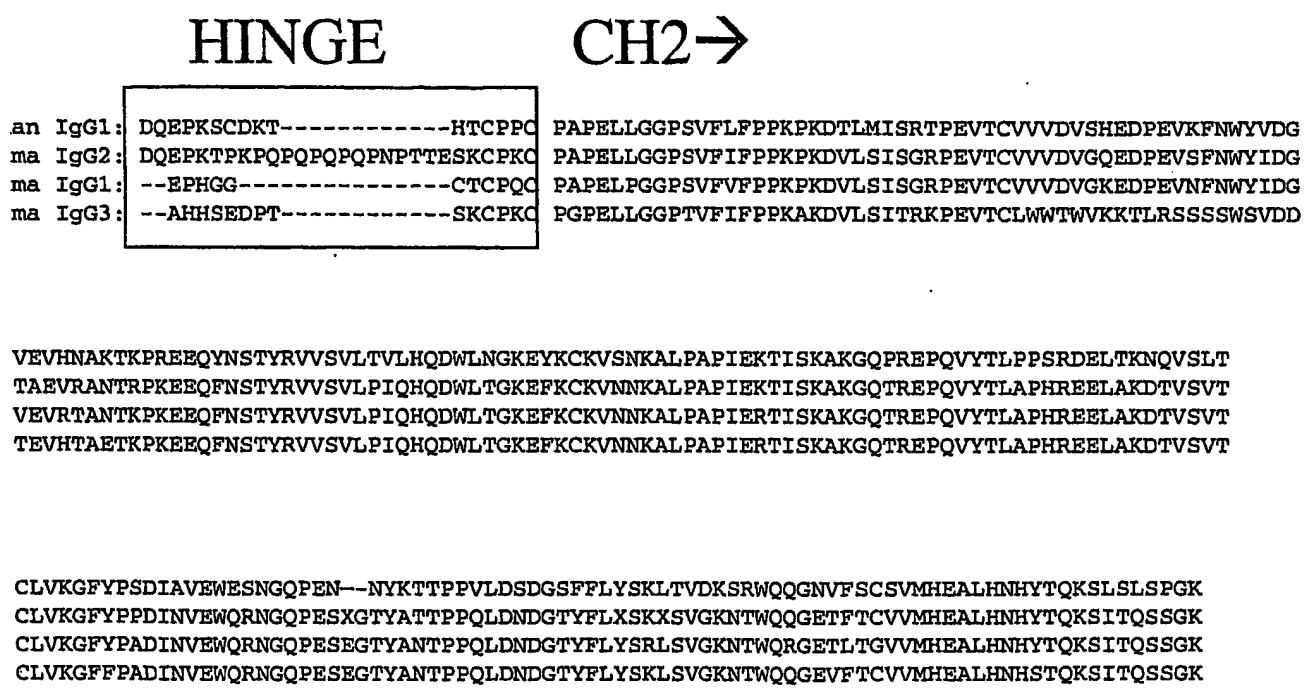

Fig. 24

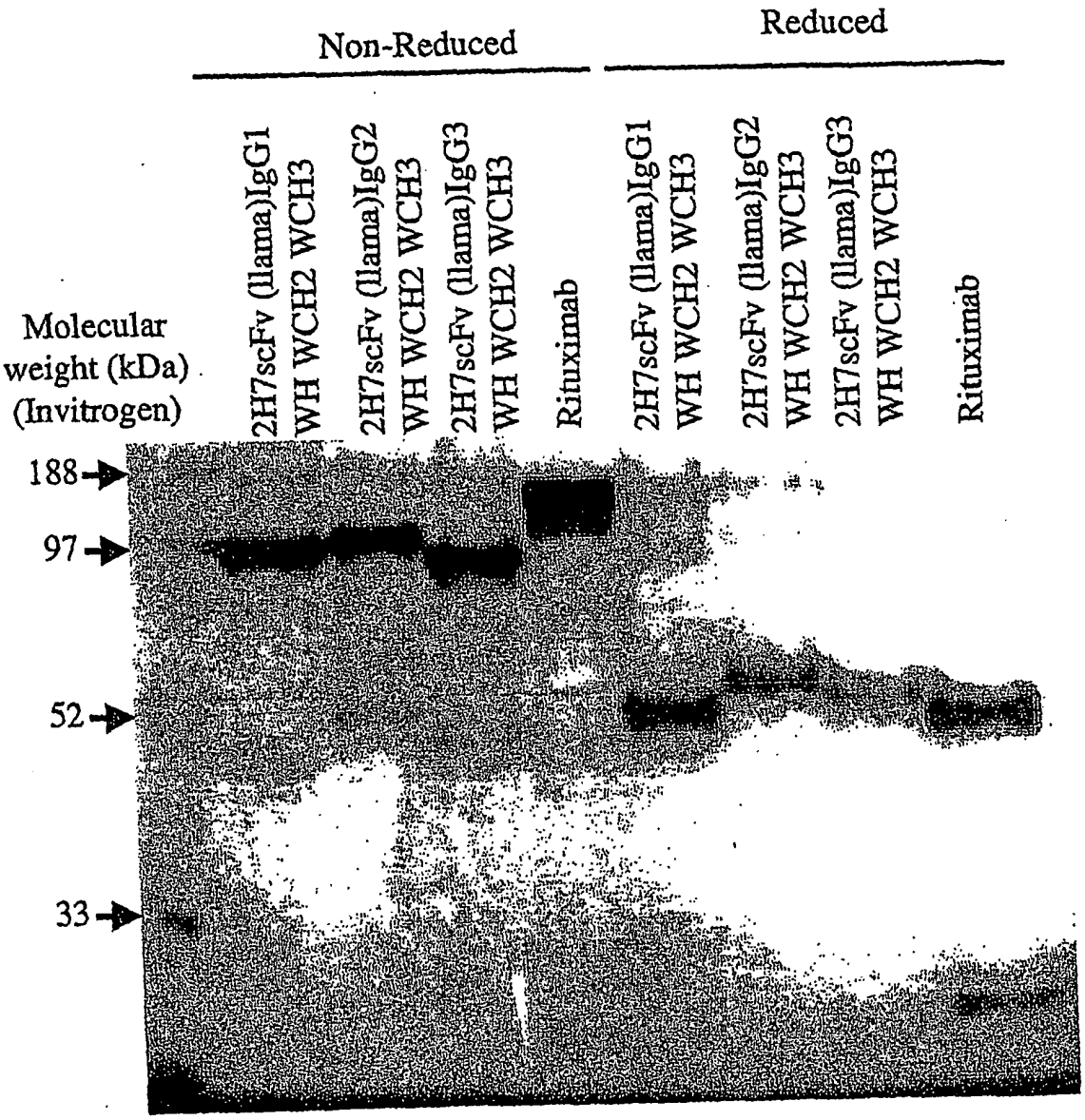
Non-Reduced
Reduced
Molecular weight (kDa) (Invitrogen)
188
97
52
33
2H7scFv (llama)IgG1 WH WCH2 WCH3
2H7scFv (llama)IgG2 WH WCH2 WCH3
2H7scFv (llama)IgG3 WH WCH2 WCH3
Rituximab
2H7scFv (llama)IgG1 WH WCH2 WCH3
2H7scFv (llama)IgG2 WH WCH2 WCH3
2H7scFv (llama)IgG3 WH WCH2 WCH3
Rituximab

Fig. 25

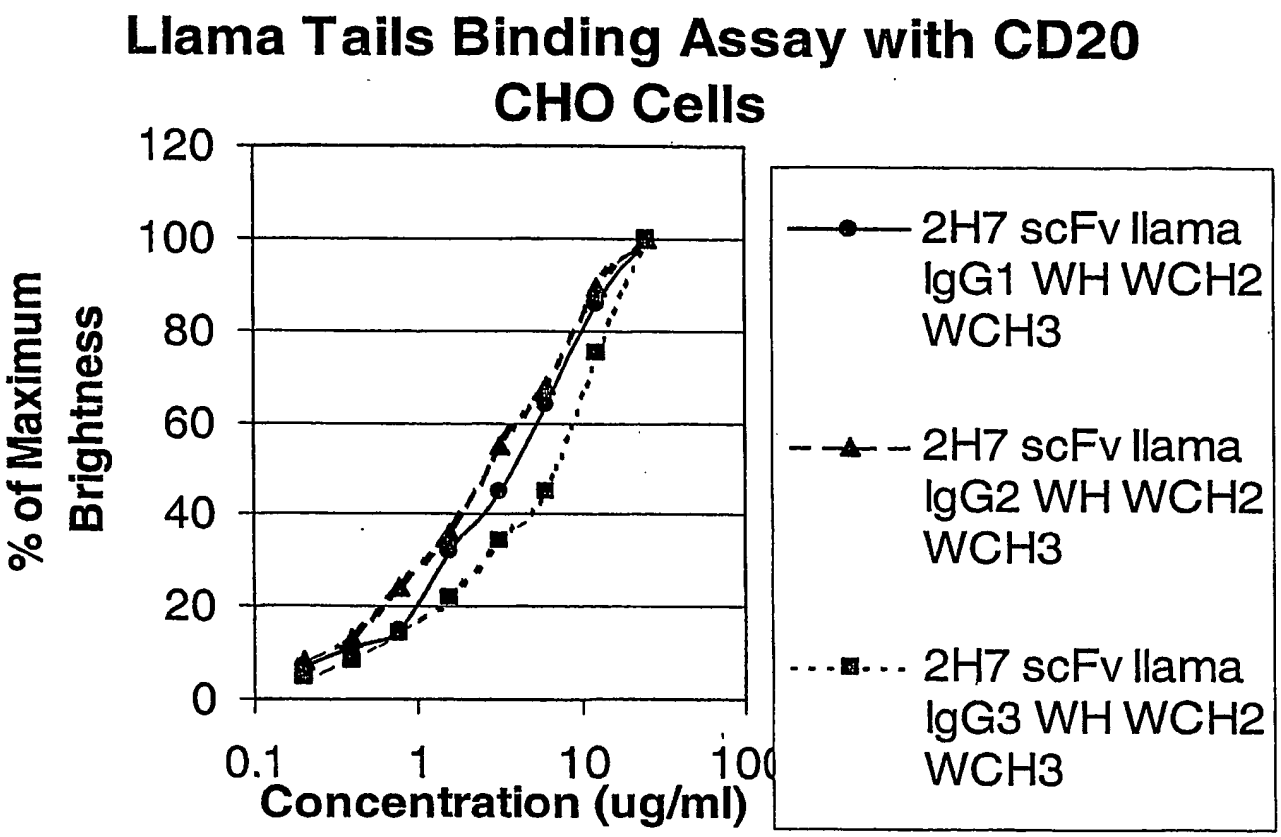
Llama Tails Binding Assay with CD20 CHO Cells
% of Maximum Brightness
120
100
80
60
40
20
0
0.1
1
10
100
Concentration (ug/ml)
2H7 scFv llama IgG1 WH WCH2 WCH3
2H7 scFv llama IgG2 WH WCH2 WCH3
2H7 scFv llama IgG3 WH WCH2 WCH3

Fig. 26

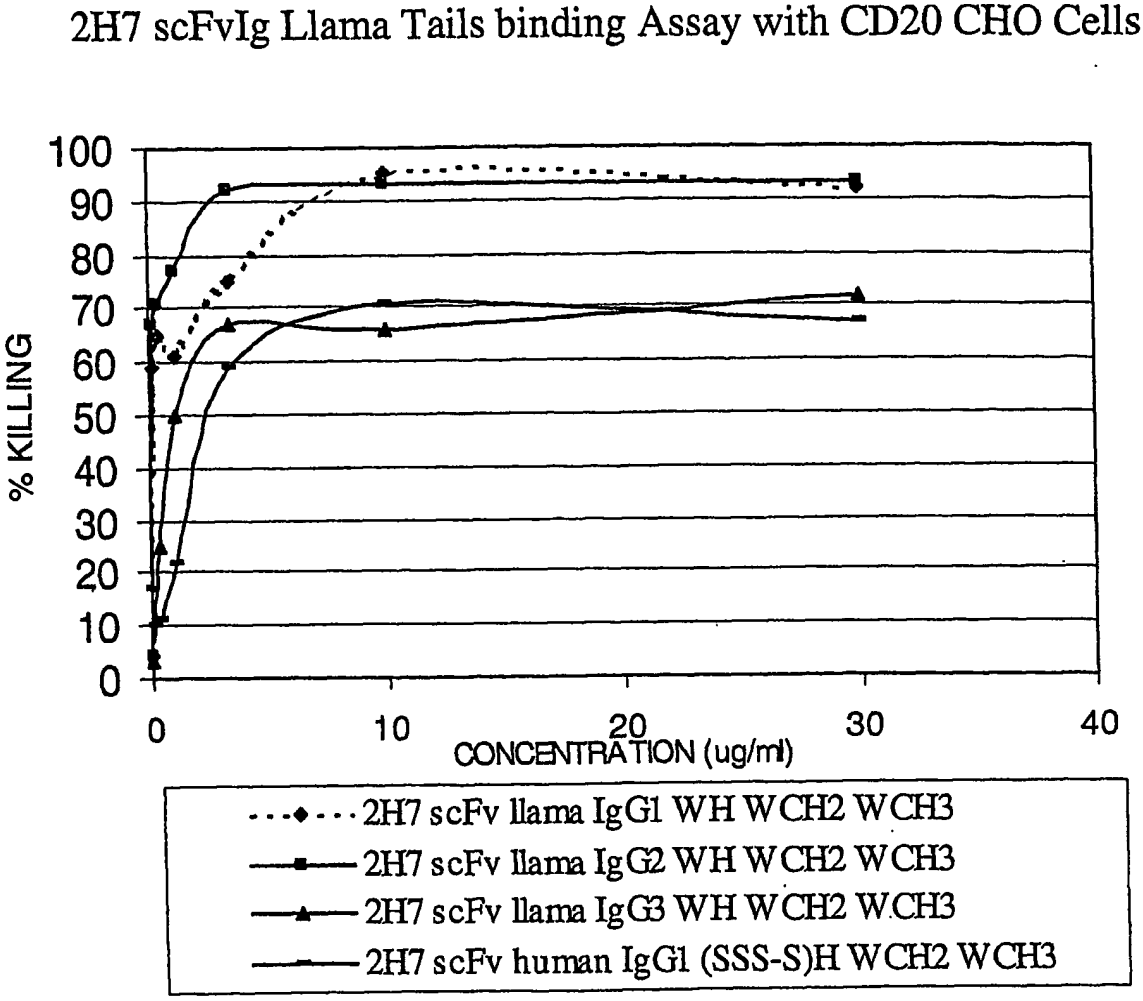
2H7 scFvIg Llama Tails binding Assay with CD20 CHO Cells
% KILLING
100
90
80
70
60
50
40
30
20
10
0
0
10
20
30
40
CONCENTRATION (ug/ml)
2H7 scFv llama IgG1 WH WCH2 WCH3
2H7 scFv llama IgG2 WH WCH2 WCH3
2H7 scFv llama IgG3 WH WCH2 WCH3
2H7 scFv human IgG1 (SSS-S)H WCH2 WCH3

Fig. 27

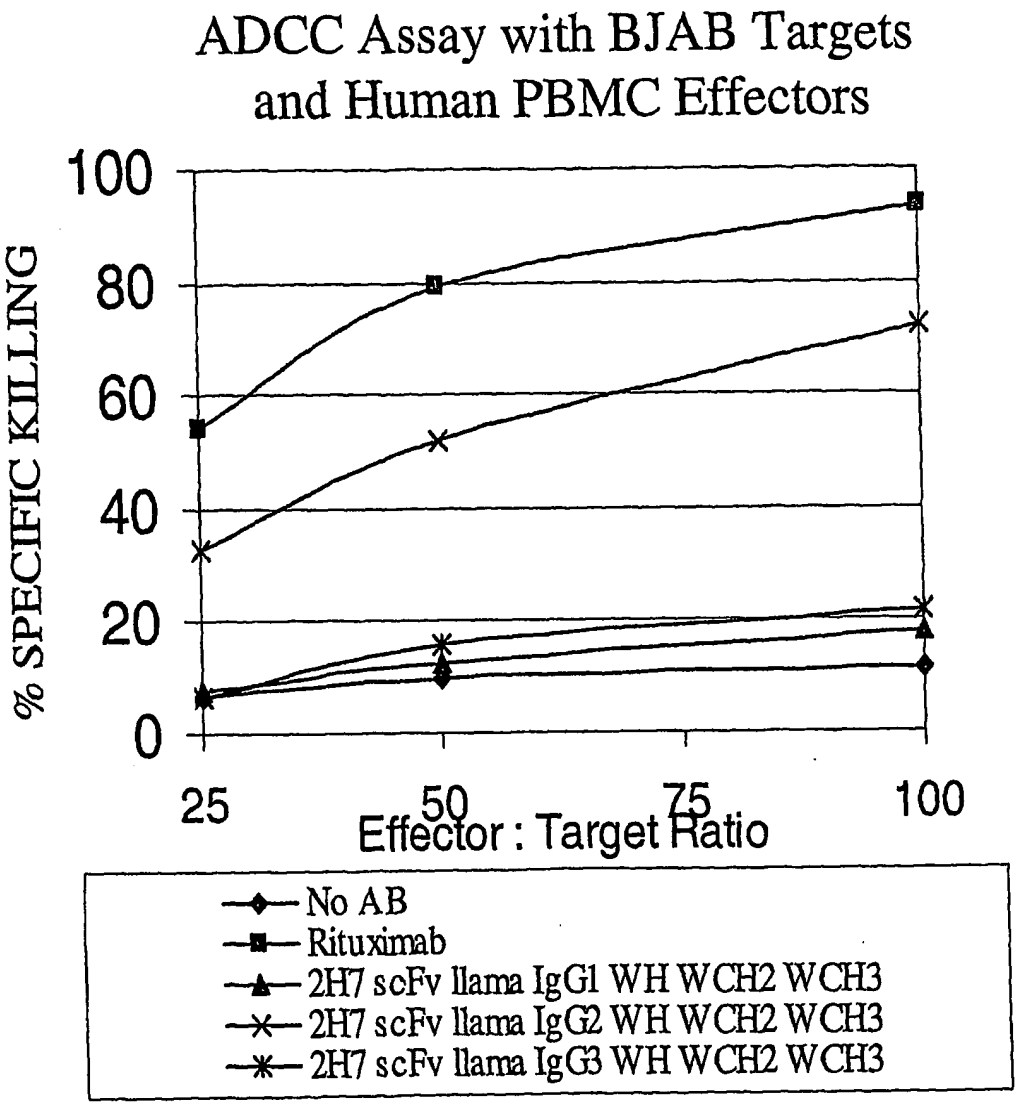
ADCC Assay with BJAB Targets and Human PBMC Effectors
% SPECIFIC KILLING
100
80
60
40
20
0
25
50
75
100
Effector : Target Ratio
No AB
Rituximab
2H7 scFv llama IgG1 WH WCH2 WCH3
2H7 scFv llama IgG2 WH WCH2 WCH3
2H7 scFv llama IgG3 WH WCH2 WCH3

Fig. 28

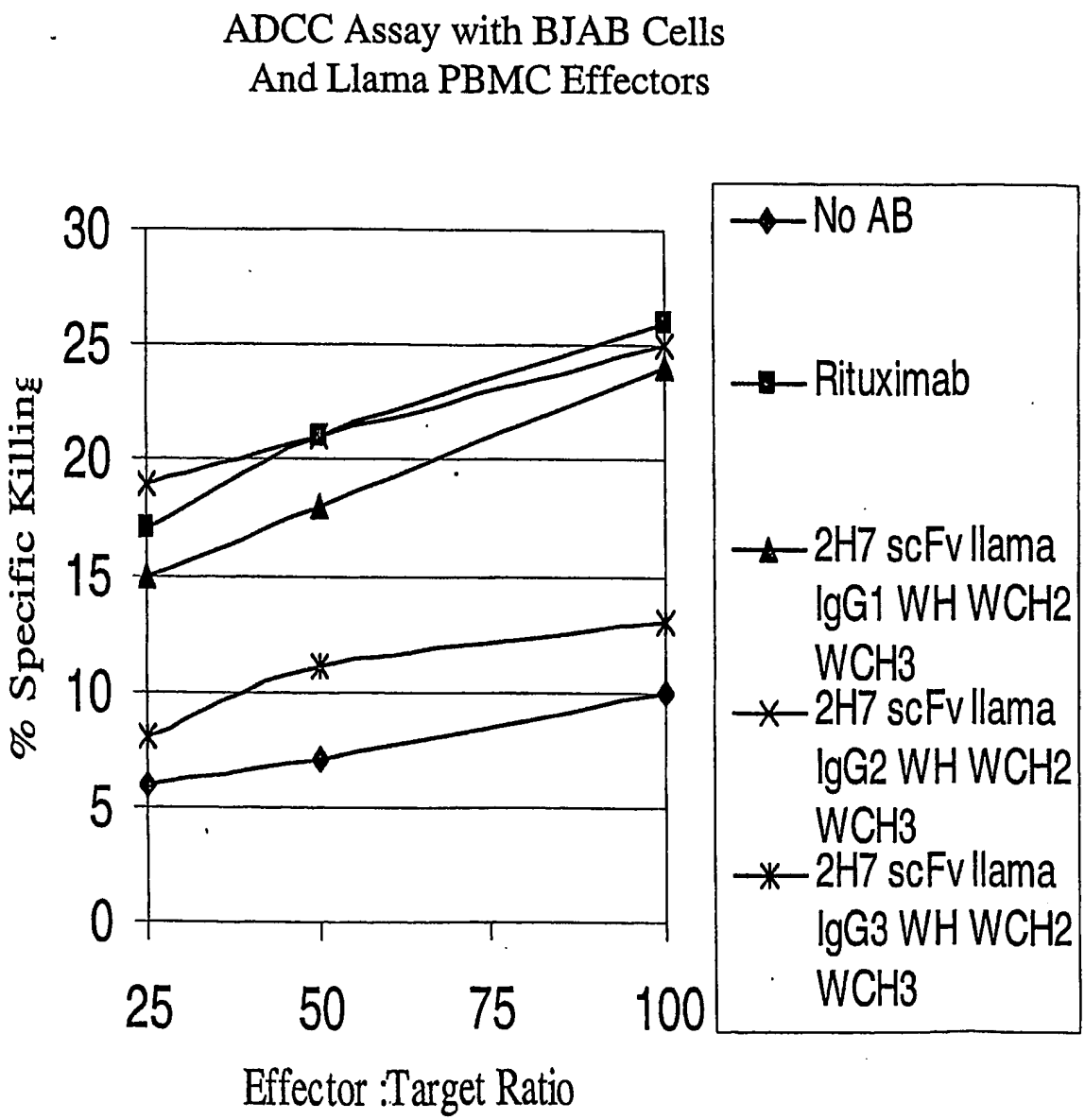
ADCC Assay with BJAB Cells
And Llama PBMC Effectors
% Specific Killing
30
25
20
15
10
5
0
25
50
75
100
Effector :Target Ratio
No AB
Rituximab
2H7 scFv llama IgG1 WH WCH2 WCH3
2H7 scFv llama IgG2 WH WCH2 WCH3
2H7 scFv llama IgG3 WH WCH2 WCH3

Fig. 29

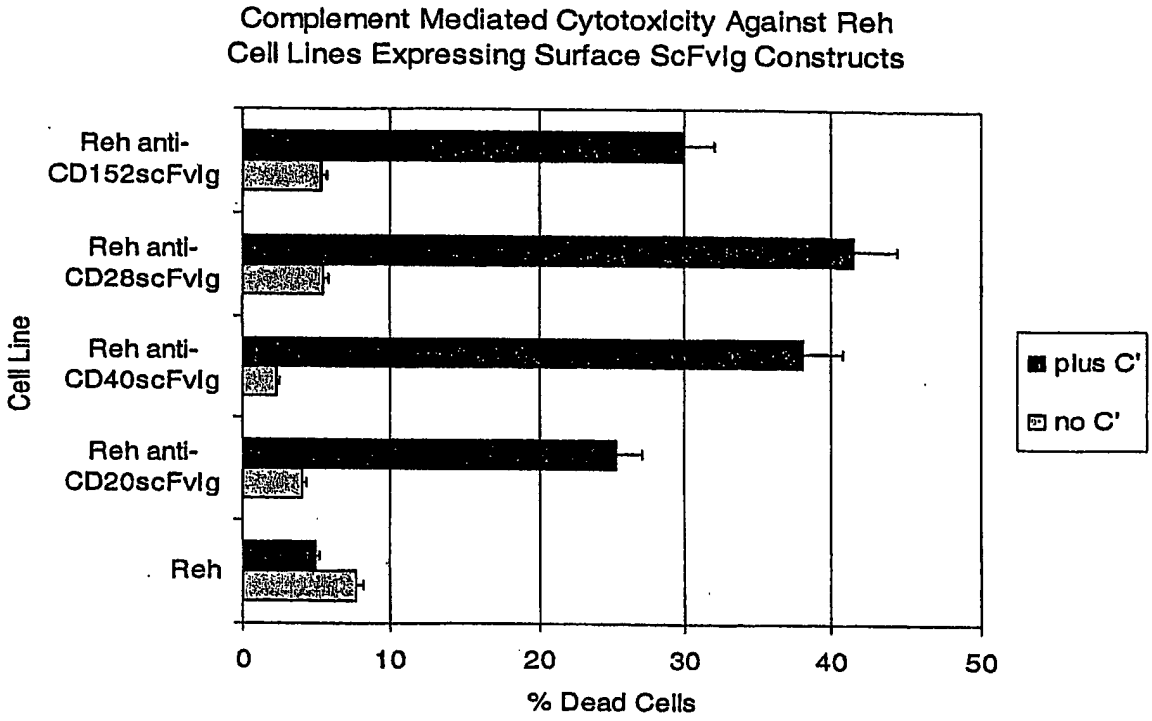

Surface scFvIg and Effector Functions

Fig. 30

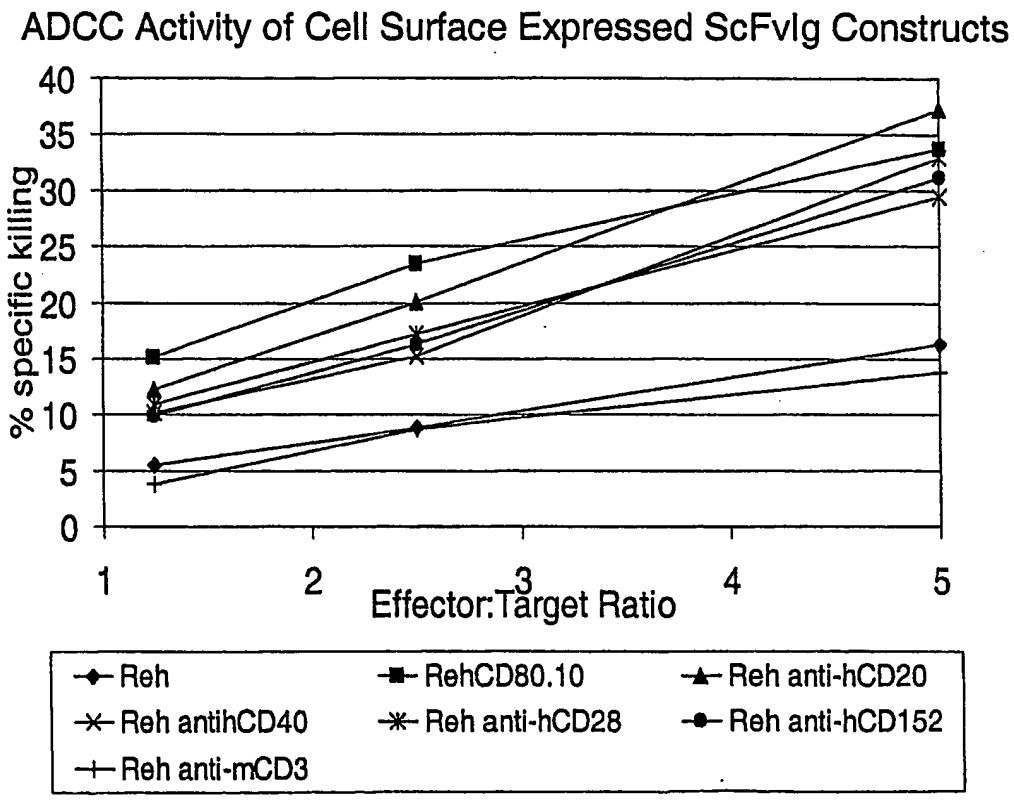

Surface scFvIg and Effector Functions

Fig. 31

Ig Constructs and Nomenclature:

Name Identifier	Hinge Sequence	CH2 Sequence	CH3 Sequence
hIgG1 (CCC-P)H WCH2 WCH3	IgG1 WT Hinge (CCC-P)	Wild Type CH2	Wild Type CH3
hIgG1 (SSS-S)H WCH2 WCH3	IgG1 Mutant Hinge (SSS-S)	Wild type CH2 (IgG1)	Wild type CH3 (IgG1)
VH L11S hIgG1 (SSS-S)H WCH2 WCH3	IgG1 Mutant Hinge (SSS-S)	Wild type CH2 (IgG1)	Wild type CH3 (IgG1)
IgG1 (SSC-S)H WCH2 WCH3	IgG1 Mutant Hinge (SSC-S)	Wild type CH2 (IgG1)	Wild type CH3 (IgG1)
IgG1 (SCS-S)H WCH2 WCH3	IgG1 Mutant Hinge (SCS-S)	Wild type CH2 (IgG1)	Wild type CH3 (IgG1)
IgG1 (CSS-S)H WCH2 WCH3	IgG1 Mutant Hinge (CSS-S)	Wild type CH2 (IgG1)	Wild type CH3 (IgG1)
IgG1 (SSS-S)H P238S CH2 WCH3	IgG1 Mutant Hinge (SSS-S)	Mutant CH2 (IgG1) Pro→Ser 238	Wild type CH3 (IgG1)
IgA WH hIgG1 WCH2 WCH3	IgA Hinge	Wild type CH2 (IgG1)	Wild type CH3 (IgG1)
IgA WH IgA WCH2 WCH3	IgA Hinge	Wild type CH2 (IgA)	Wild type CH3 (IgA)
IgA WH IgA WCH2 T4CH3	IgA Hinge	Wild type CH2 (IgA)	Truncated CH3 (IgA) Missing 4 aa at COOH

Fig. 32

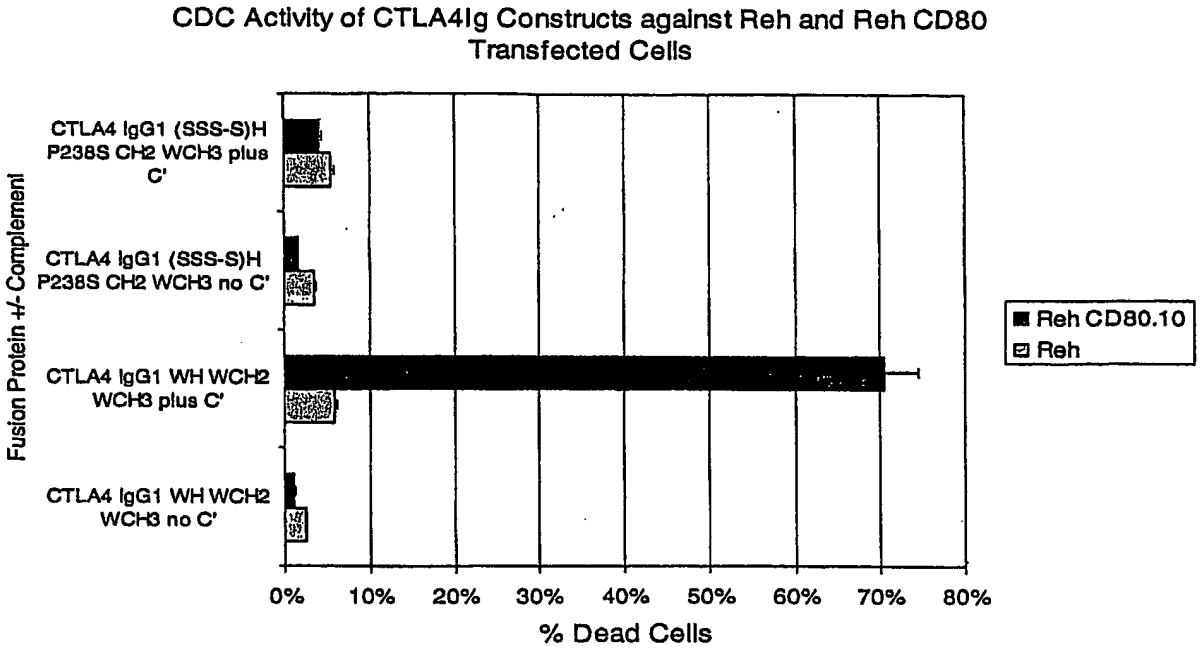
CDC Activity of CTLA4Ig Constructs against Reh and Reh CD80 Transfected Cells
CTLA4 IgG1 (SSS-S)H P238S CH2 WCH3 plus C'
CTLA4 IgG1 (SSS-S)H P238S CH2 WCH3 no C'
CTLA4 IgG1 WH WCH2 WCH3 plus C'
CTLA4 IgG1 WH WCH2 WCH3 no C'
Fusion Protein +/- Complement
0%
10%
20%
30%
40%
50%
60%
70%
80%
% Dead Cells
Reh CD80.10
Reh

Fig. 33

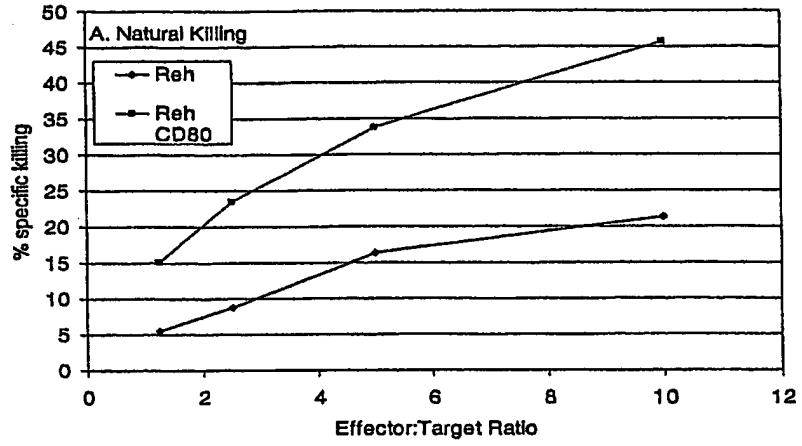
A. Natural Killing
Reh
Reh CD80
% specific killing
Effector:Target Ratio

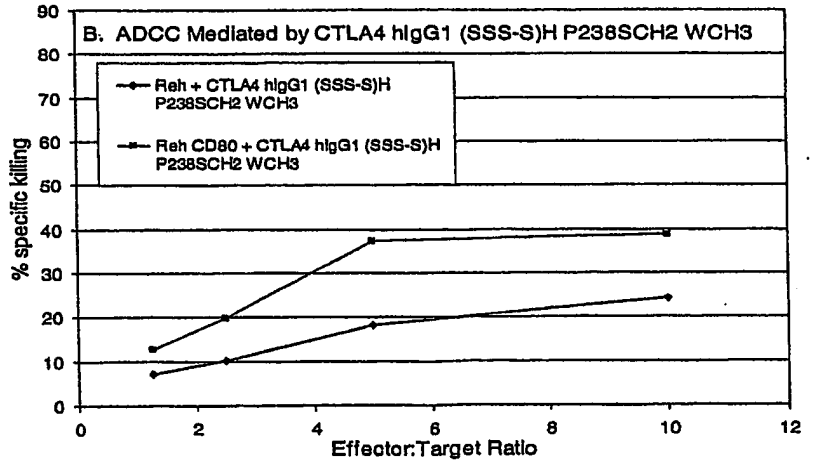
B. ADCC Mediated by CTLA4 hIgG1 (SSS-S)H P238SCH2 WCH3
Reh + CTLA4 hIgG1 (SSS-S)H P238SCH2 WCH3
Reh CD80 + CTLA4 hIgG1 (SSS-S)H P238SCH2 WCH3
% specific killing
Effector:Target Ratio

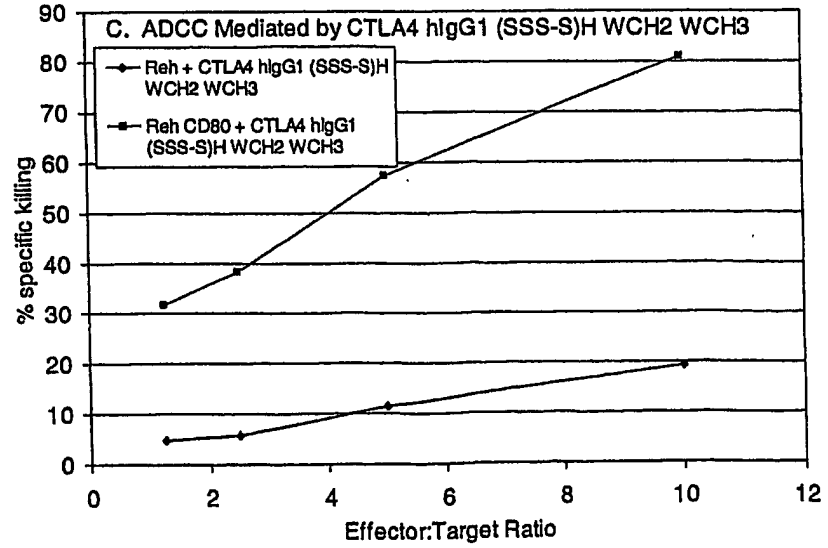
C. ADCC Mediated by CTLA4 hIgG1 (SSS-S)H WCH2 WCH3
Reh + CTLA4 hIgG1 (SSS-S)H WCH2 WCH3
Reh CD80 + CTLA4 hIgG1 (SSS-S)H WCH2 WCH3
% specific killing
Effector:Target Ratio

Fig. 34

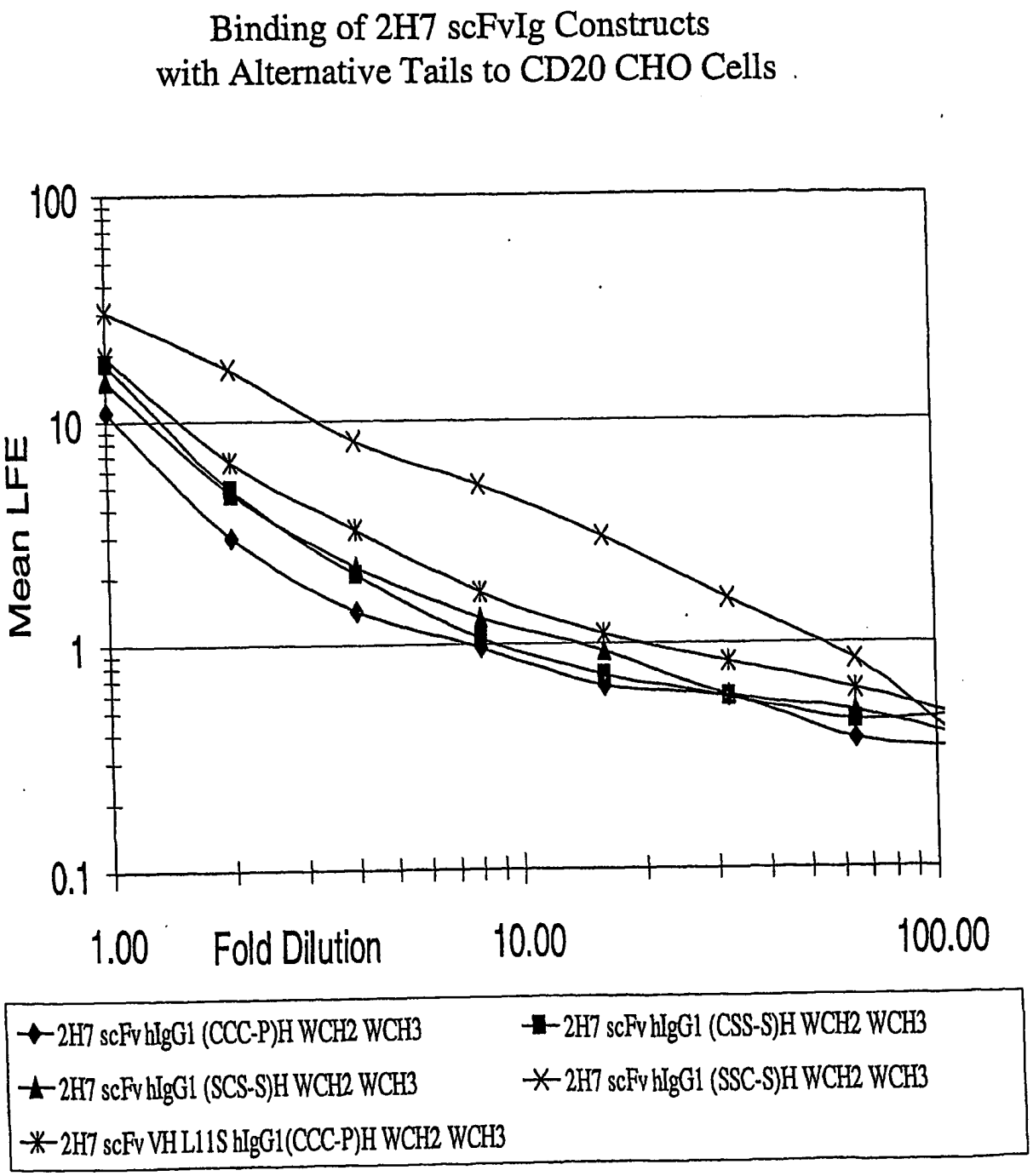
Binding of 2H7 scFvIg Constructs
with Alternative Tails to CD20 CHO Cells
100
10
1
0.1
Mean LFE
1.00
Fold Dilution
10.00
100.00
2H7 scFv hIgG1 (CCC-P)H WCH2 WCH3
2H7 scFv hIgG1 (CSS-S)H WCH2 WCH3
2H7 scFv hIgG1 (SCS-S)H WCH2 WCH3
2H7 scFv hIgG1 (SSC-S)H WCH2 WCH3
2H7 scFv VH L11S hIgG1(CCC-P)H WCH2 WCH3

Fig. 35

Immunoblot Analysis of protein immunoprecipitates from COS transfections of 2H7 scFvIg Constructs

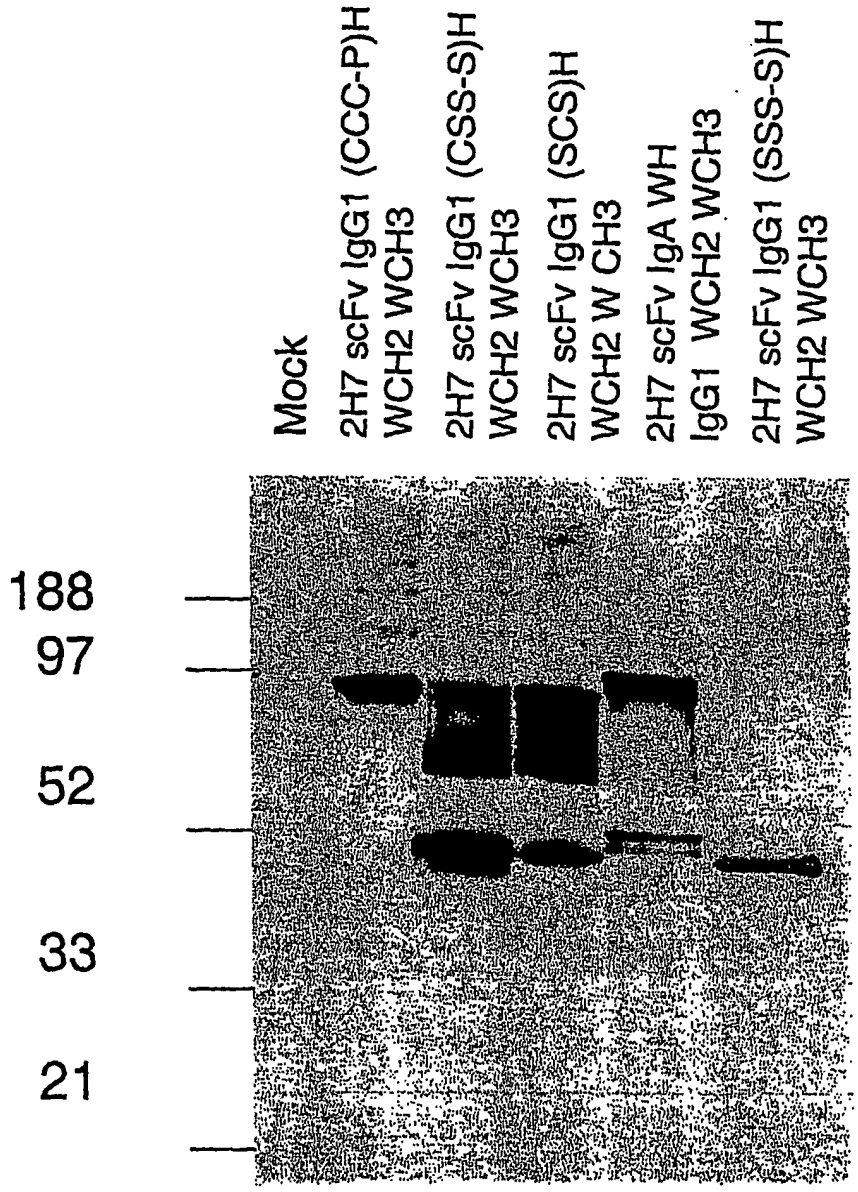

Fig. 36

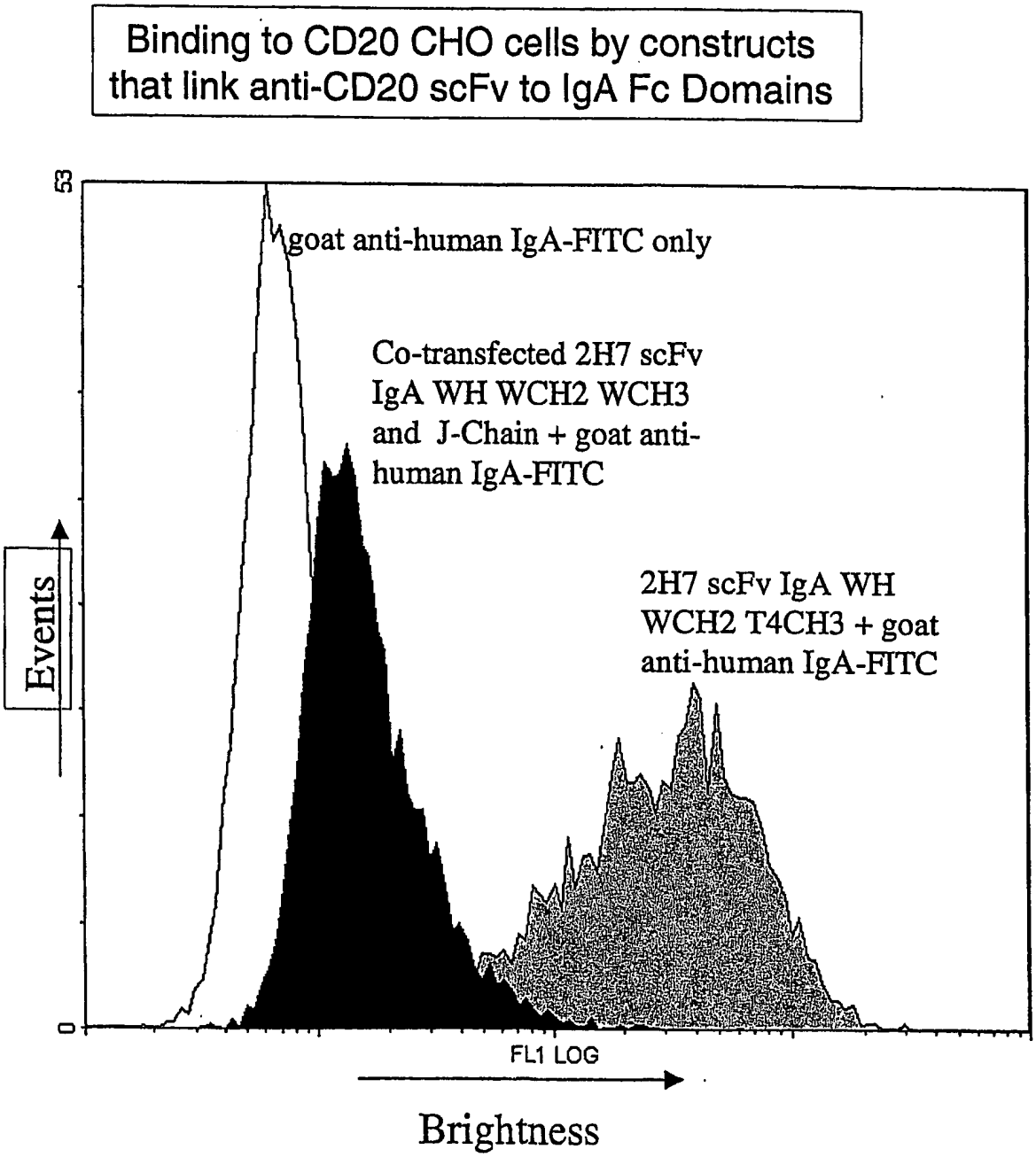
Binding to CD20 CHO cells by constructs that link anti-CD20 scFv to IgA Fc Domains
53
0
Events
goat anti-human IgA-FITC only
Co-transfected 2H7 scFv IgA WH WCH2 WCH3 and J-Chain + goat anti-human IgA-FITC
2H7 scFv IgA WH WCH2 T4CH3 + goat anti-human IgA-FITC
FL1 LOG
Brightness

Fig. 37

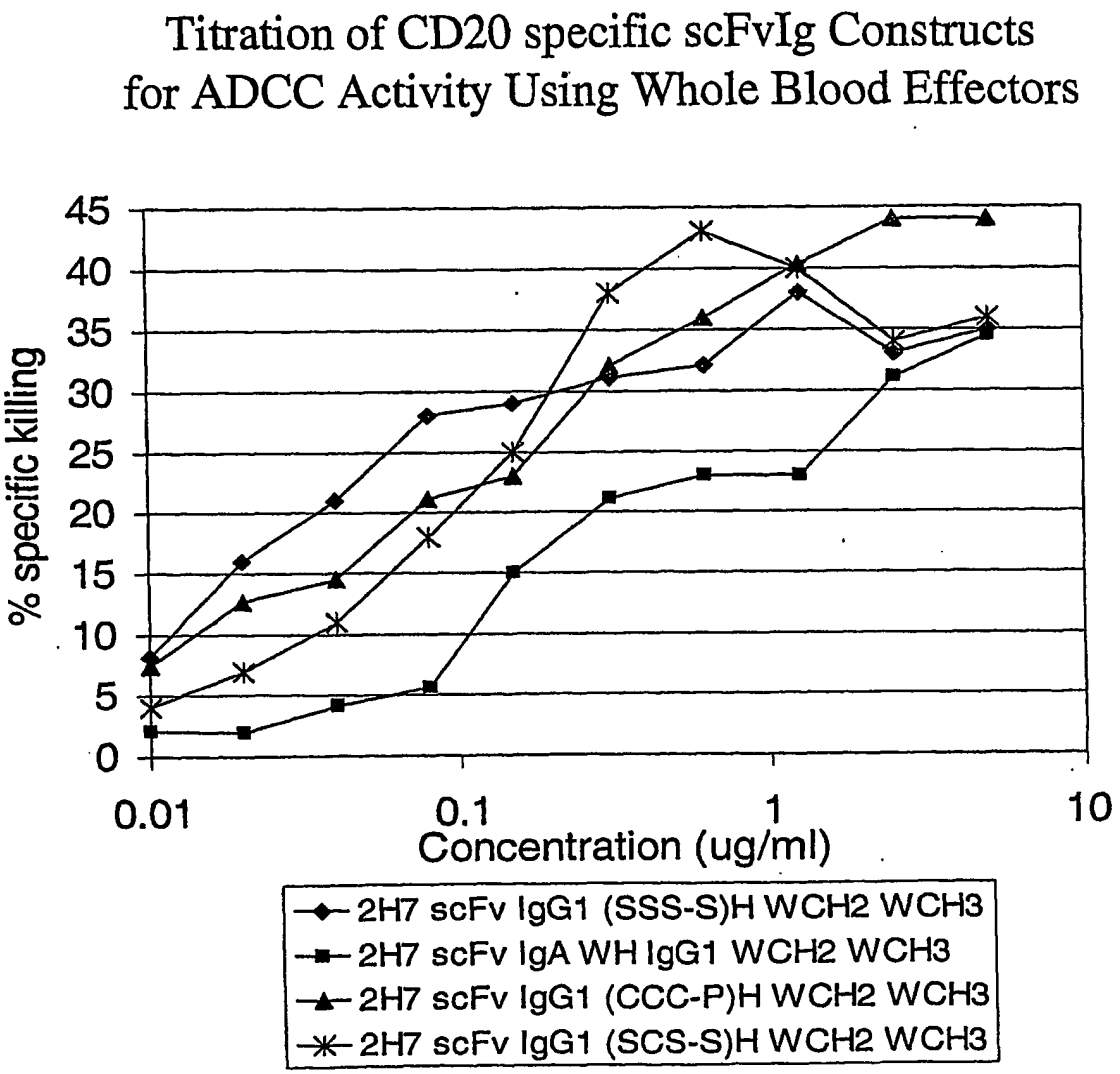
Titration of CD20 specific scFvIg Constructs
for ADCC Activity Using Whole Blood Effectors
% specific killing
45
40
35
30
25
20
15
10
5
0
0.01
0.1
1
10
Concentration (ug/ml)
2H7 scFv IgG1 (SSS-S)H WCH2 WCH3
2H7 scFv IgA WH IgG1 WCH2 WCH3
2H7 scFv IgG1 (CCC-P)H WCH2 WCH3
2H7 scFv IgG1 (SCS-S)H WCH2 WCH3

Fig. 38

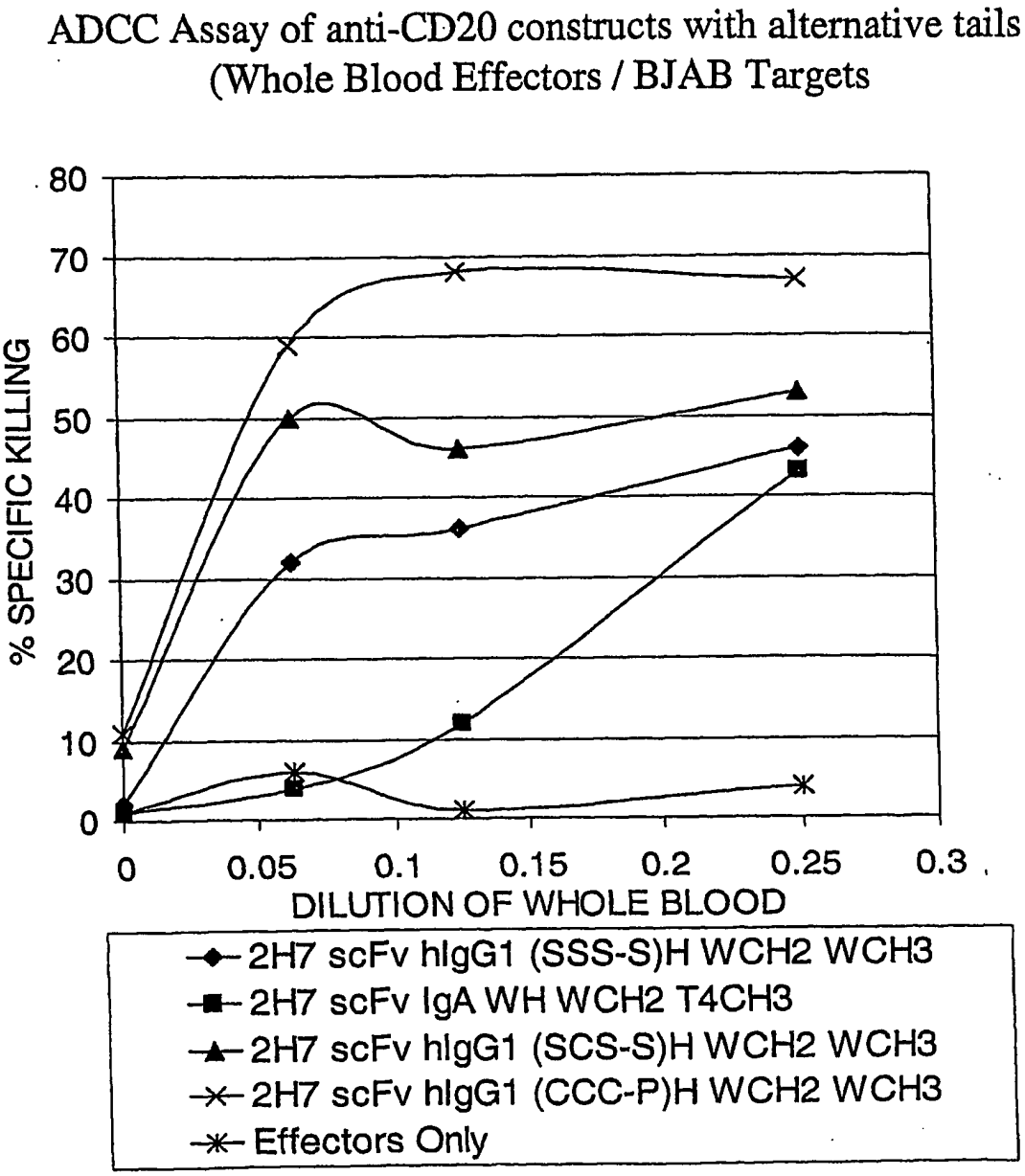
ADCC Assay of anti-CD20 constructs with alternative tails
(Whole Blood Effectors / BJAB Targets
% SPECIFIC KILLING
80
70
60
50
40
30
20
10
0
0
0.05
0.1
0.15
0.2
0.25
0.3
DILUTION OF WHOLE BLOOD
2H7 scFv hIgG1 (SSS-S)H WCH2 WCH3
2H7 scFv IgA WH WCH2 T4CH3
2H7 scFv hIgG1 (SCS-S)H WCH2 WCH3
2H7 scFv hIgG1 (CCC-P)H WCH2 WCH3
Effectors Only

Fig. 39

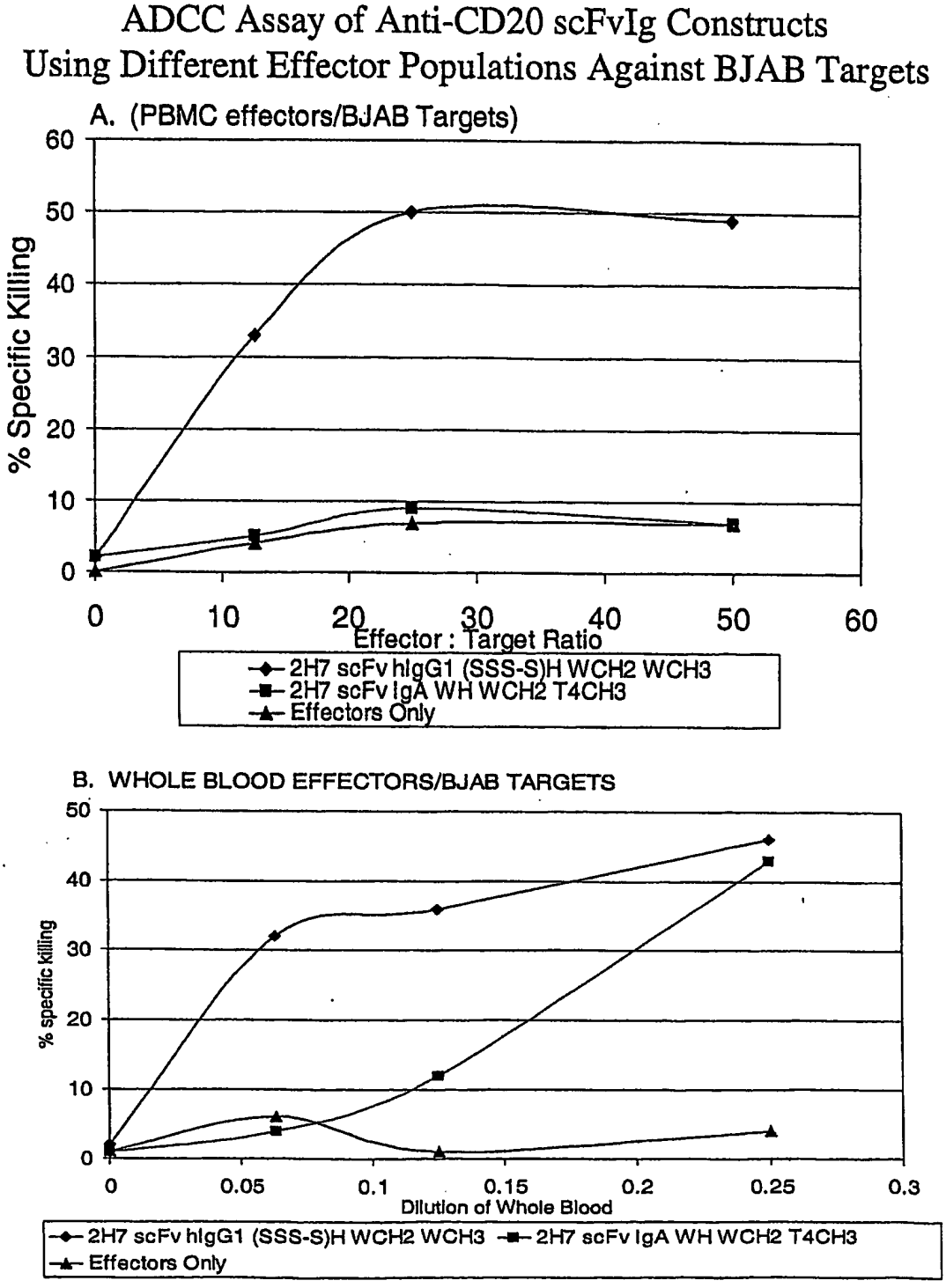
ADCC Assay of Anti-CD20 scFvIg Constructs
Using Different Effector Populations Against BJAB Targets
A. (PBMC effectors/BJAB Targets)
% Specific Killing
Effector : Target Ratio
2H7 scFv hIgG1 (SSS-S)H WCH2 WCH3
2H7 scFv IgA WH WCH2 T4CH3
Effectors Only
B. WHOLE BLOOD EFFECTORS/BJAB TARGETS
% specific killing
Dilution of Whole Blood
2H7 scFv hIgG1 (SSS-S)H WCH2 WCH3
2H7 scFv IgA WH WCH2 T4CH3
Effectors Only

Fig. 40

Immunoblot of 2H7 scFv Ig constructs from COS Transfections (1 µl/well) compared to a Concentration Standard

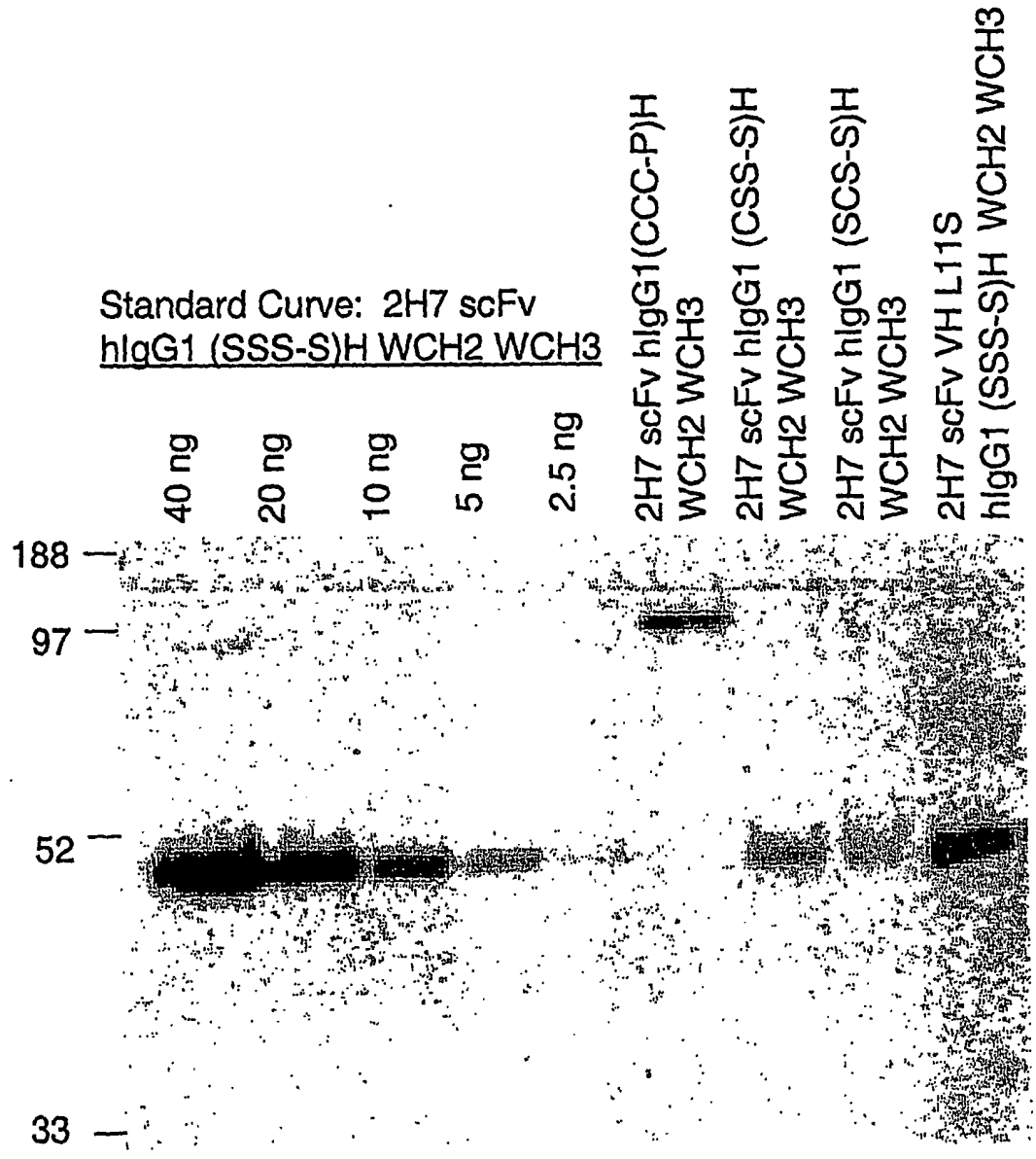

Figures 41A, 41B and 41C

A.

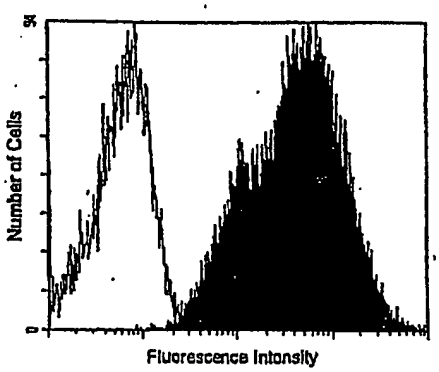

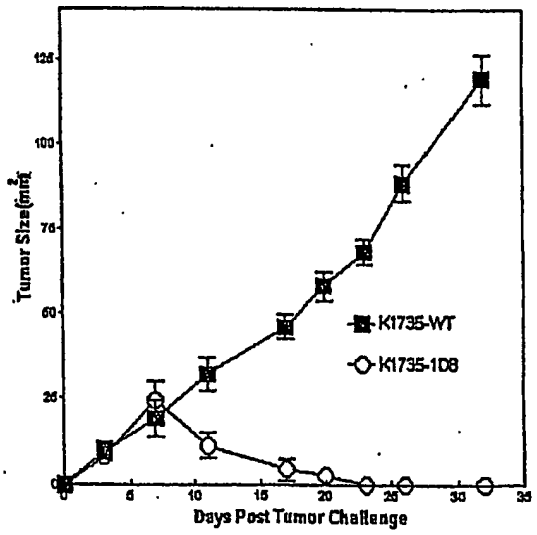

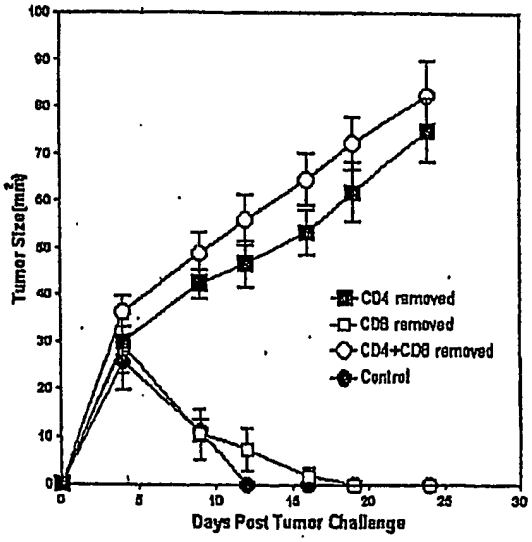

B.

C.

Fig. 42

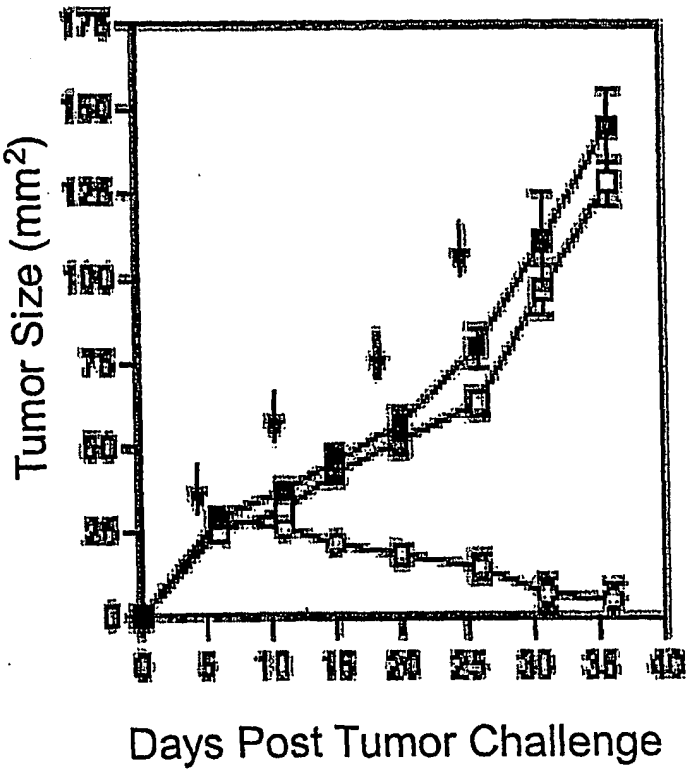
Tumor Size (mm2)
175
150
125
100
75
50
25
0
0
5
10
15
20
25
30
35
40
Days Post Tumor Challenge

Fig. 43

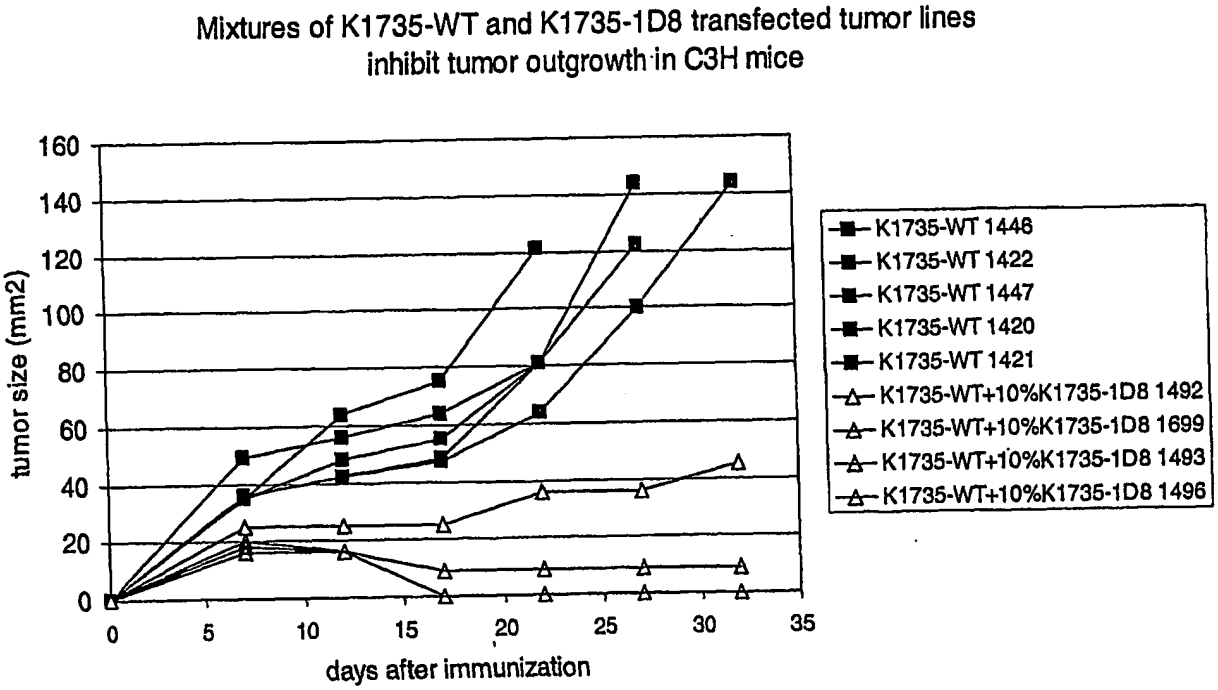
Mixtures of K1735-WT and K1735-1D8 transfected tumor lines inhibit tumor outgrowth in C3H mice
tumor size (mm2)
160
140
120
100
80
60
40
20
0
0
5
10
15
20
25
30
35
days after immunization
K1735-WT 1446
K1735-WT 1422
K1735-WT 1447
K1735-WT 1420
K1735-WT 1421
K1735-WT+10%K1735-1D8 1492
K1735-WT+10%K1735-1D8 1699
K1735-WT+10%K1735-1D8 1493
K1735-WT+10%K1735-1D8 1496

Fig. 44

Expression of anti-mouse CD137 (1D8) scFv-hIgG1 (SSS-S)H P238SCH2 WCH3
On the surface of panned Ag104-1D8 Transfected Tumor Cells

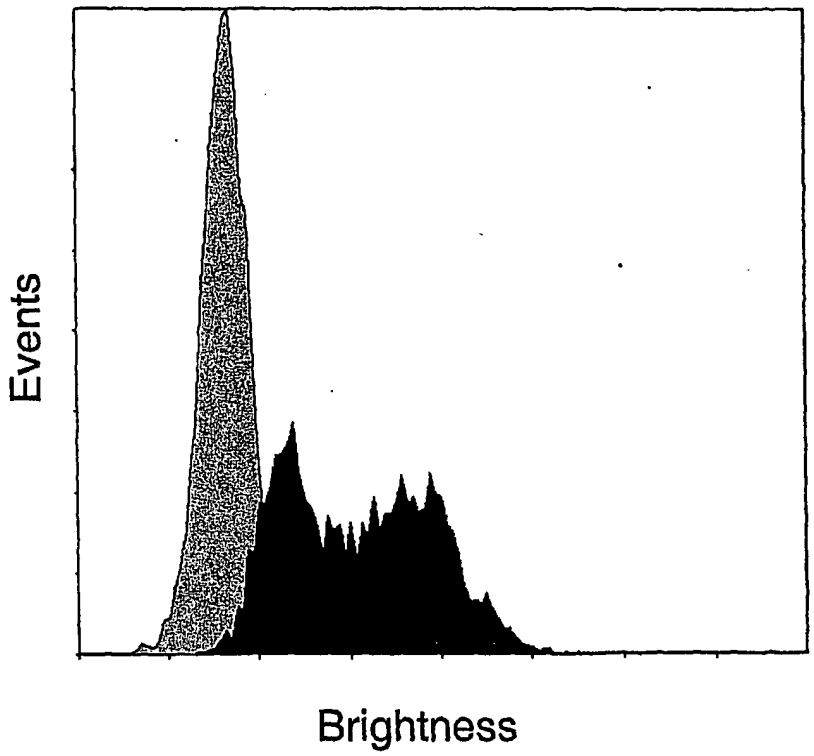

Fig. 45

Coomassie Stained SDS-PAGE Gel of 2H7 scFv Ig Constructs

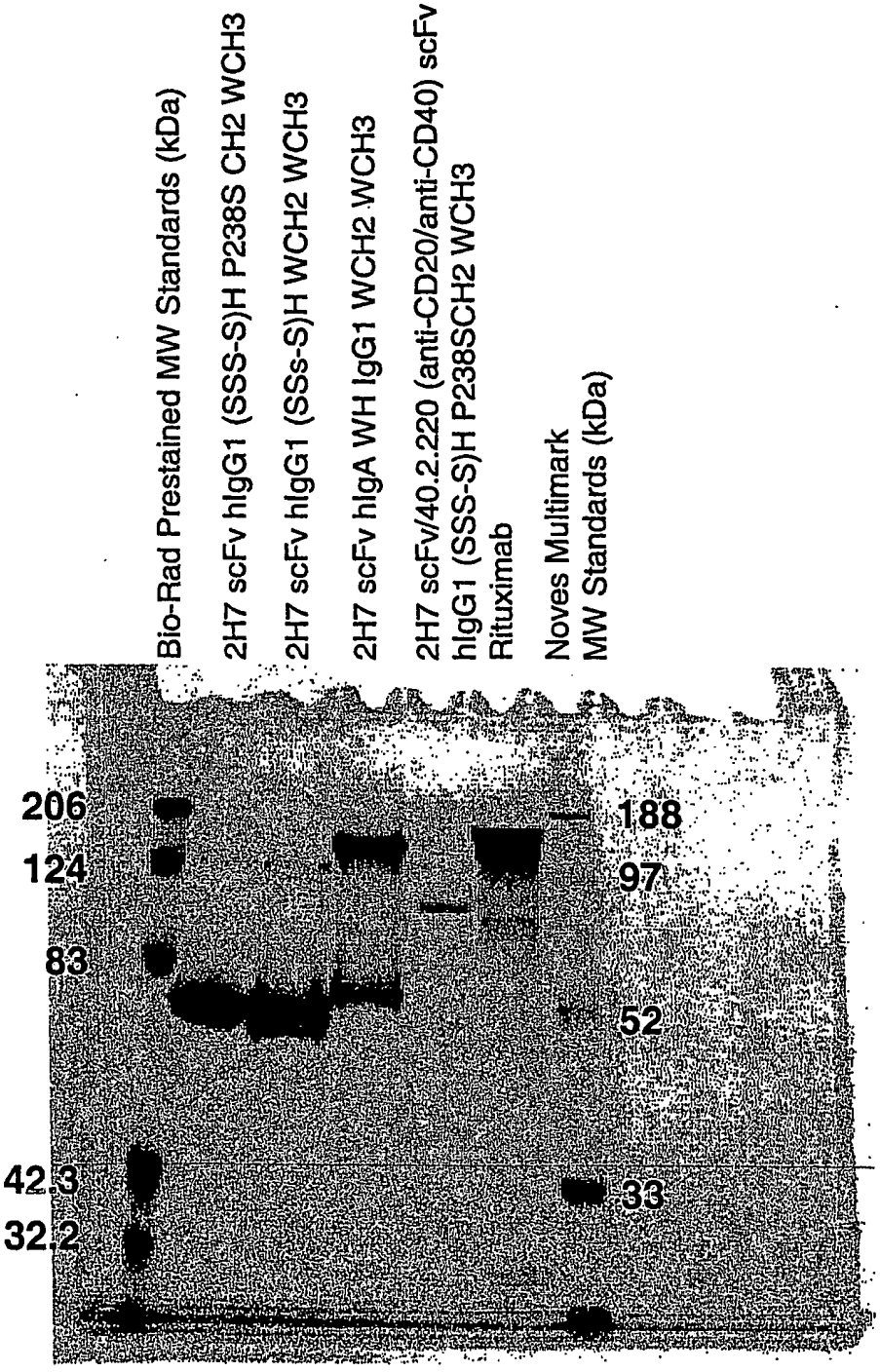

Fig. 46

ADCC mediated by 2H7 scFvIg Constructs by human PBMC effector cells against Bjab targets

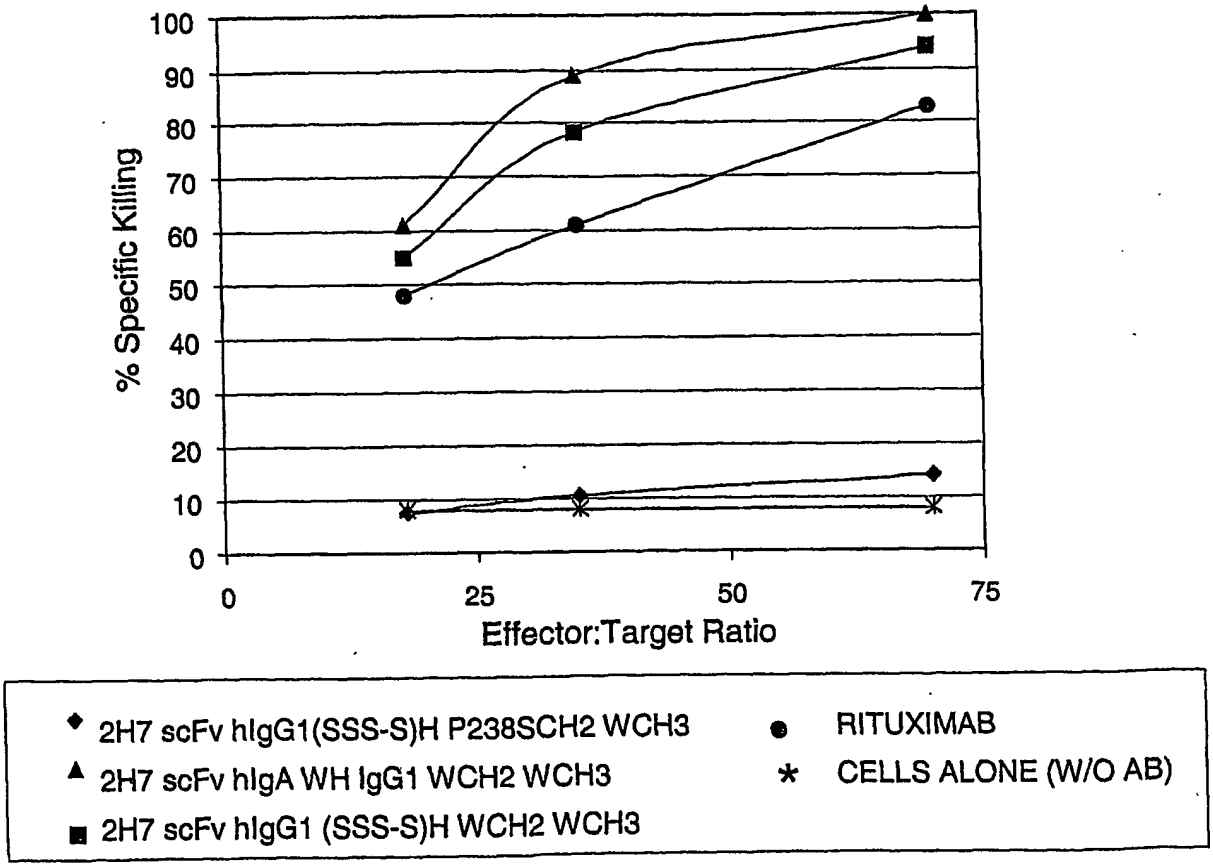

Fig. 47

Cell surface expression of anti-human CD3 G19-4 scFv hIgG1 (SSS-S)H P238SCH2 WCH3-hCD80TM/CT on Reh and T51 Cells.

Reh anti-CD3 (G19-4) scFv hIgG1 (SSS-S)H P238SCH2 WCH3-hCD80TM/CT

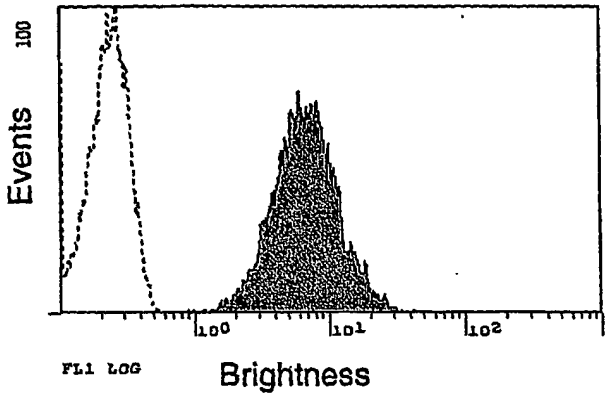

T51 G19-4 scFv hIgG1 (SSS-S)H P238SCH2 WCH3-hCD80TM/CT:

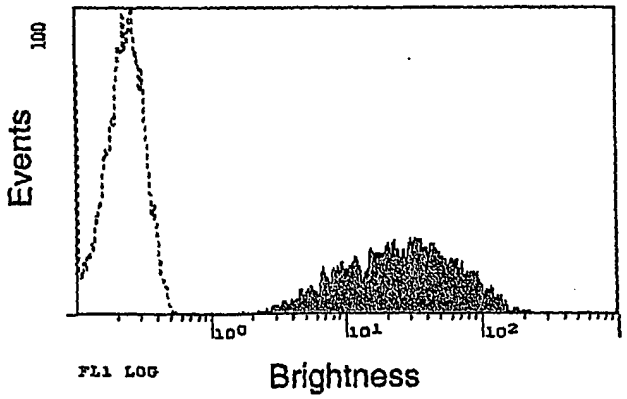

Figure 48.

Targeting of Cytotoxicity to Transfected Cell Lines by Surface expression of CD3 scFvIg

A

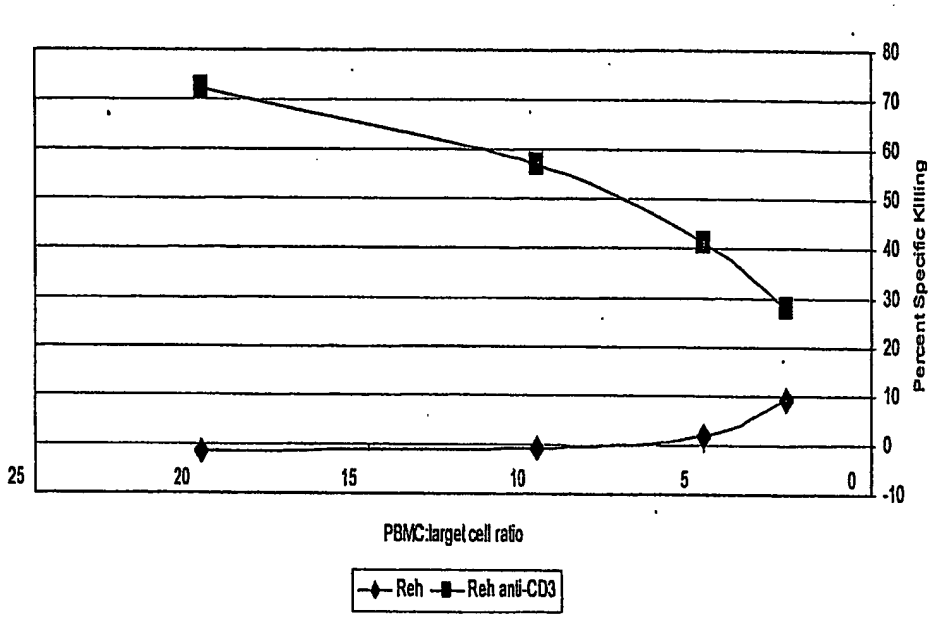

B

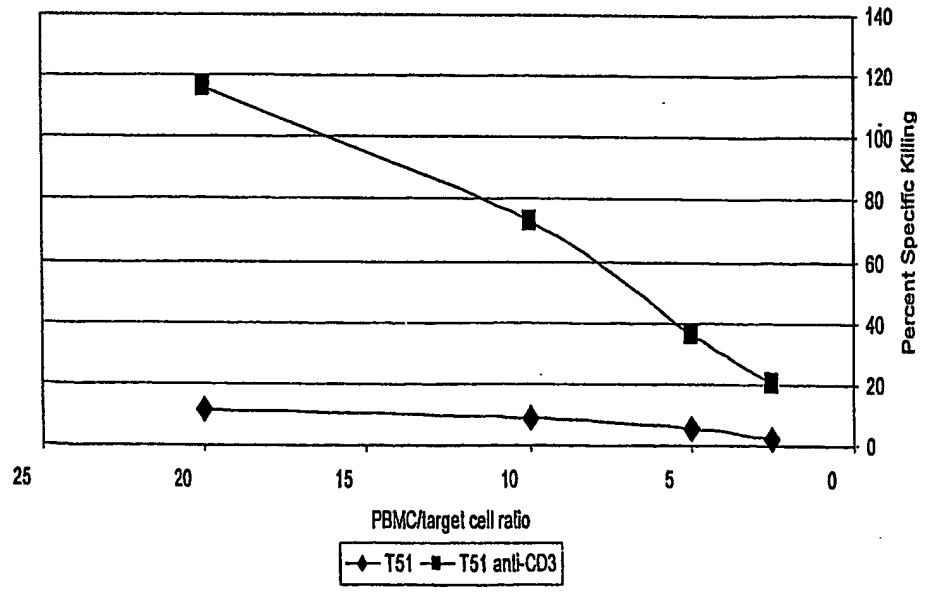

Fig. 49

Binding of 5B9, a mouse anti-human CD137 scFv hIgG1 (SSS-S)H WCH2WCH3 to stimulated human PBMC

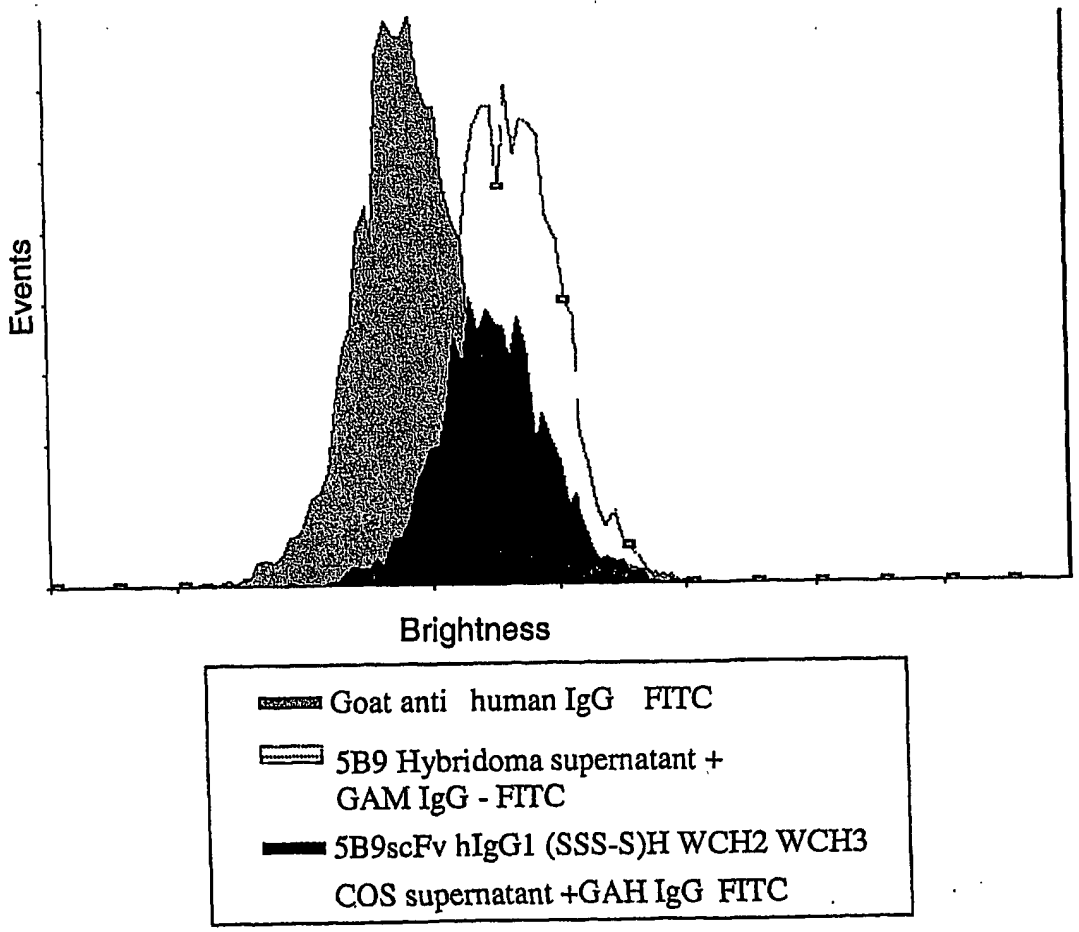

Fig. 50

Effect of V_HL11S Mutation on CytoxB20
2H7 scFv hIgG1 (SSS-S)H WCH2 WCH3 Protein Expression

50A. Standard Curve: 2H7VH-L11S-IgG1 (SSS-S)H WCH2 WCH3

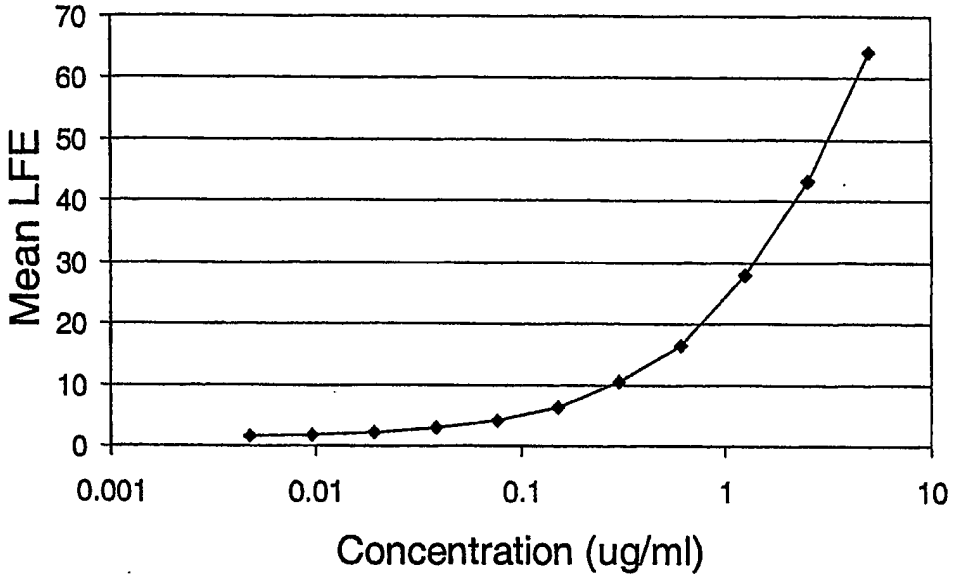

50B. CHO supernatant Brightness and Estimation of Protein concentrations from Standard Curve:

	CHO clone name				
	4F2	**4F5**	**3E5**	**6B11A**	**2B8A**
Mean LFE					
1/100	71.7	40.6	31.5	99.7	101.5
1/500	27.1	12.4	11.2	40.8	43
approx conc. µg/ml	**600**	**225**	**125**	**1000**	**1250**

Fig. 51

Production Levels of 2H7scFv VH L11S hIgG1 (SSS-S)H WCH2 WCH3 From CHO Clone Culture Supernatants

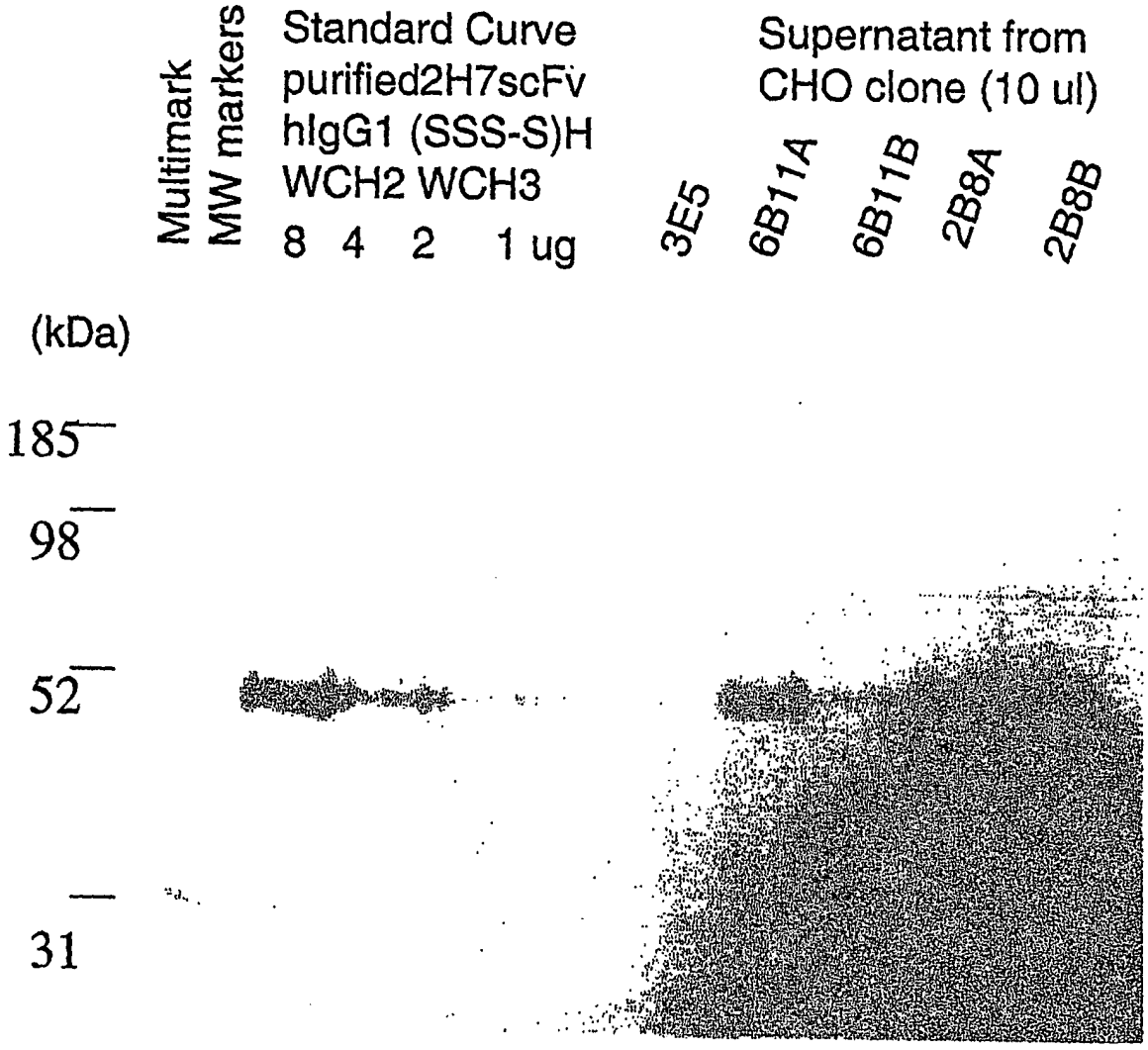

Fig. 52

Effect of VHL11S Mutation on G28-1 scFvIg Construct Protein Production from COS cells

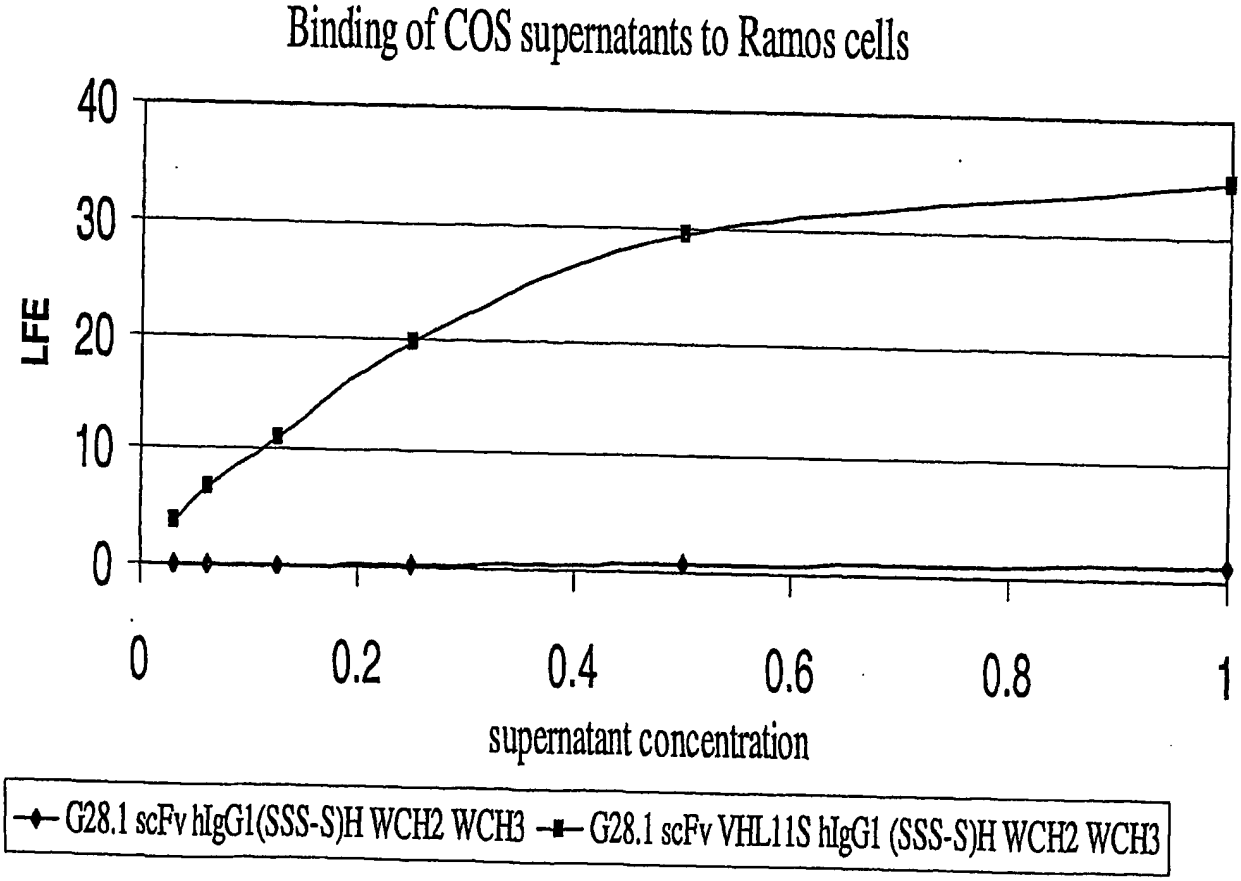

Fig. 53

Immunoblot of G28-1 scFvIg Constructs

Increased Protein Levels in COS supernatants
transfected with G28-1scFv hIgG1 (SSS-S)H WCH2 WCH3
After Substitution of Leucine with Serine at position 11 of VH (VHL11S)

Fig. 53A.

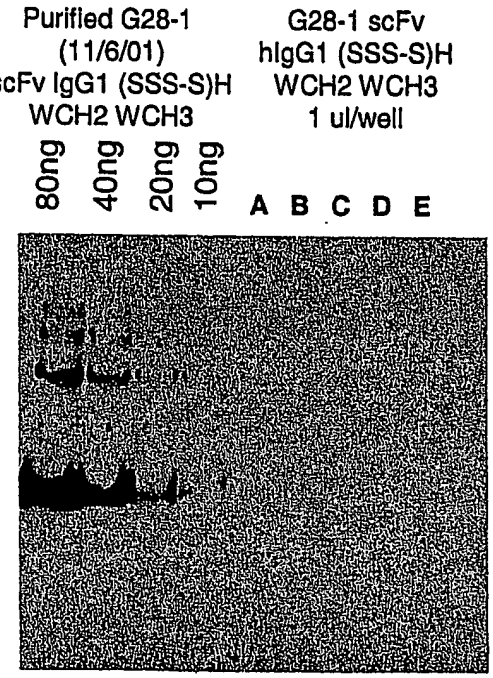

Fig. 53B.

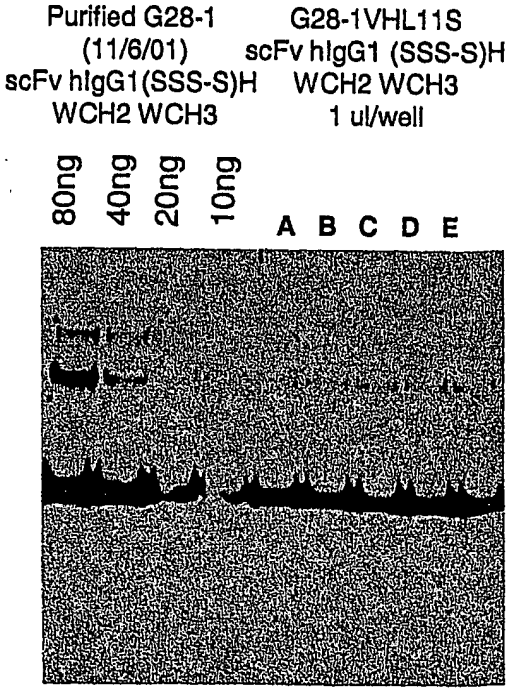

Fig. 54

Binding of 2H7 scFvIg Constructs with Altered Hinges and CH3 domains to CD20 CHO Cells

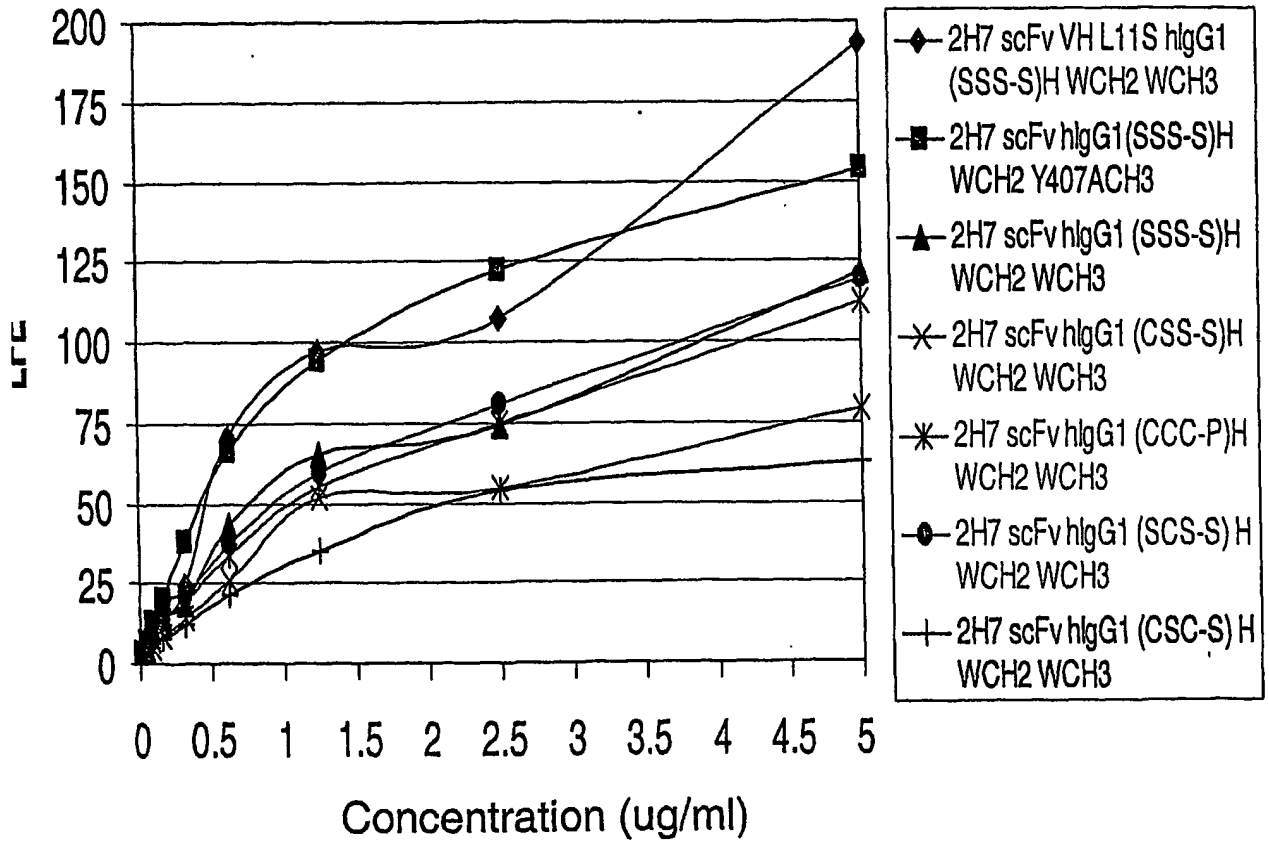

Fig. 55

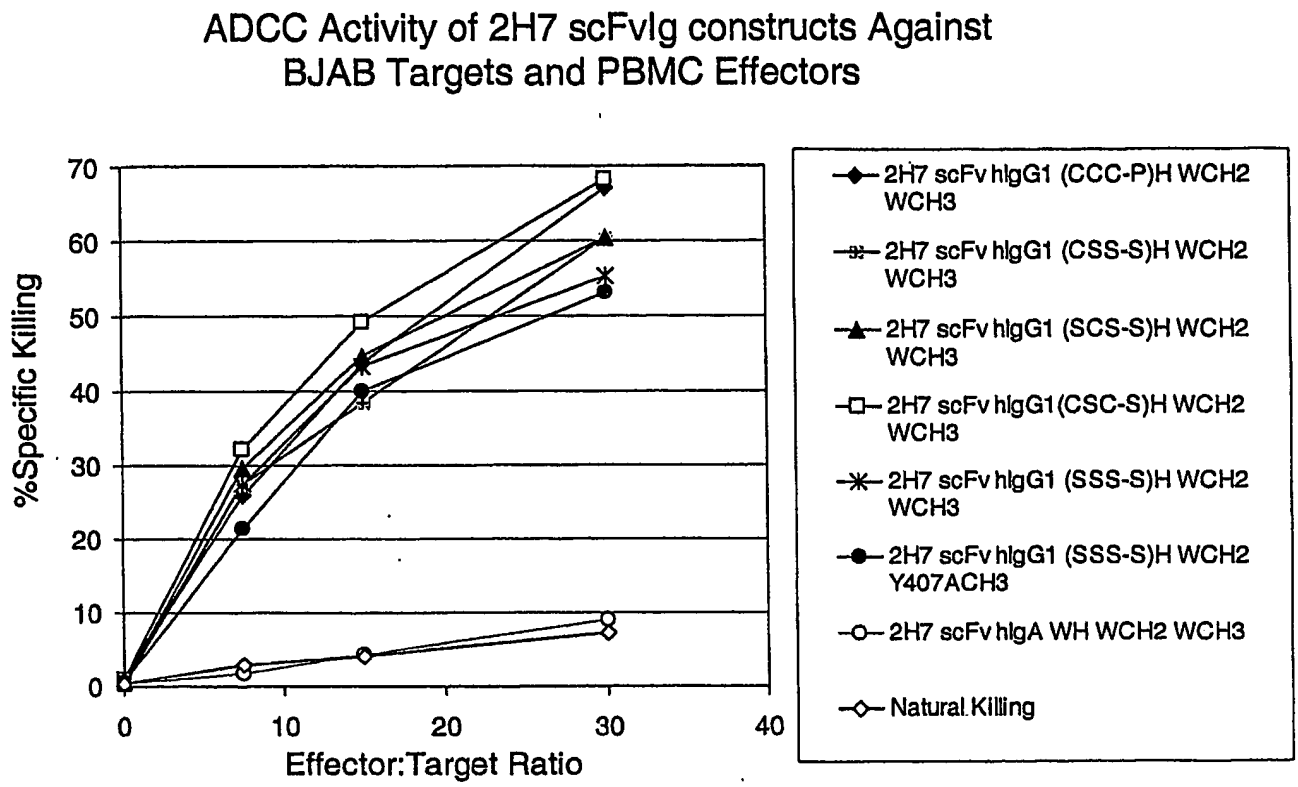
ADCC Activity of 2H7 scFvIg constructs Against BJAB Targets and PBMC Effectors
%Specific Killing
Effector:Target Ratio
0
10
20
30
40
50
60
70
2H7 scFv hIgG1 (CCC-P)H WCH2 WCH3
2H7 scFv hIgG1 (CSS-S)H WCH2 WCH3
2H7 scFv hIgG1 (SCS-S)H WCH2 WCH3
2H7 scFv hIgG1(CSC-S)H WCH2 WCH3
2H7 scFv hIgG1 (SSS-S)H WCH2 WCH3
2H7 scFv hIgG1 (SSS-S)H WCH2 Y407ACH3
2H7 scFv hIgA WH WCH2 WCH3
Natural Killing

Fig. 56

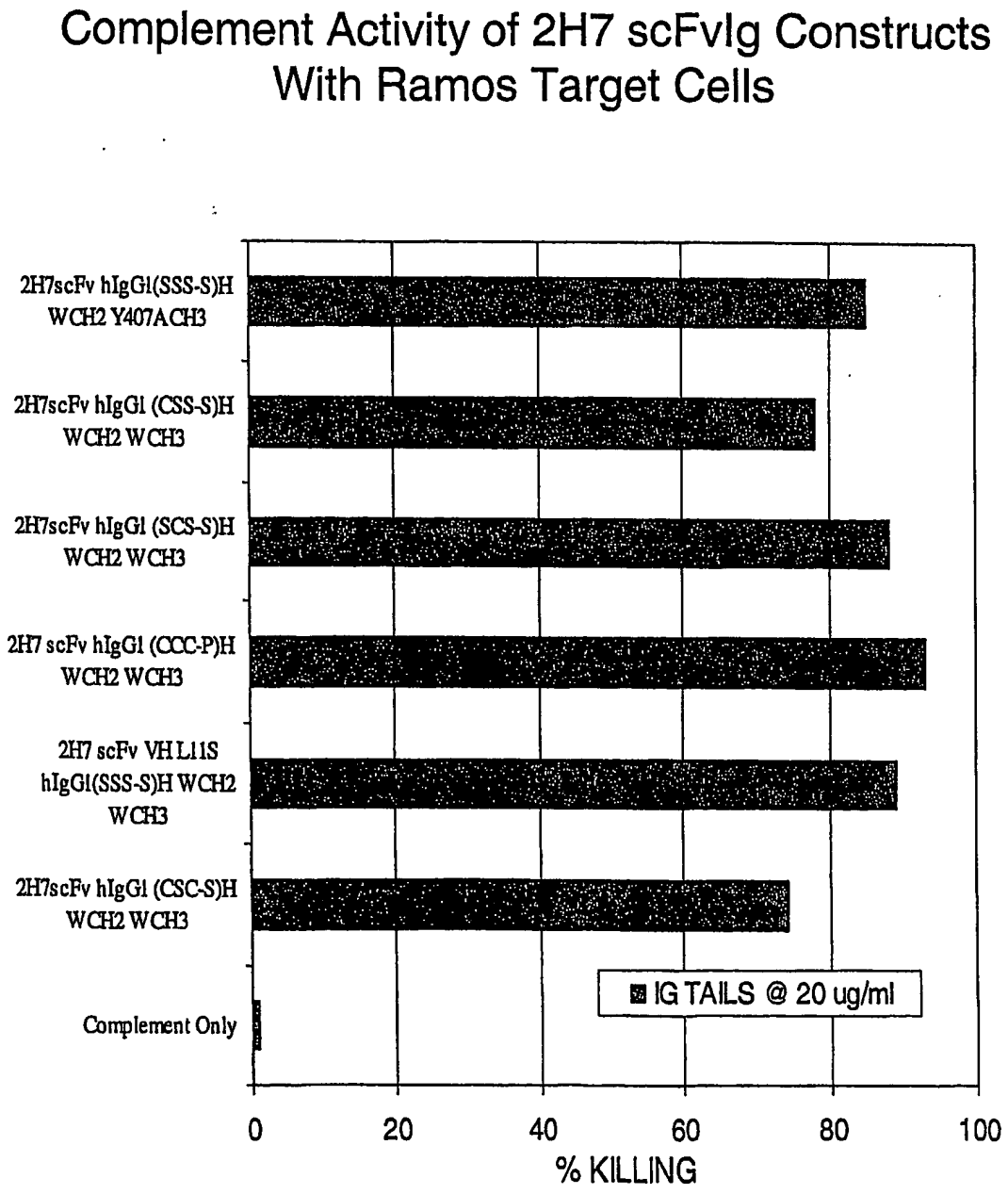
Complement Activity of 2H7 scFvIg Constructs With Ramos Target Cells
2H7scFv hIgG1(SSS-S)H WCH2 Y407ACH3
2H7scFv hIgG1 (CSS-S)H WCH2 WCH3
2H7scFv hIgG1 (SCS-S)H WCH2 WCH3
2H7 scFv hIgG1 (CCC-P)H WCH2 WCH3
2H7 scFv VH L11S hIgG1(SSS-S)H WCH2 WCH3
2H7scFv hIgG1 (CSC-S)H WCH2 WCH3
Complement Only
IG TAILS @ 20 ug/ml
0
20
40
60
80
100
% KILLING

Fig. 57

Binding of 2H7 scFvIg Derivatives to CD20CHO Cells

A. No fusion protein

B. 2H7 scFv hIgE CH2CH3CH4

C. 2H7 scFv hIgA WH WCH2 WCH3

D. 2H7 scFv hIgG1 (SSS-S)H WCH2 WCH3

FITC anti-hIgG

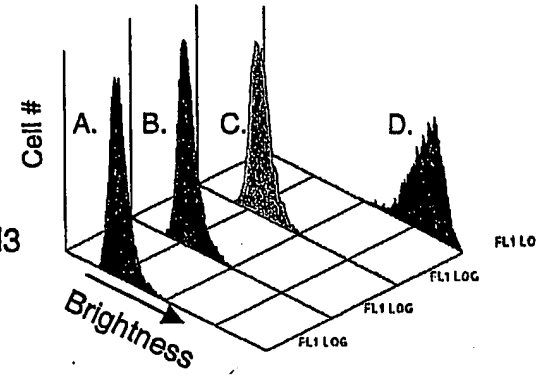

FITC anti-hIgA

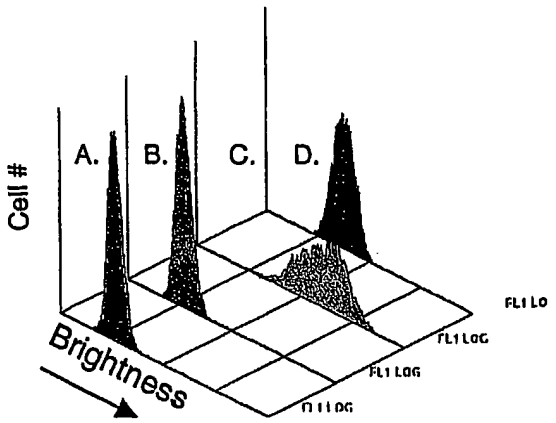

FITC anti-hIgE

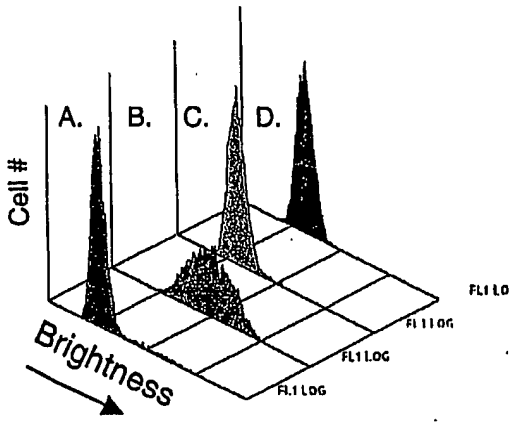

Fig. 58

Fig. 58A. 2H7 scFv VH L11S human IgE (WCH2 WCH3 WCH4) Binding to CD20 CHO at 30 ug/ml

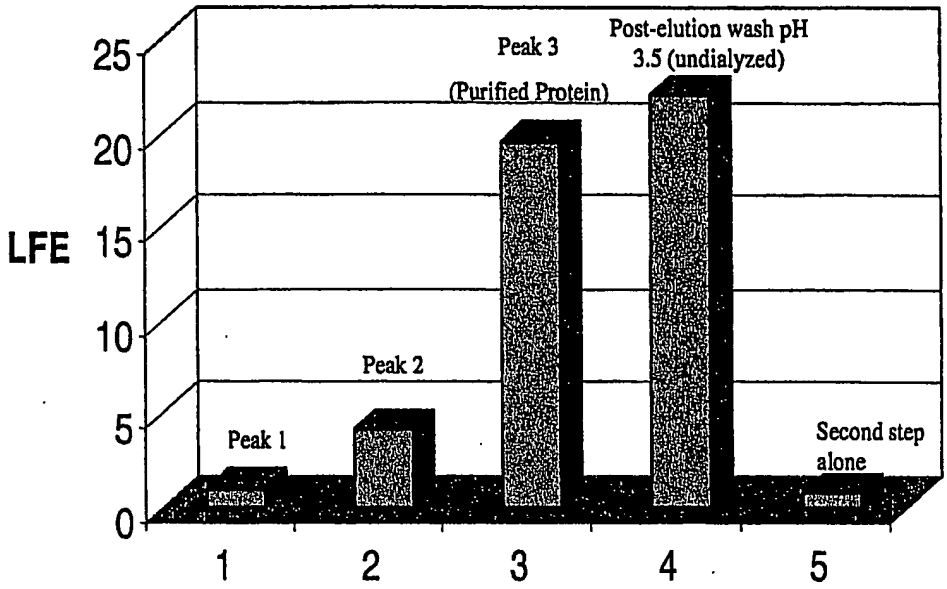

Fig. 58B. ADCC Activity of 2H7 VHL11S IgE (WCH2 WCH3 WCH4) Protein Fractions with **PBMC** Effectors and Bjab Targets

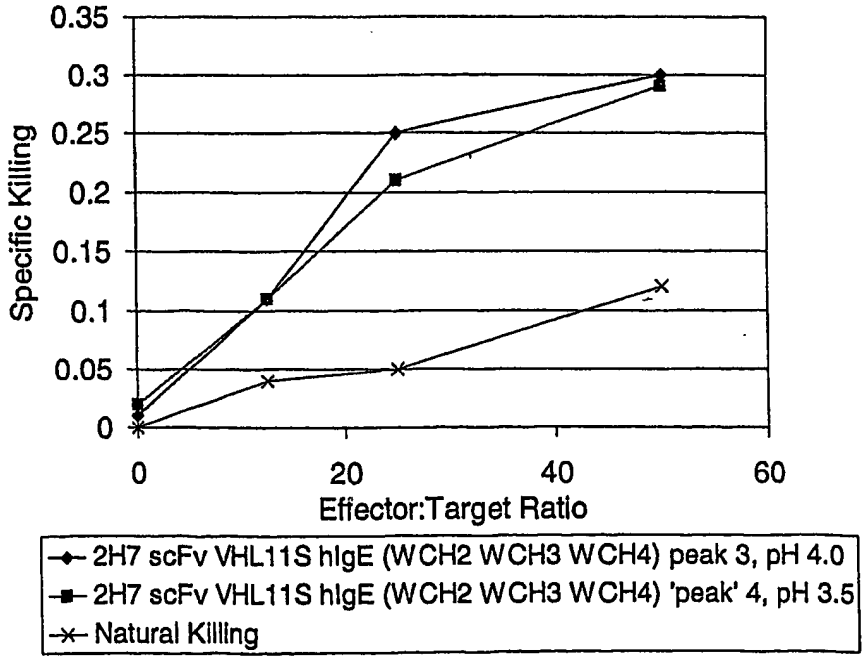

Fig. 59

Binding Data for COS derived α-CD20 (2H7) scFv VHL11S mIg E (WCH2 WCH3 WCH4) and mIgA (WH WCH2 WCH3)Tailed Molecules

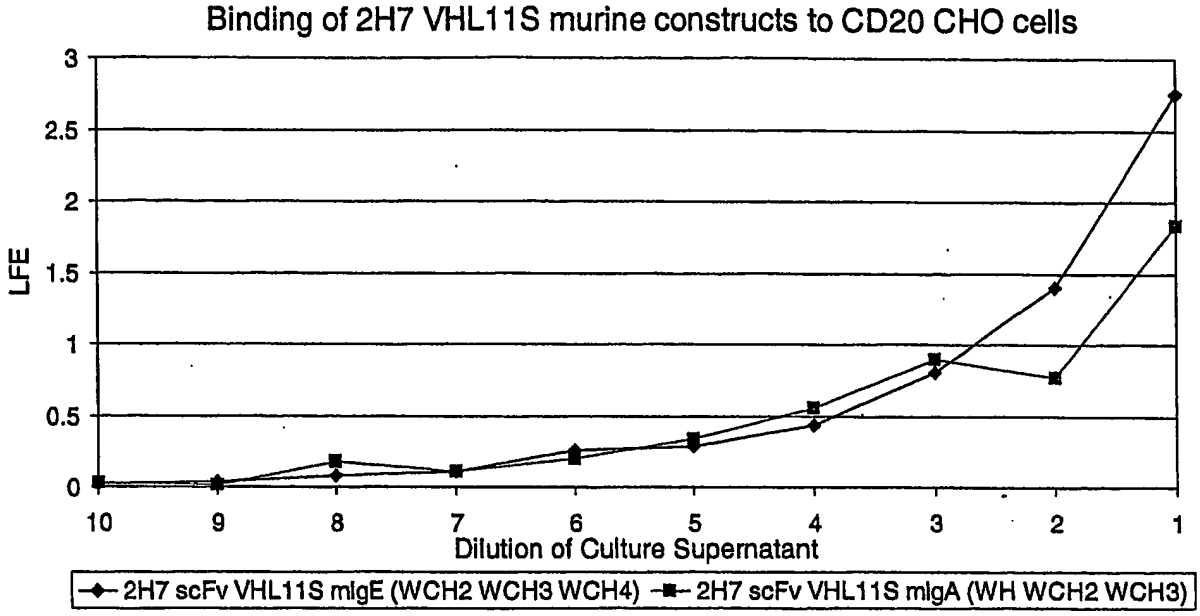

Fig. 60

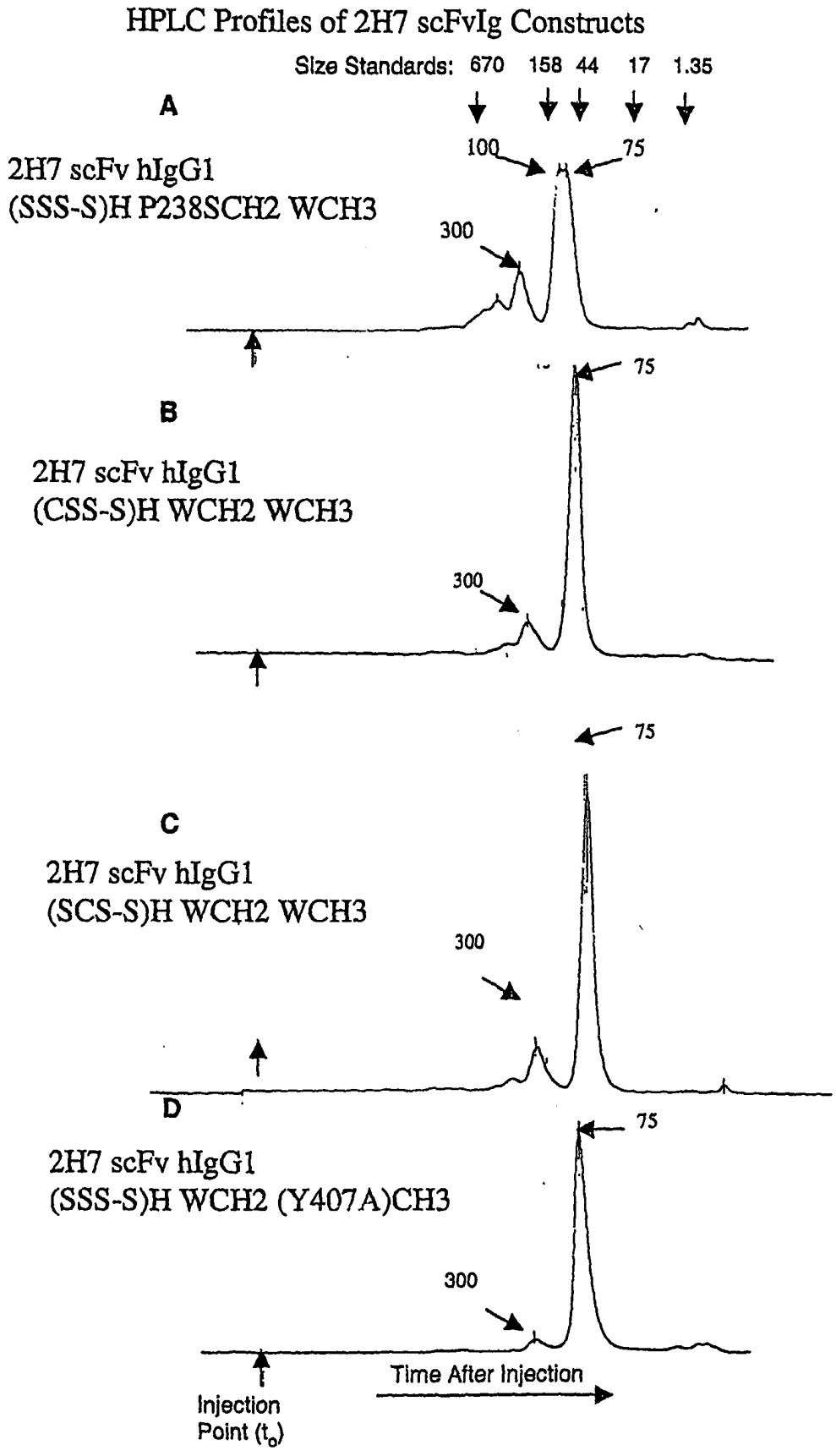
HPLC Profiles of 2H7 scFvIg Constructs
Size Standards: 670 158 44 17 1.35
A
2H7 scFv hIgG1
(SSS-S)H P238SCH2 WCH3
100
75
300
B
2H7 scFv hIgG1
(CSS-S)H WCH2 WCH3
75
300
C
2H7 scFv hIgG1
(SCS-S)H WCH2 WCH3
75
300
D
2H7 scFv hIgG1
(SSS-S)H WCH2 (Y407A)CH3
75
300
Time After Injection
Injection
Point (t0)

Fig. 61

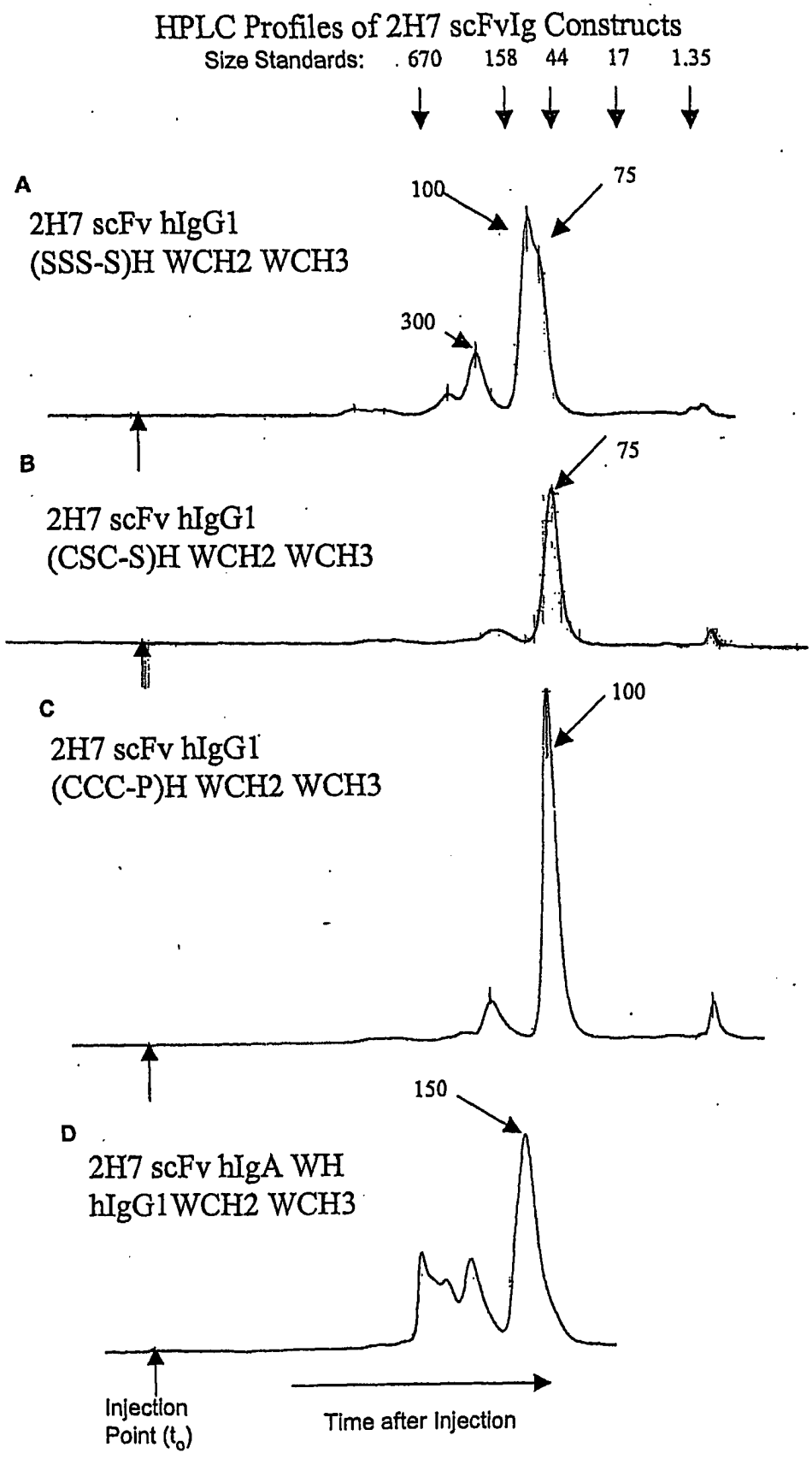
HPLC Profiles of 2H7 scFvIg Constructs
Size Standards: 670 158 44 17 1.35
A
2H7 scFv hIgG1
(SSS-S)H WCH2 WCH3
100
75
300
B
2H7 scFv hIgG1
(CSC-S)H WCH2 WCH3
75
C
2H7 scFv hIgG1
(CCC-P)H WCH2 WCH3
100
D
2H7 scFv hIgA WH
hIgG1WCH2 WCH3
150
Injection
Point (t_o)
Time after Injection

Fig. 62

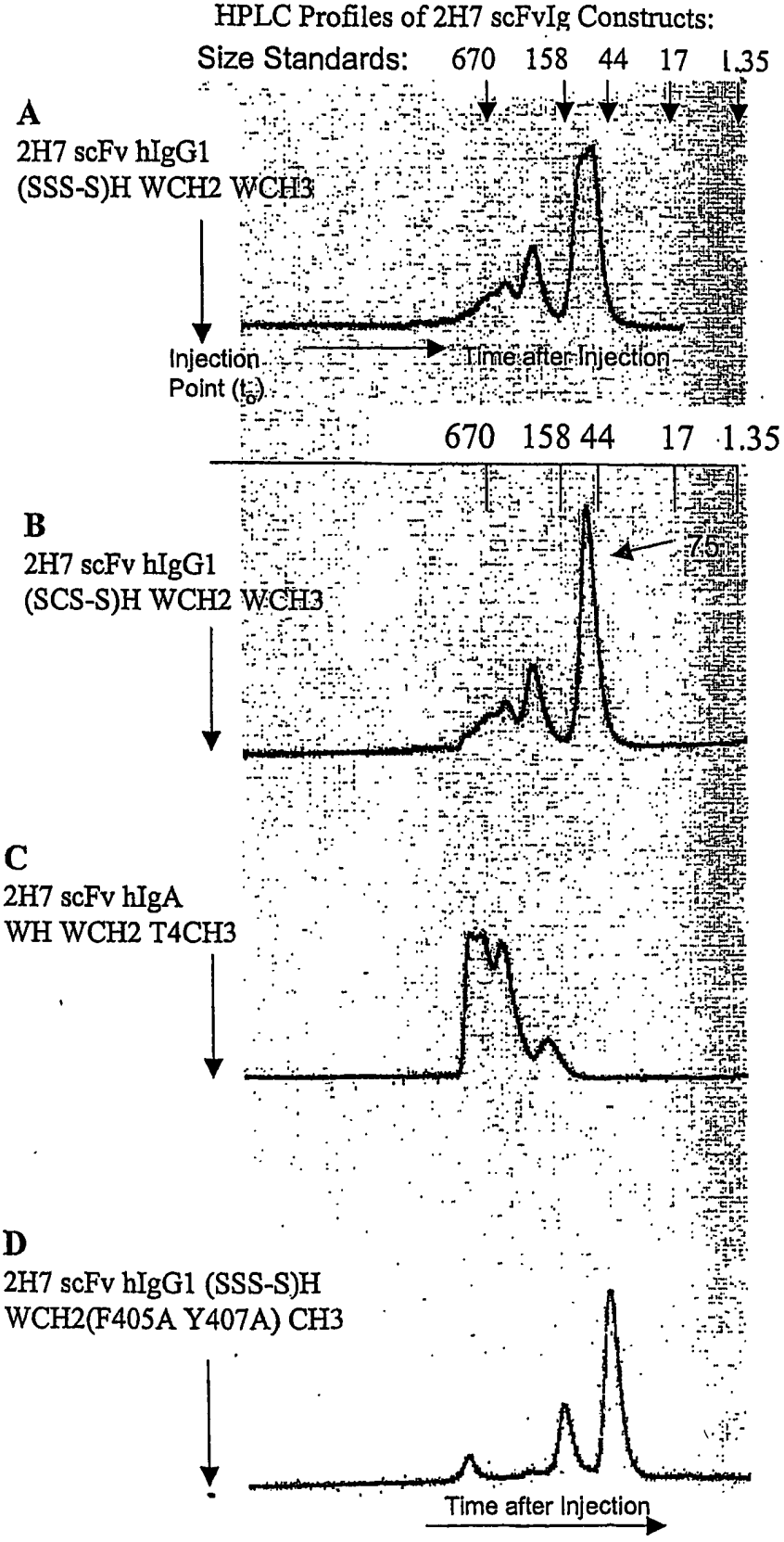
HPLC Profiles of 2H7 scFvIg Constructs:
Size Standards: 670 158 44 17 1.35
A
2H7 scFv hIgG1
(SSS-S)H WCH2 WCH3
Injection Point (t_o)
Time after Injection
670 158 44 17 1.35
B
2H7 scFv hIgG1
(SCS-S)H WCH2 WCH3
7.5
C
2H7 scFv hIgA
WH WCH2 T4CH3
D
2H7 scFv hIgG1 (SSS-S)H
WCH2(F405A Y407A) CH3
Time after Injection

Fig. 63

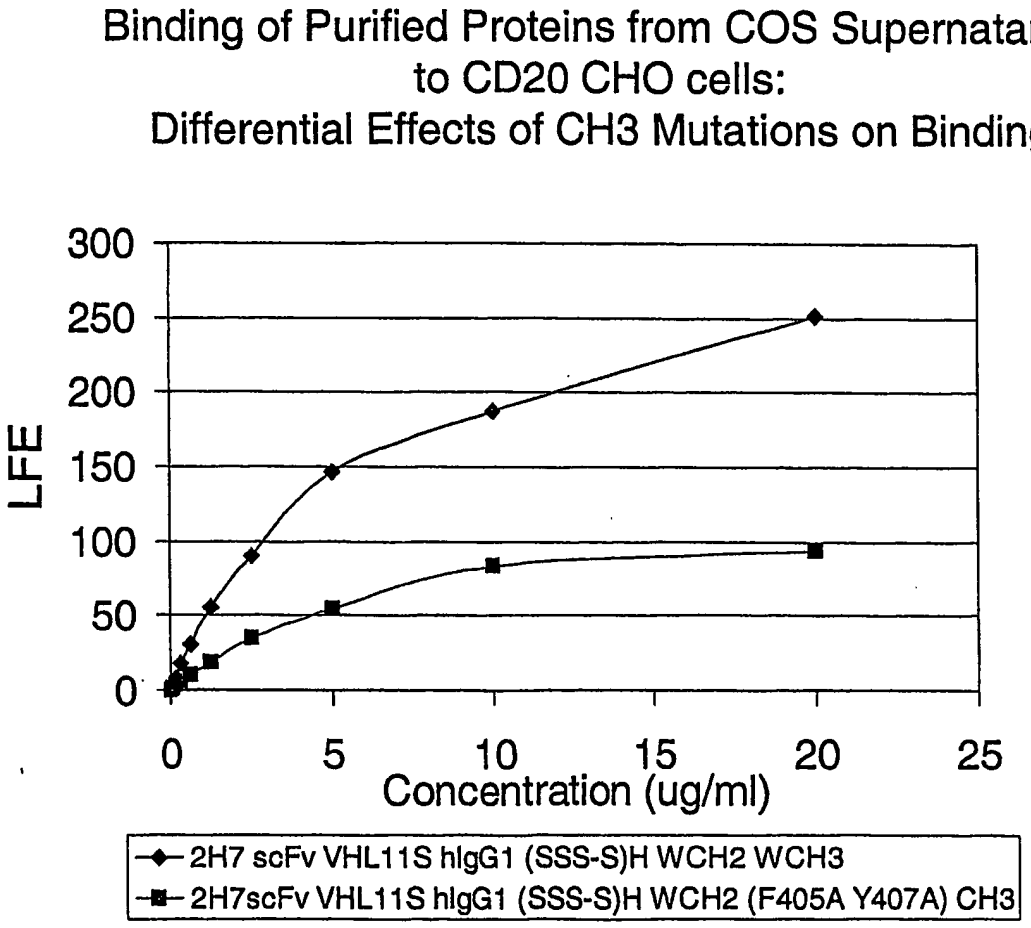
Binding of Purified Proteins from COS Supernatants
to CD20 CHO cells:
Differential Effects of CH3 Mutations on Binding
LFE
300
250
200
150
100
50
0
0
5
10
15
20
25
Concentration (ug/ml)
2H7 scFv VHL11S hIgG1 (SSS-S)H WCH2 WCH3
2H7scFv VHL11S hIgG1 (SSS-S)H WCH2 (F405A Y407A) CH3

Fig. 64

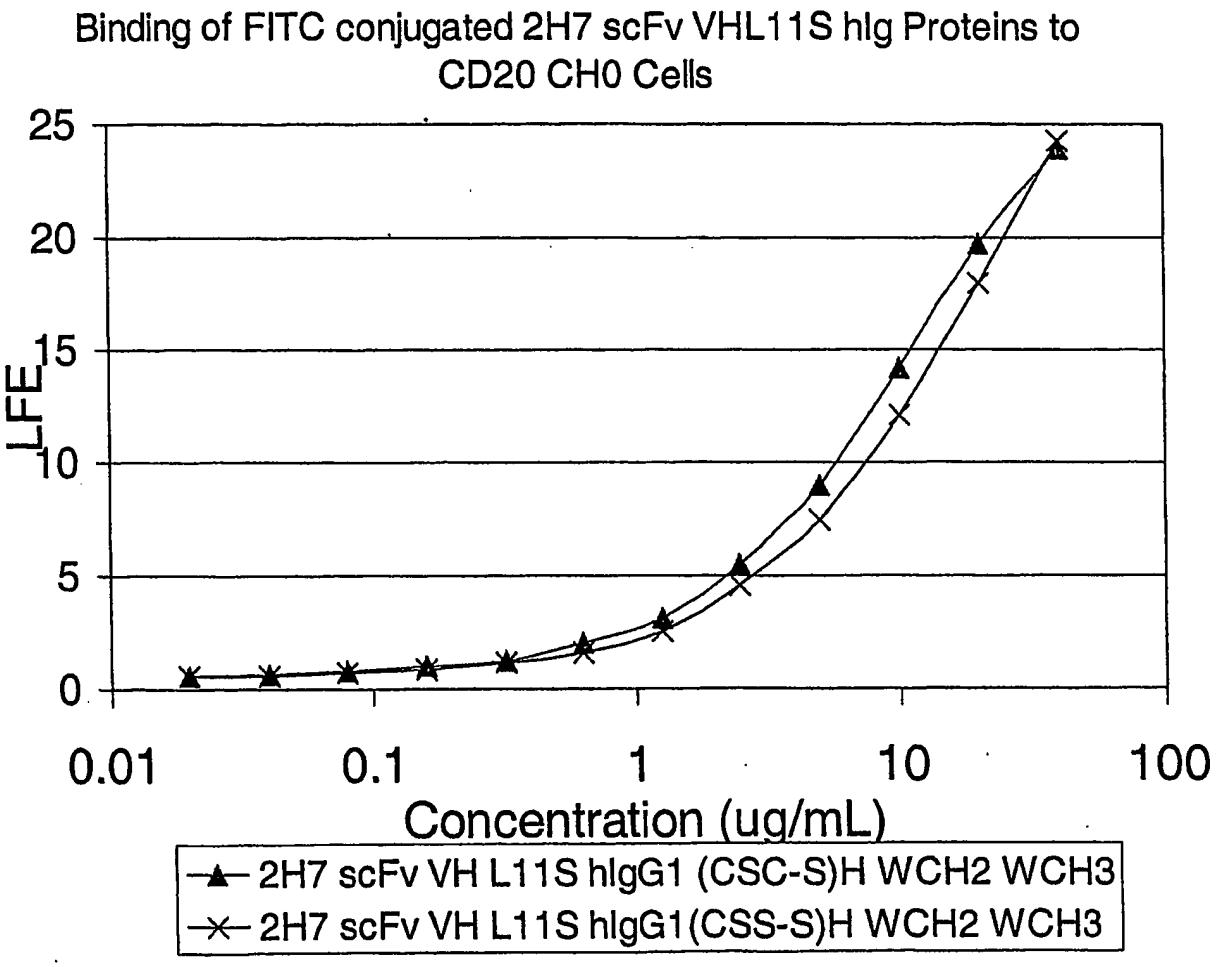
Binding of FITC conjugated 2H7 scFv VHL11S hIg Proteins to CD20 CH0 Cells
25
20
15
10
5
0
LFE
0.01
0.1
1
10
100
Concentration (ug/mL)
2H7 scFv VH L11S hIgG1 (CSC-S)H WCH2 WCH3
2H7 scFv VH L11S hIgG1(CSS-S)H WCH2 WCH3

Fig. 65

Nonreducing SDS-PAGE on Protein A-Purified Lots of 2H7 scFv VHL11S hIg Constructs (10 ug/lane)

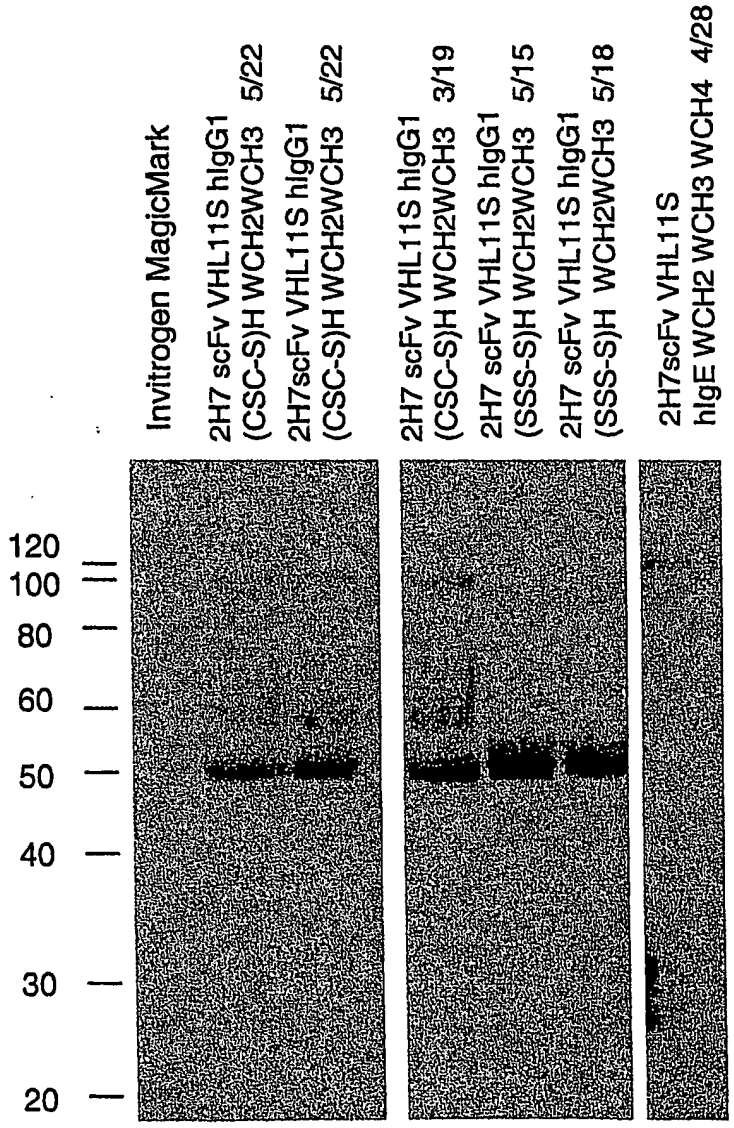

Fig. 66

Alterations in Human IgG Fc sequence
that differentially change effector function efficiency

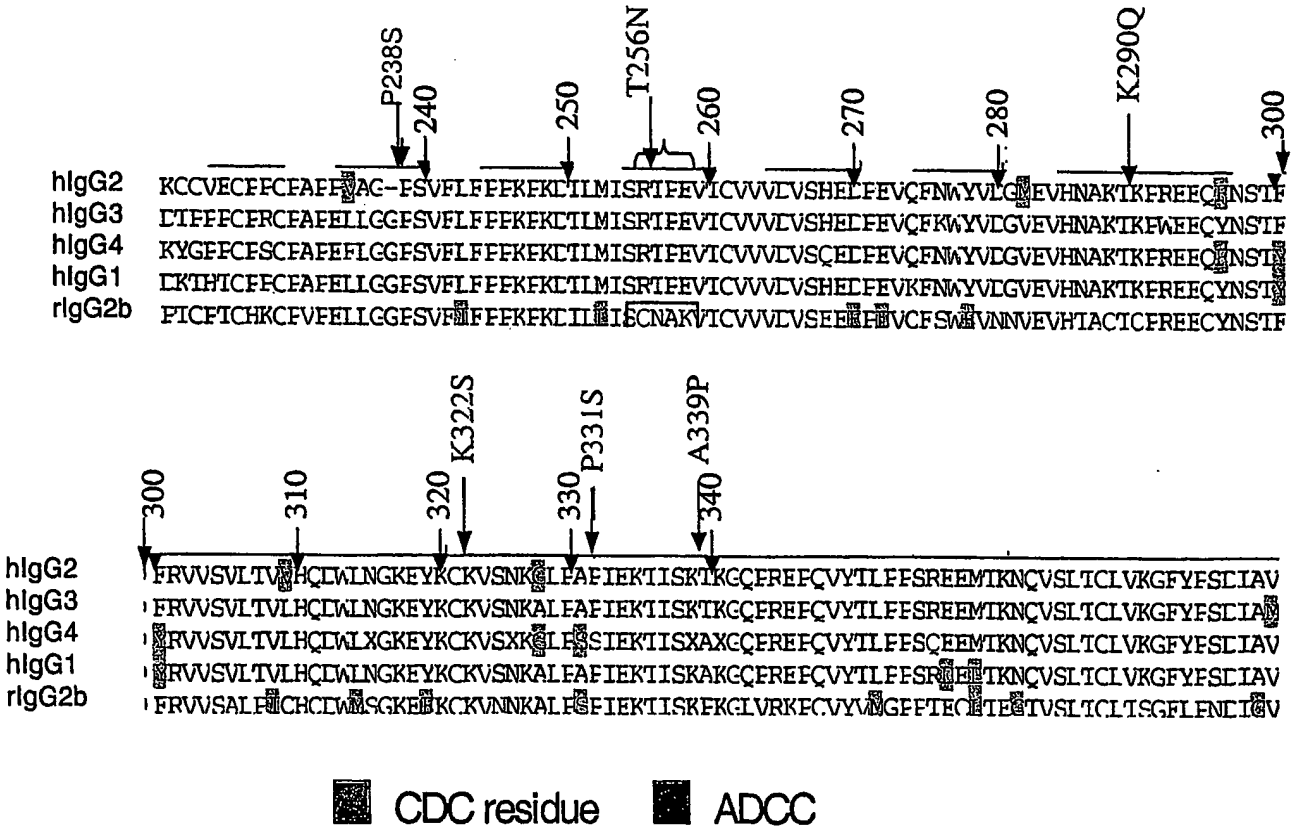

Figure 67.

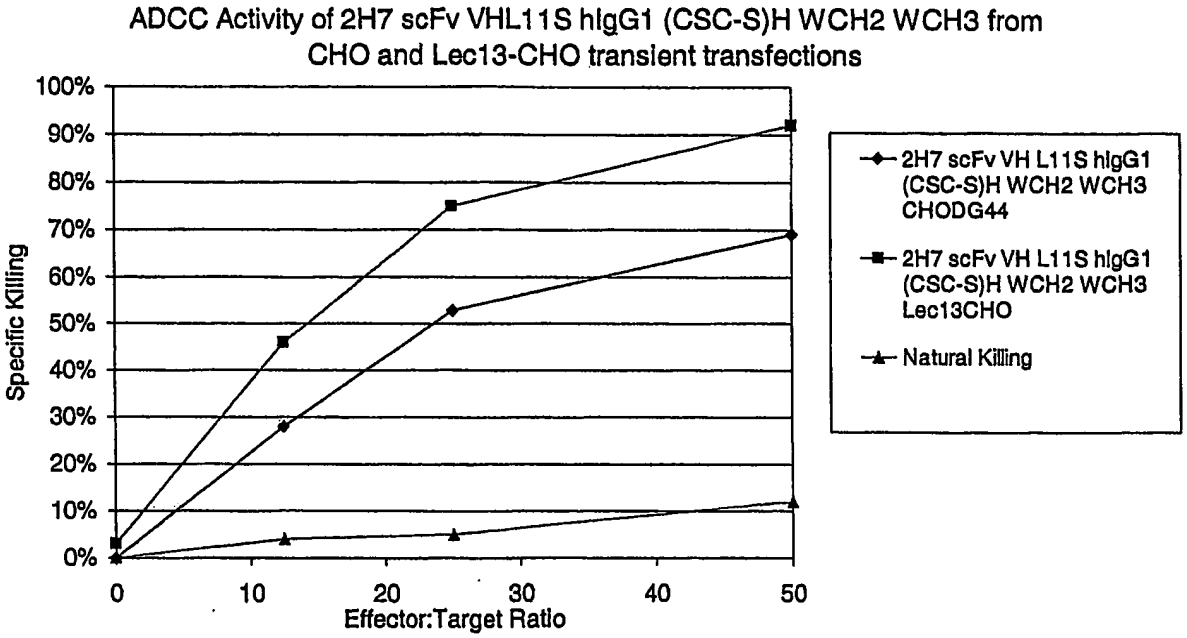
ADCC Activity of 2H7 scFv VHL11S hIgG1 (CSC-S)H WCH2 WCH3 from CHO and Lec13-CHO transient transfections
Specific Killing
100%
90%
80%
70%
60%
50%
40%
30%
20%
10%
0%
0
10
20
30
40
50
Effector:Target Ratio
2H7 scFv VH L11S hIgG1 (CSC-S)H WCH2 WCH3 CHODG44
2H7 scFv VH L11S hIgG1 (CSC-S)H WCH2 WCH3 Lec13CHO
Natural Killing

Fig. 68

CD16(ED) hIgG1(SSS-S)H P238S CH2 WCH3 high and low affinity alleles expressed as soluble molecules

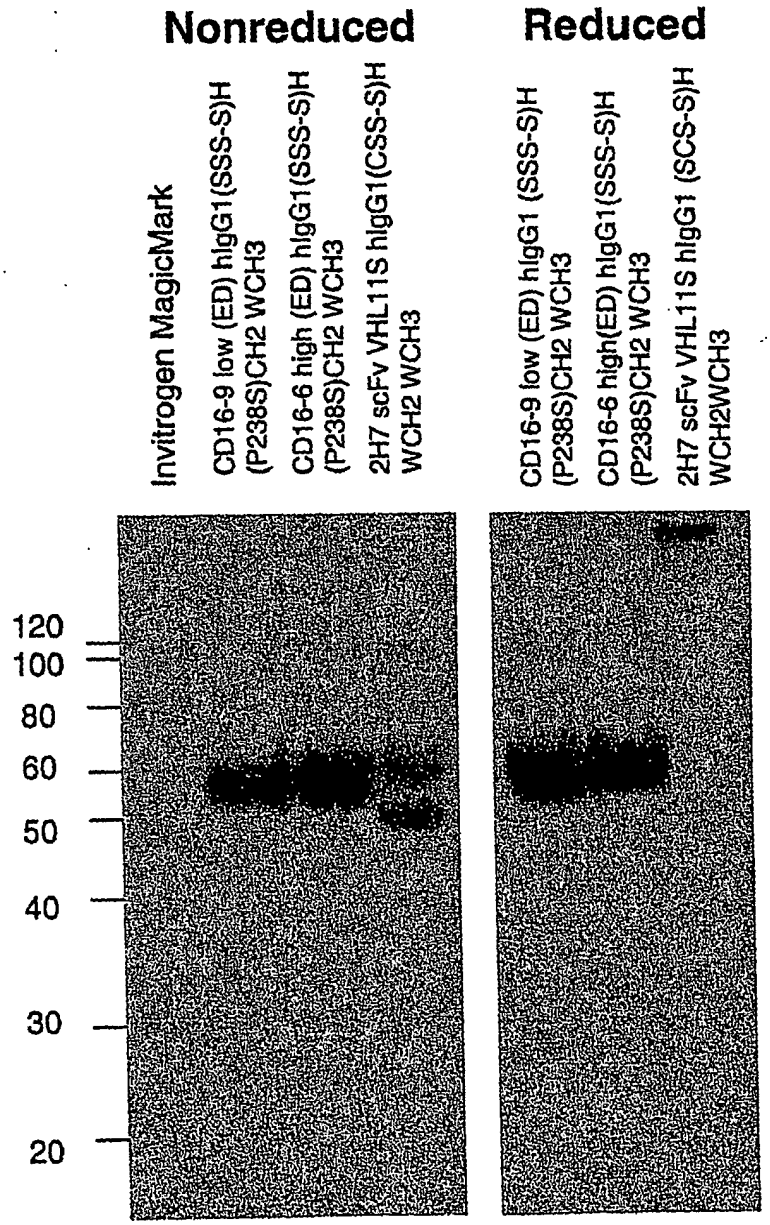

Fig. 69

Binding of soluble CD16-FITC high and low affinity fusion proteins to 2H7 scFv VHL11S hIgG1 (CSC-S)H WCH2WCH3 or (SSS-S)H (P238S)CH2WCH3 on CD20CHO Targets

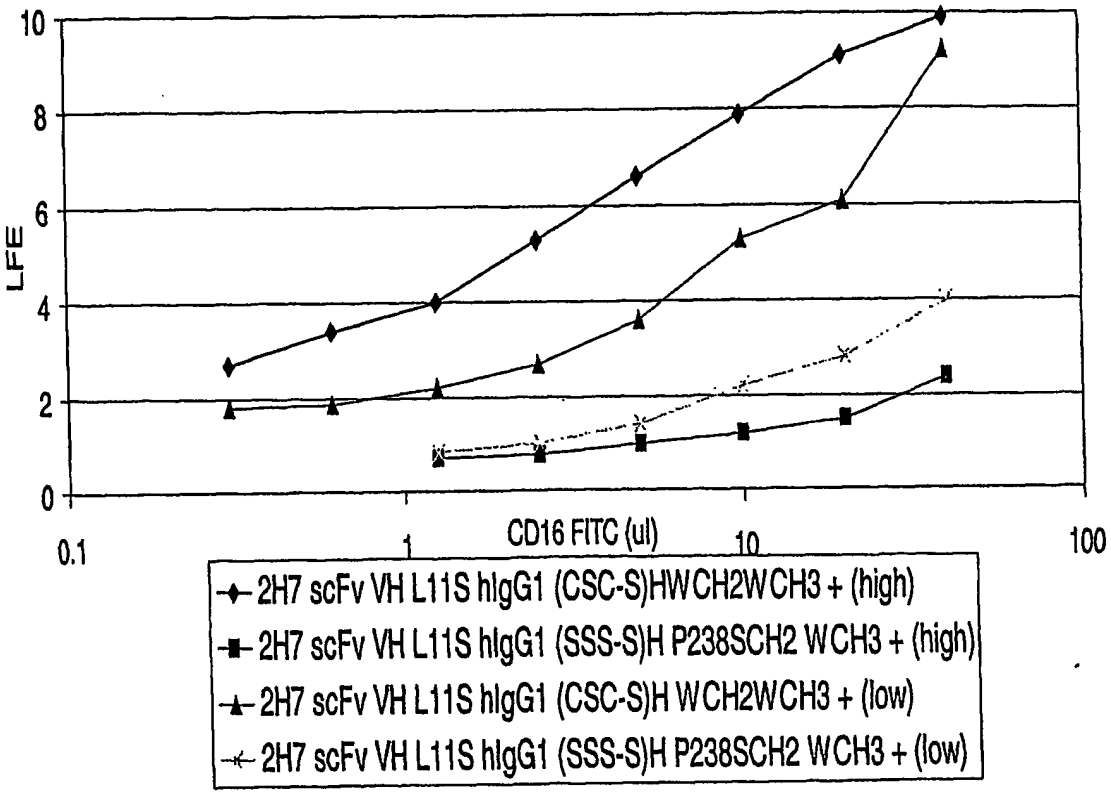

Fig. 70

Binding of FITC Labeled, Recombinant Human CD16(ED) extracellular domain -Ig Fusion Protein to CytoxB Derivatives on CD20 CHO Cells

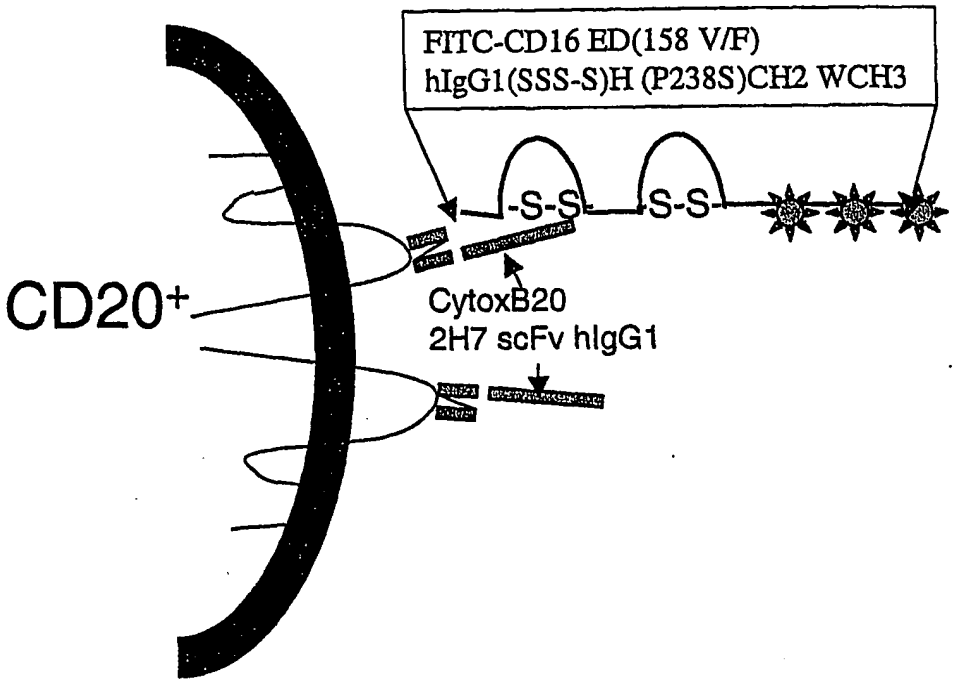

Expression of surface displayed SMIPs links modified cDNAs with the altered fusion proteins

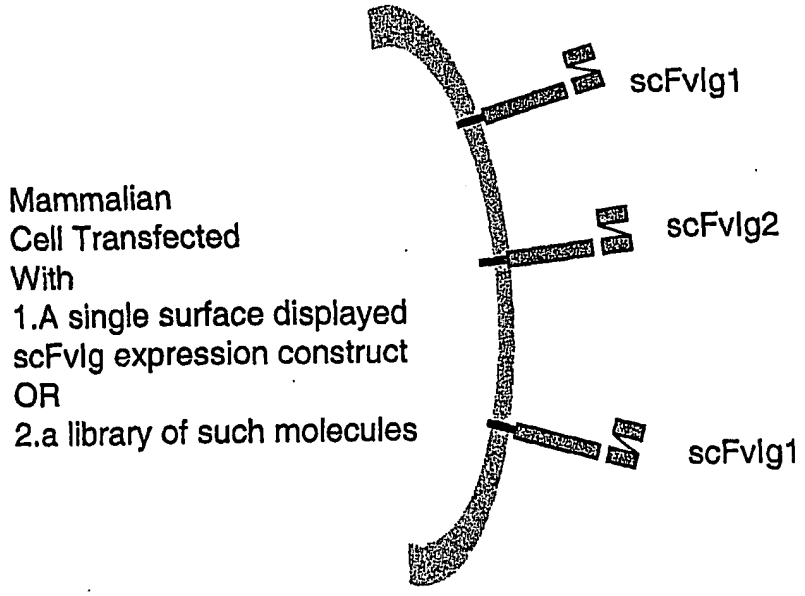

Fig. 71

CD37 mAbs and scFvIg Induce Apoptosis

	Bjab Staining	Annexin V Positive	
scFvIg	No scFvIg	17.5	
	2H7 MH	27	
	G28-1 MH	30.6	
	G28-1 IgAH	28.9	
	HD37 MH	29.1	
	(2H7+G28-1)MH	41	
	(2H7+HD37) MH	37.1	
	(G28-1+HD37) MH	35.3	
			plus GAM
	Ramos	AnnexinV Positive	AnnexinV positive
mAbs	cells alone	3	3.3
	2H7 Mab	1.4	3.1
	G28-1 Mab	18.3	8.7
	HD37 Mab	3.7	3.1
	G28-5	3.9	8.3
	2H7+G28-1	32.3	35.7
	2H7+HD37	5	10.5
	2H7+G28-5	5.7	19.4
	HD37+G28-1	26.9	50
	HD37+G28-5	8.2	18.4
	G28-1+G28-5	39.5	68.3

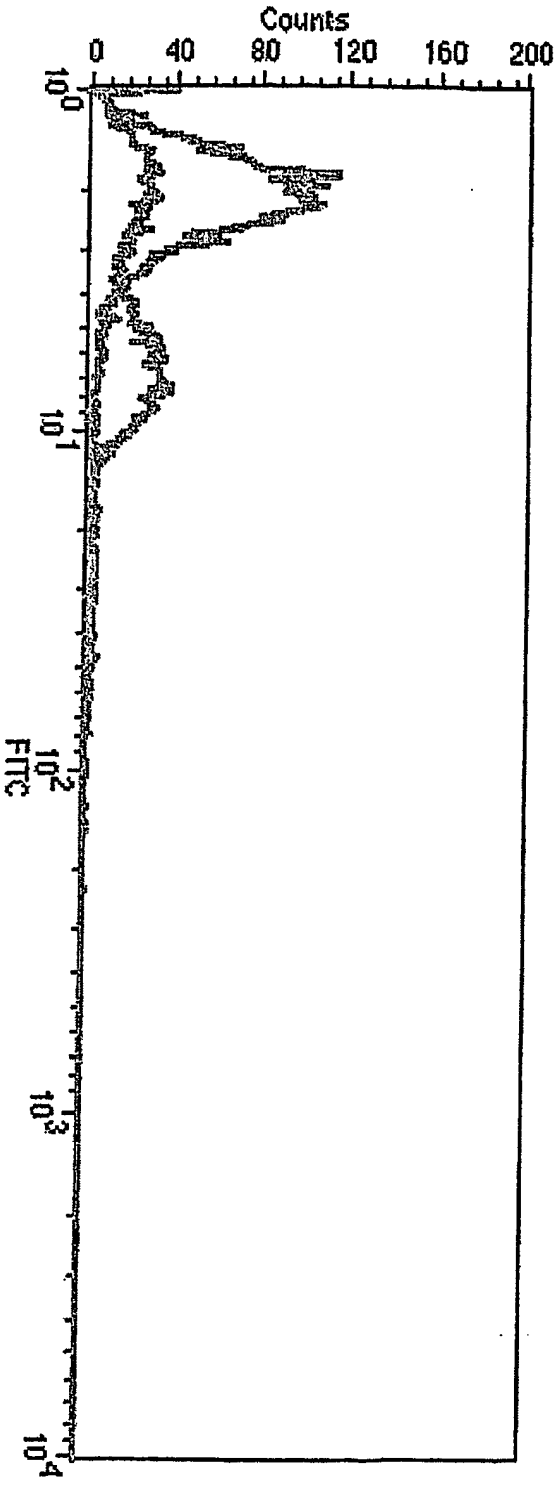
Caspase 3 Activity in Ramos Cells after 4 Hour
Incubation With CytoxB20G SMIP
Counts
0
40
80
120
160
200
10^0
10^1
10^2
10^3
10^4
FITC
media
CD20 SMIP

Fig. 72

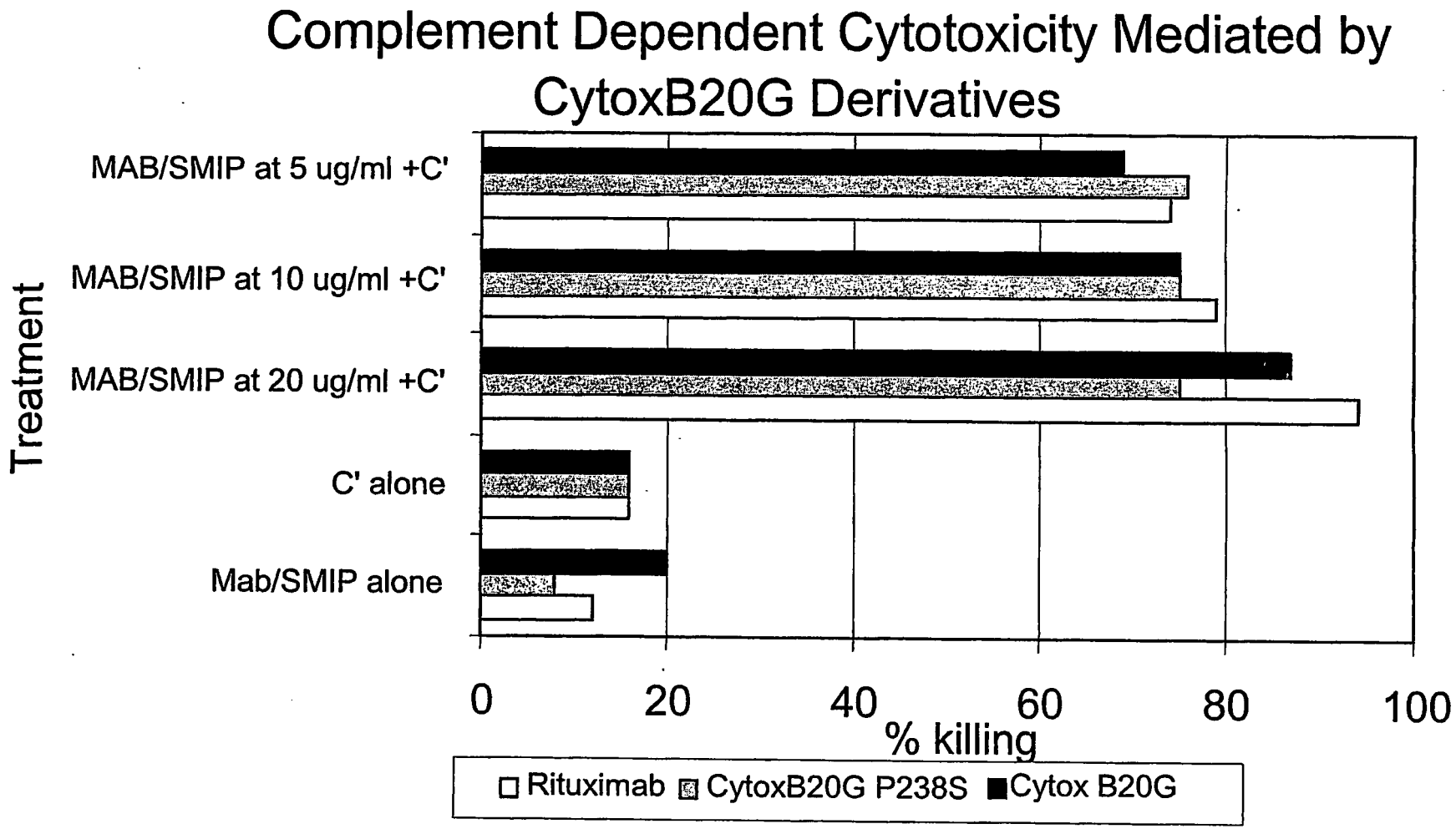

Fig. 73

Figure 76: CDC Activity of CytoxB20G SMIPS. CytoxB20G, CytoxB20GP238, or Rturximab were incubated at increasing concentrations with 10^4 Bjab Target Cells and a 1:10 dilution of rabbit complement (PelFreez) in a volume of 100 microliters for sixty minutes. Aliquots were stained with trypan blue (Invitrogen), and counted using a hemacytometer to determine the percentage of the cell population killed during treatment. Negative controls with cells and only one reagent were also included.

ADCC Activity of CytoxB20G SMIPS

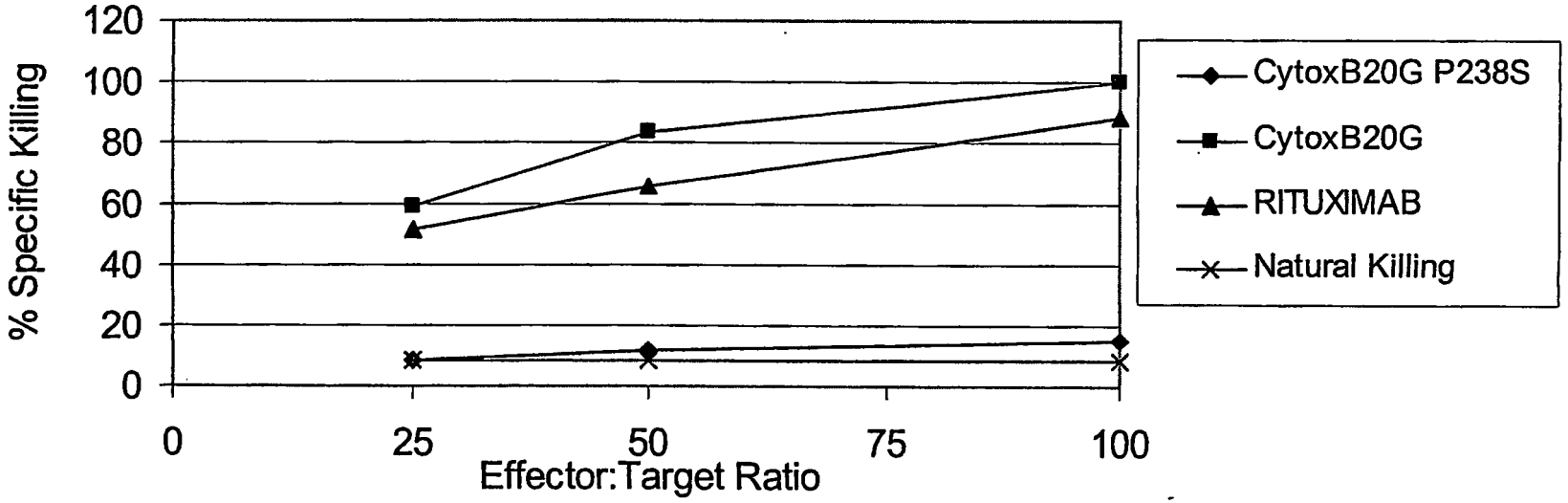

Fig. 74

Figure 77: ADCC Activity of CytoxB20G SMIPS. ADCC activity of CytoxB20G or Rituximab was measured *in vitro* against BJAB B lymphoma cell line as target and using fresh human PBMC as effector cells. Effector to target ratios were varied as follows: 100:1, 50:1, and 25:1, with the number of BJAB cells per well remaining constant but varying the number of PBMC. Bjab cells were labeled for 2 hours with ^{51}Cr and aliquoted at a cell density of $5x10^4$ cells/well to each well of flat-bottom 96 well plates. Purified fusion proteins or rituximab were added at a concentration of 10 µg/ml, and PBMC were added at 1.25 x 10^6 cells /well (25:1), 2.5 x 10^6 cells/well (50:1), or 5 x 10^6 cells/well (100:1), in a final volume of 200 µl. Natural Killing was measured at each effector:target ratio by omission of SMIP or MAb. Spontaneous release was measured without addition of PBMC or fusion protein, and maximal release was measured by the addition of detergent (1% NP-40) to the appropriate wells. Reactions were incubated for 5 hours, and 100 µl culture supernatant harvested to a Lumaplate (Packard Instruments) and allowed to dry overnight prior to counting cpm released on a Packard Top Count NXT Microplate Scintillation Counter.

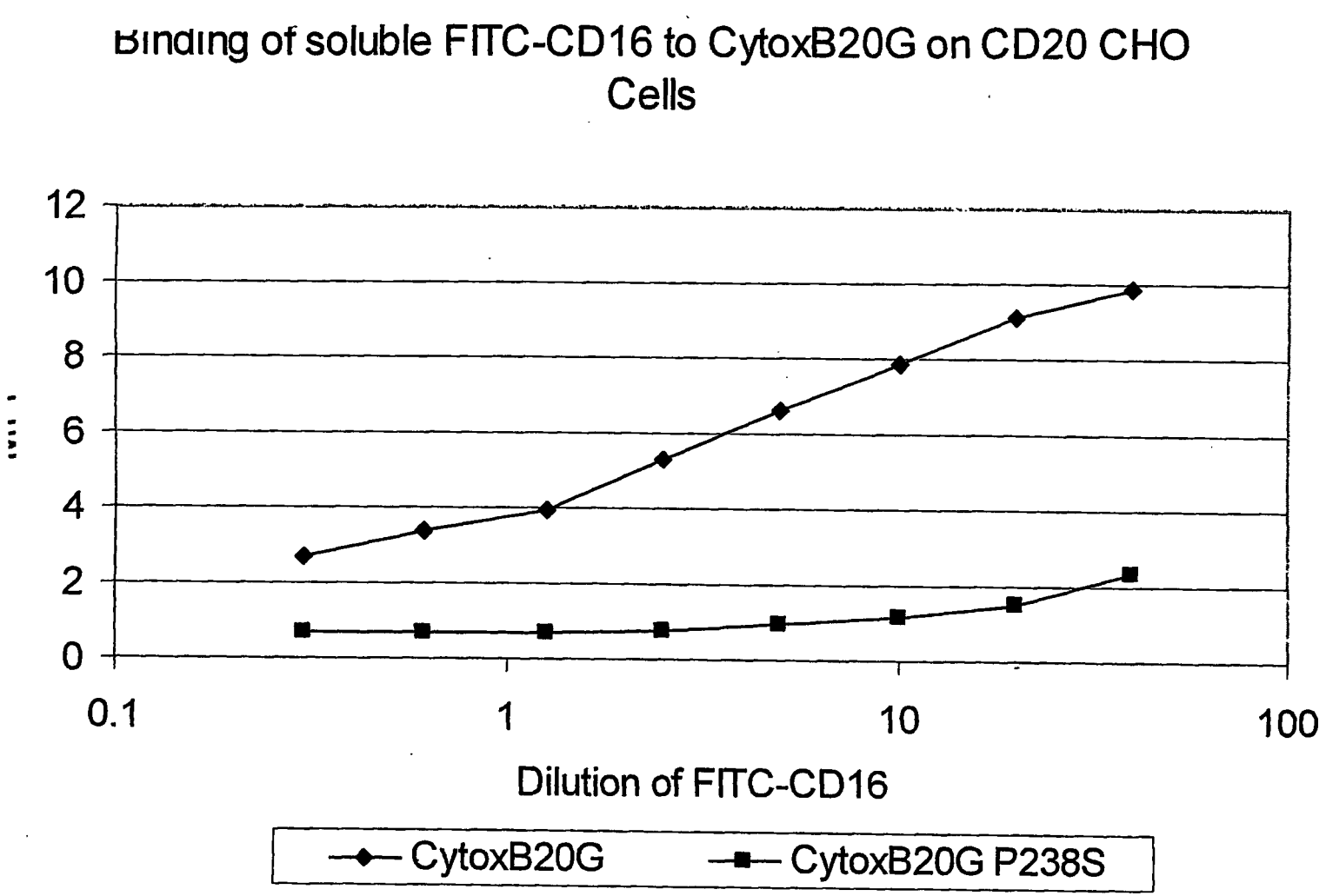

Fig. 75

re 78: Binding of soluble FITC-CD16 to CytoxB20G on CD20 CHO cells. CD20 CHO cells (10^6) were incubated
ı saturating amounts of CytoxB20G or CytoxB20G P238S(10 ug/ml) for one hour on ice in PBS/2% FBS. Cells
: washed in PBS/2% FBS and incubated with serial dilutions of 0.5 mg/ml FITC-CD16 for one hour on ice. Cells
: washed and specific binding measured by flow cytometry using a Beckman-Coulter Epics C machine. Results
: analyzed using Expo analysis software and normalized fluorescence units graphed as a function of concentration.

WO 2005/017148

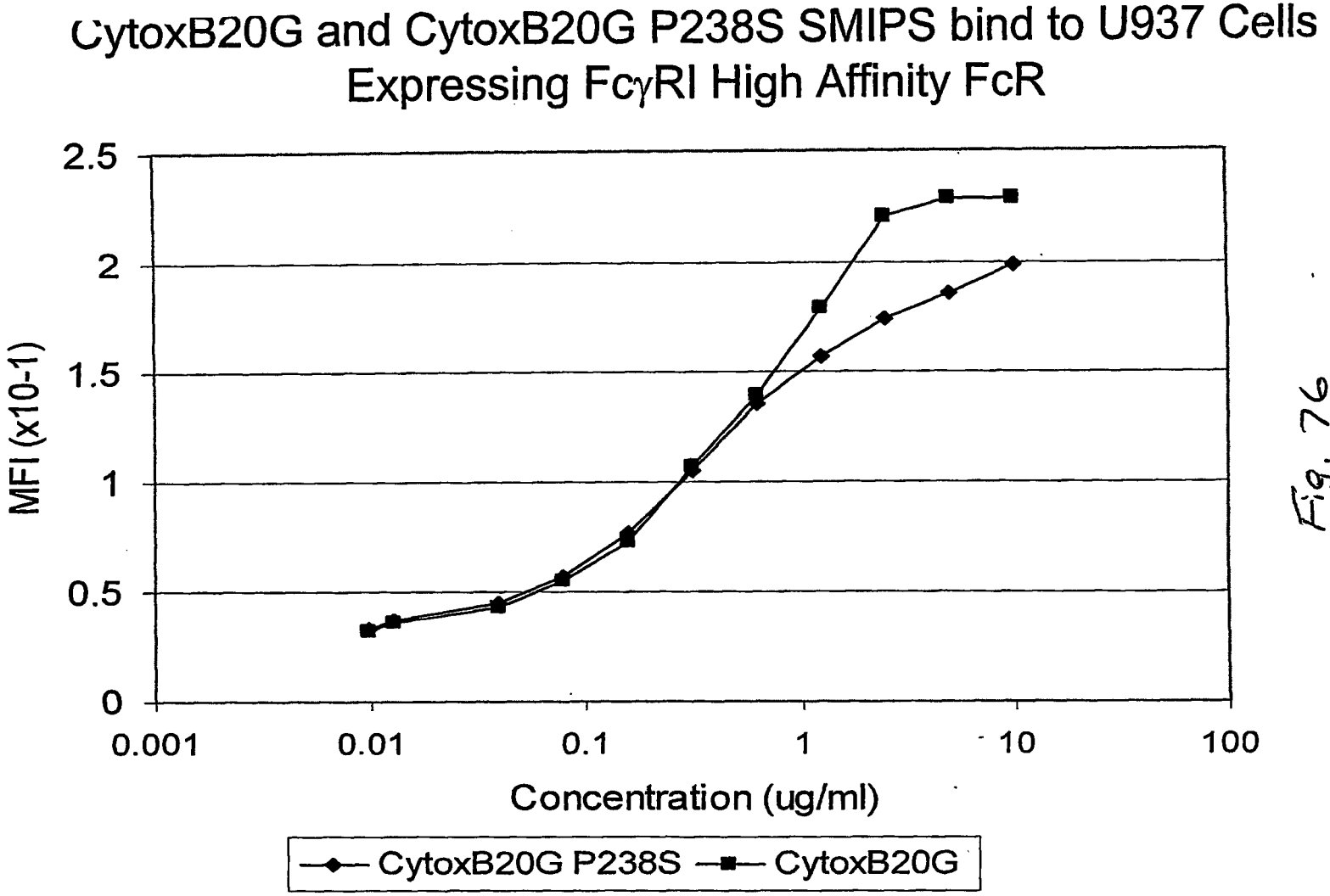

Fig. 76

re 79: CytoxB20G SMIPs bind similarly to U937 cells expressing the high affinity FcR (FcγRI, CD64). U937 cells
) expressing CD64 were incubated in PBS/2%FBS for one hour on ice with CytoxB20G orCytoxB20G P238S. Cells
: washed and incubated for one hour on ice with FITC-goat anti-human IgG1 (Fc specific) (Caltag) at a final dilution
100. Cells were washed and fluorescence analysed on a Beckman-Coulter EpicsC flow cytometer. Data was
yzed using Expo analysis software, and fluorescence intensity graphed as a function of SMIP concentration.

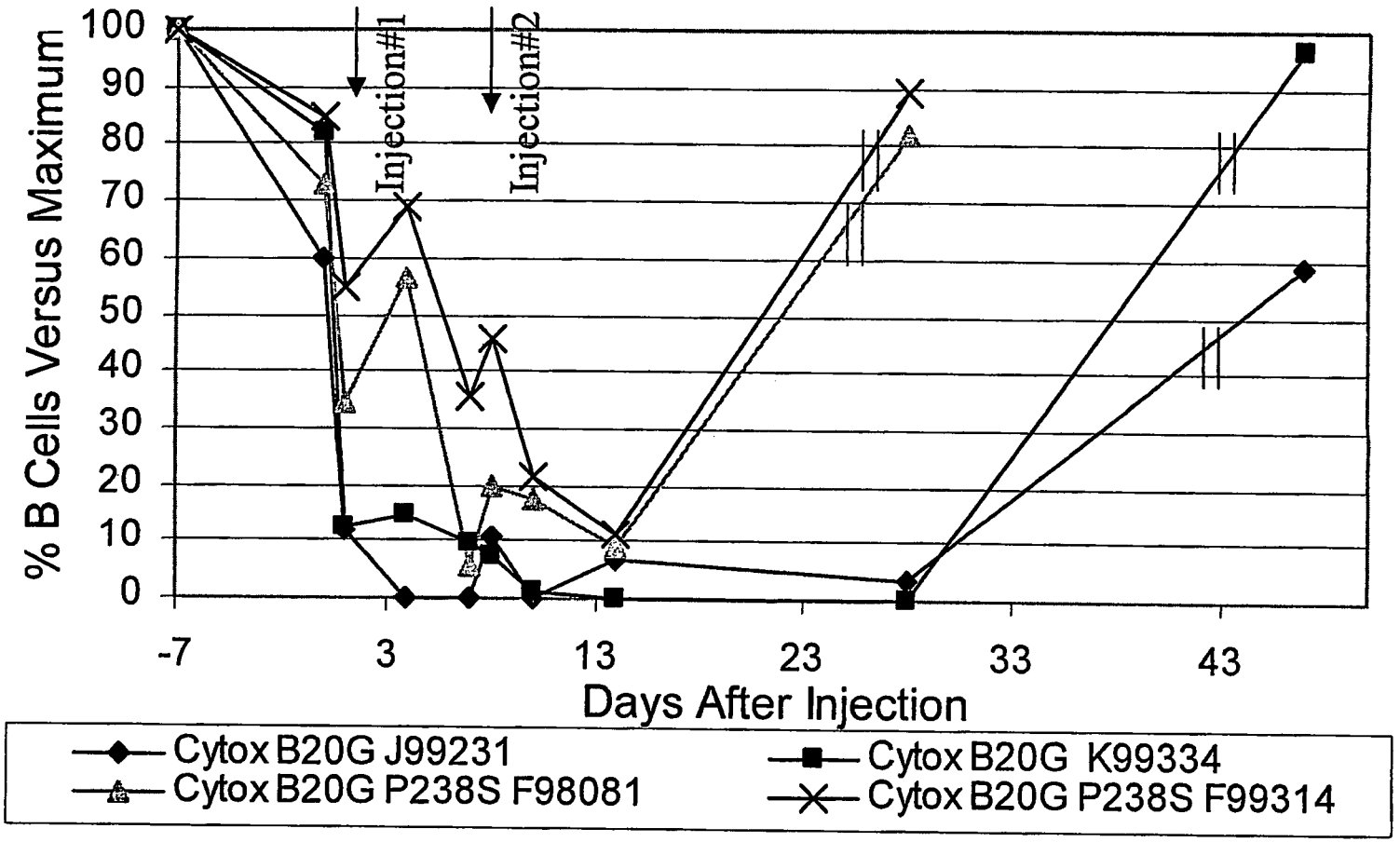

Fig. 77

30: CytoxB20G or CytoxB20G P238S were administered to macaques by intravenous injection at 6 mg/kg, with isions given one week apart. The effect on circulating B cells was measured by detection of CD40 positive B cells heral blood. Blood samples were drawn from injected animals at days -7,0,1,3,7,8,10,14, 28, and 43. B cell n was estimated by performing CBC (complete blood counts) and two color flow cytometry analysis on monkey FITC or PE conjugates of antibodies against CD40, CD19,CD20, IgG, CD3, CD8 were used in various itions. Data are plotted as the number of CD40 positive blood B cells tabulated in thousands of cells per er over time relative to the initial pre-injection time point level of B cells (maximum).

Figure 81: SEC on CytoxB37G SMIPs containing SSS and SSC hinge Domains from Human IgG1

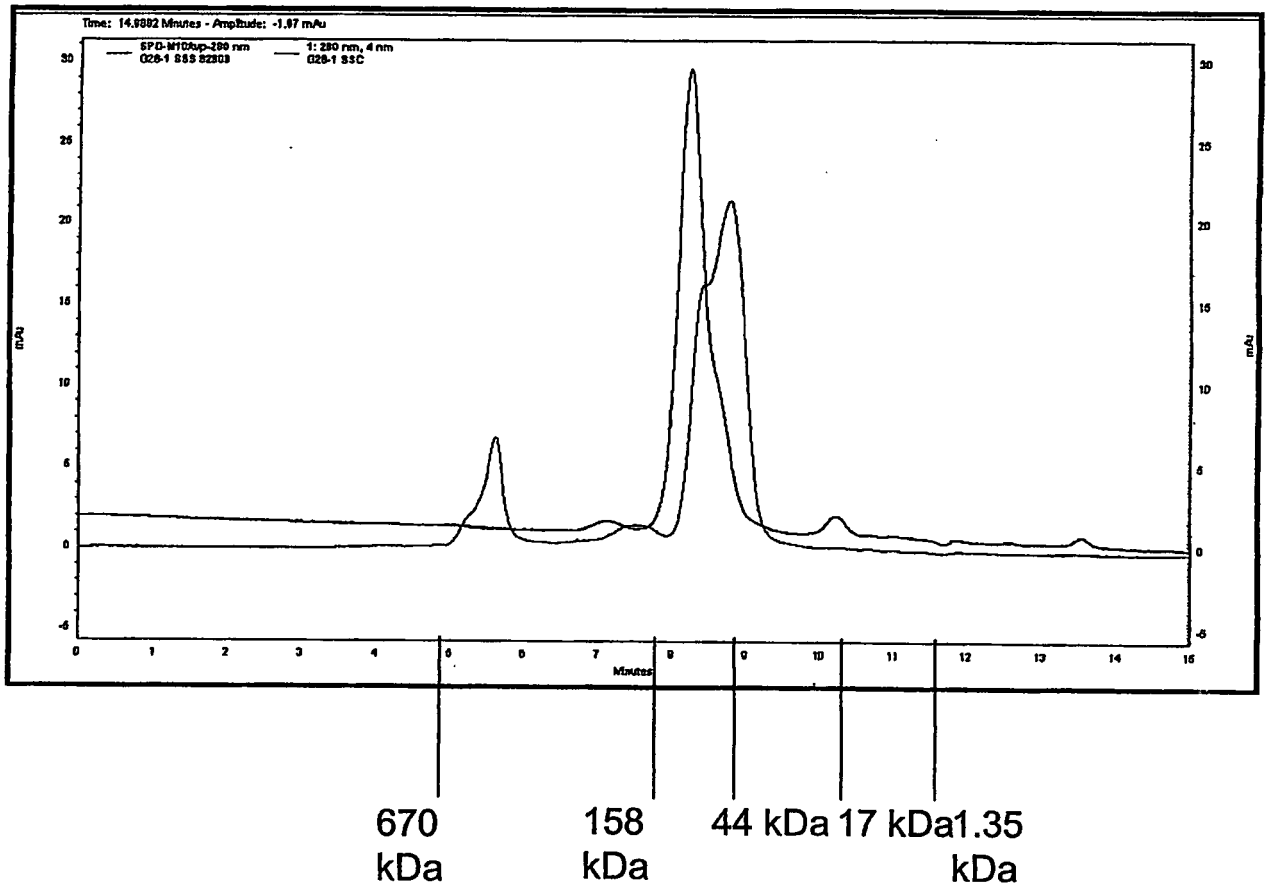

Fig. 78

Figure 81: SEC (Size Exclusion Chromatography) CytoxB37G SMIPs were purified from CHO culture supernatants by Protein A affinity chromatography. Purified aliquots of 10-25 µg were subjected to HPLC over a Tosoh Biosep, Inc. TSK 3000 SWXL HPLC column, por size 5 µm. The flow rate was 1ml/min, in PBS, pH 7.2 running buffer. Migration rates of molecular weight standards are indicated below the tracing. The CytoxB37G (SSS)H SMIP indicated in blue, while the CytoxB37G (CSS)H is indicated in red.

gure 82: Binding of CytoxB37G SMIPs to B Cell Lymphoma Cell Lines

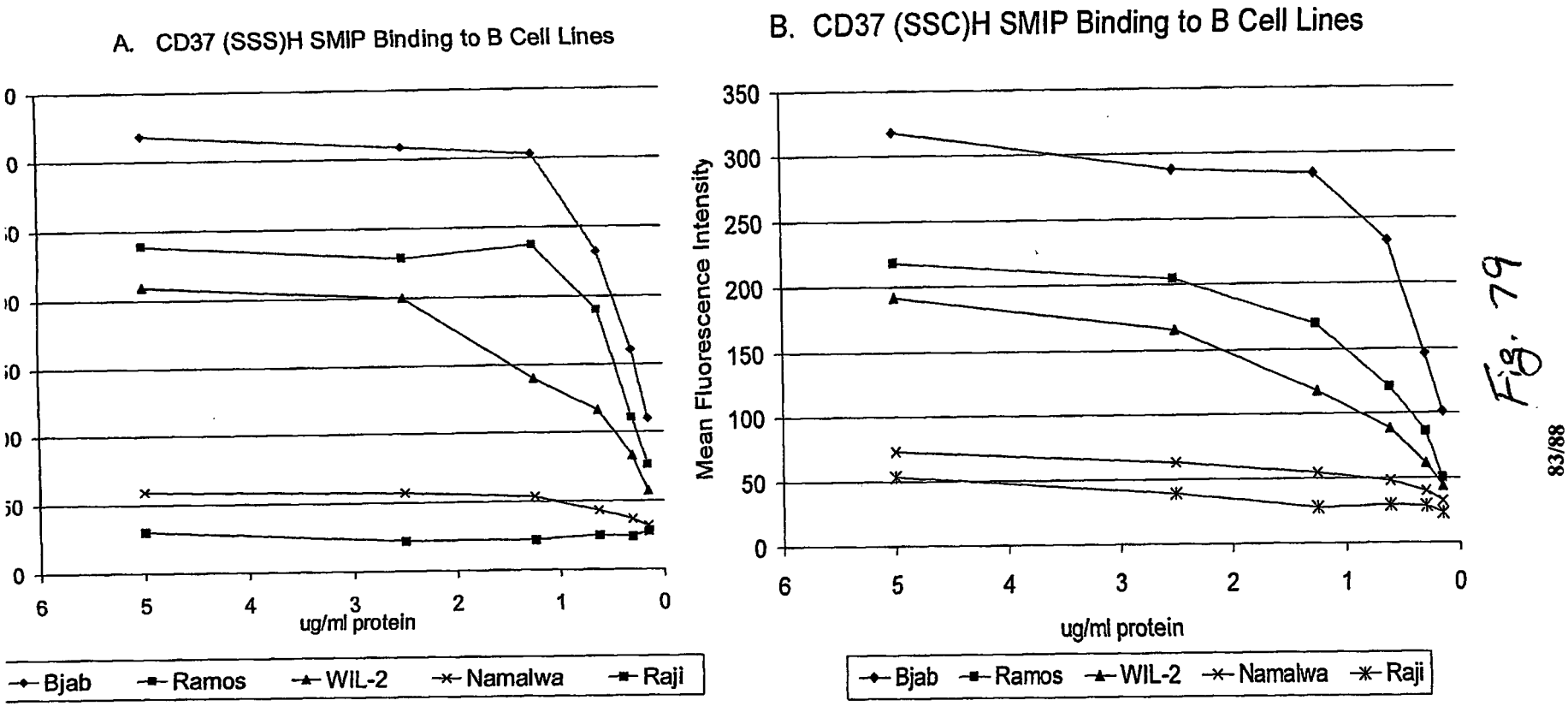

Fig. 79

ure 82 : Binding of CytoxB37G SMIPS to B cell lymphoma cell lines. Serial dilutions of ified CytoxB37 (SSS)H G or CytoxB37 (SSC)H G SMIPS were incubated with 10^6 cells of each cell type for 60 iutes on ice in PBS/2%FBS. Samples were washed twice, and incubated with a mixture of FITC goat anti-human i and FITC goat anti-human IgG F(ab')2 (CalTag) at 1:100 each, on ice for 45 minutes. Samples were washed and lyzed by flow cytometry using a FACsCalibur (Becton-Dickinson)

Fig. 80: AnnexinV-PI Staining of Ramos Cells Incubated 24 hours with CD37 SMIPS

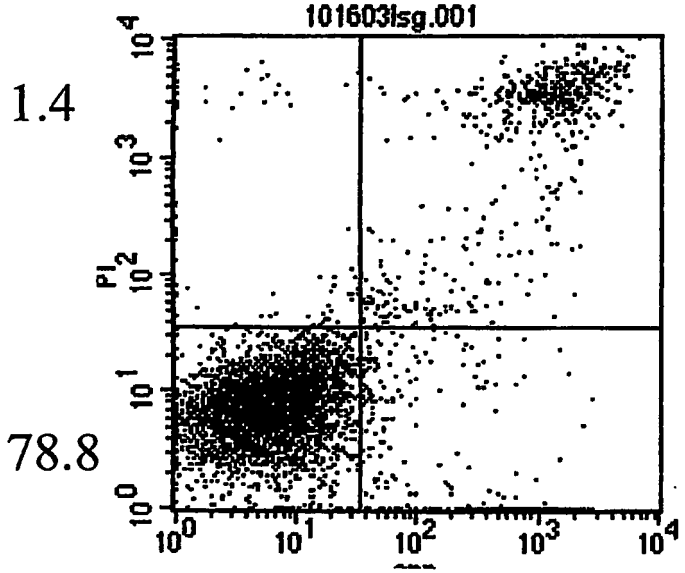

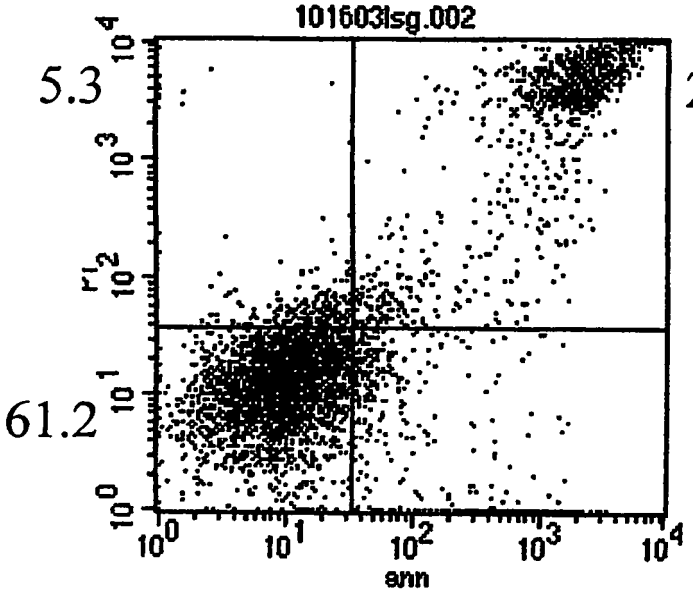

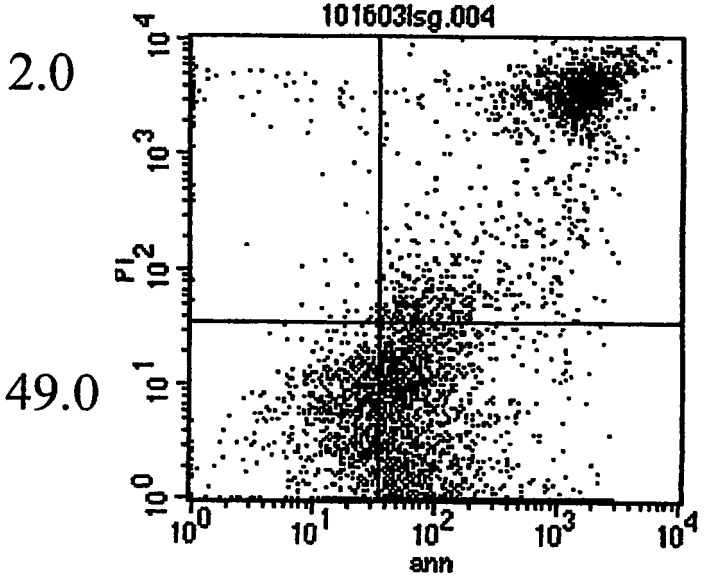

Figure 84: Thymidine Incorporation (Growth Inhibition) in Ramos B-cells after a 48 Hour Incubation with anti-CD37 SMIPS

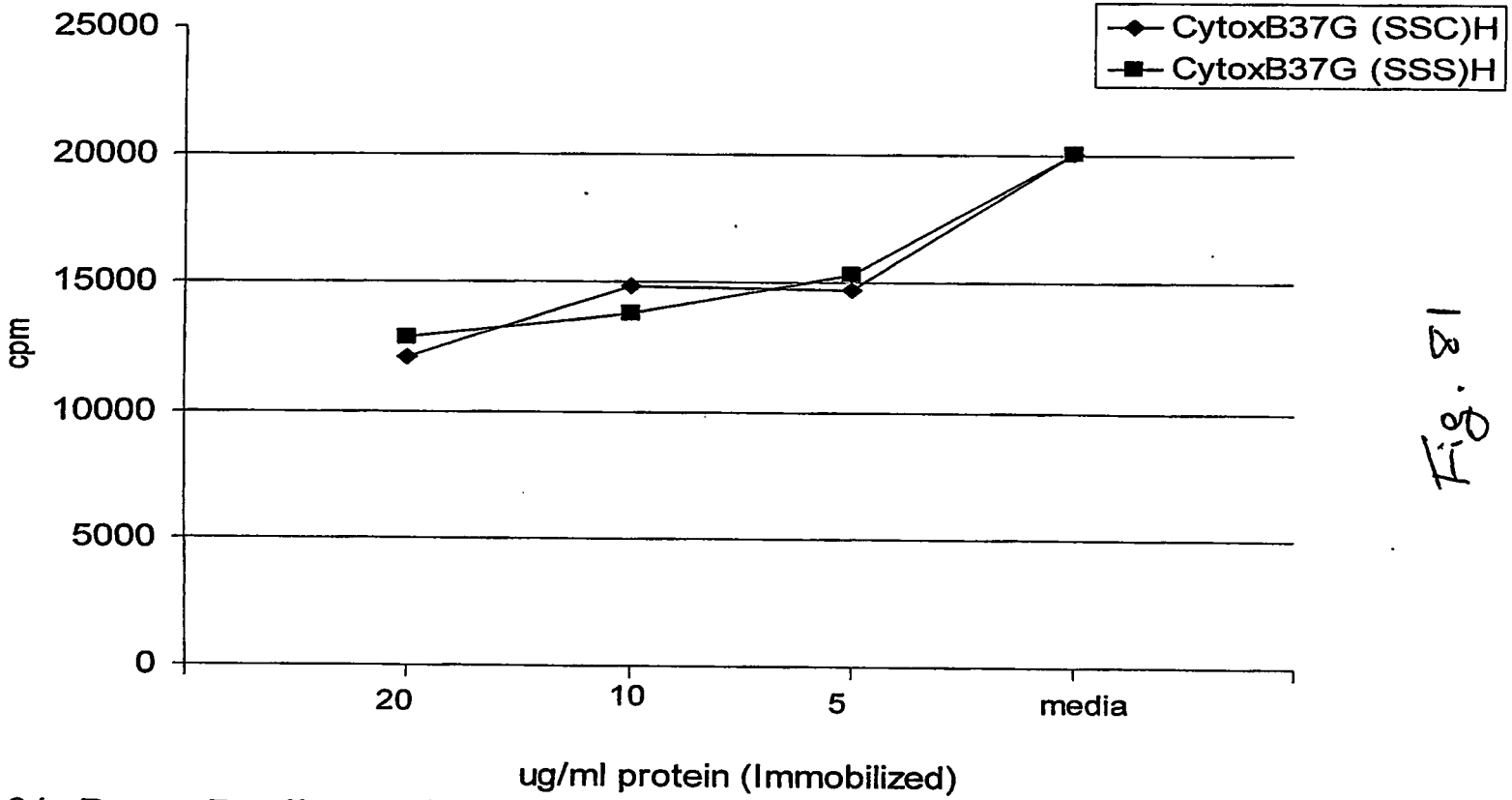

Fig. 84

ıre 84: Ramos B cells were incubated with serial dilutions of purified CD37G SMIPS containing ɜr the IgG1 hinge identified as (SSS)H or (SSC)H. Cultures were incubated in 96 well flat bottom ıe culture dishes (Costar) at 37°C, 5%CO_2 for 36 hours prior to pulsing with ^{3}H-thymidine for the 12 hours of a 48 hour incubation (0.75 µCi/well). Cells were harvested onto 96-well GFC plates g a Packard harvester, dried, and 25 µl Microscint scintillation fluid added to each well prior to ıting on a TopCount NXT microplate (Packard) scintillation counter. Data are plotted as cpm rporated versus protein concentration. Each SMIP show increasing inhibition of proliferation with ɜasing protein concentration.

WO 2005/017148

ure 85: The Induction of Apoptosis in Ramos B-cells after a 20 hour incubation with different combinations of CD20 and CD37 targeted SMIPS

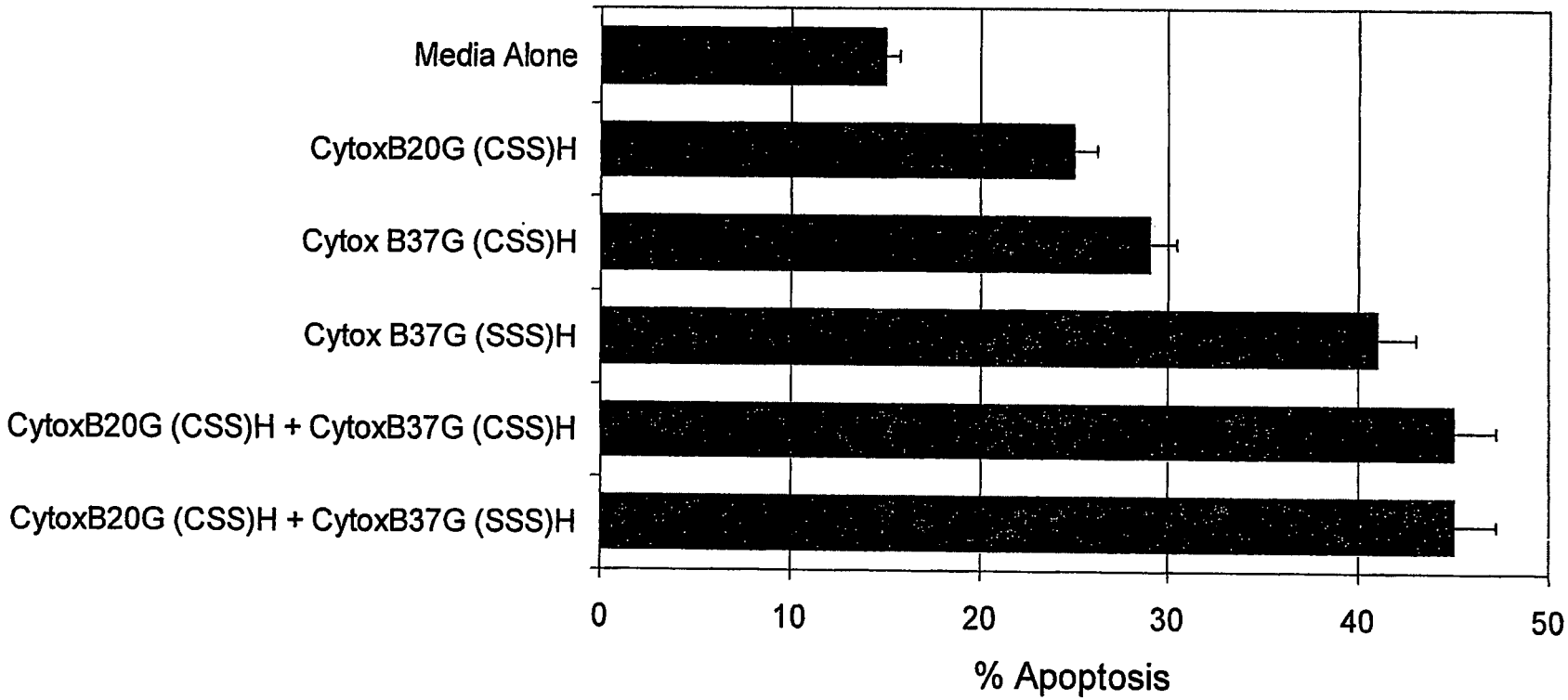

Fig. 82

gure 85: Ramos B cells were incubated with CD20 and/or CD37 targeted SMIPs (10 /ml) in solution for 20 hours. Cells were then harvested, washed, and incubated in nexinV and propidium iodide using a staining kit from Immunotech prior to two color w cytometry using a FACsCalibur flow cytometer (Becton-Dickinson). The graph show percentage of annexin V positive cells identified by their staining in the right quadrants the dot plots.

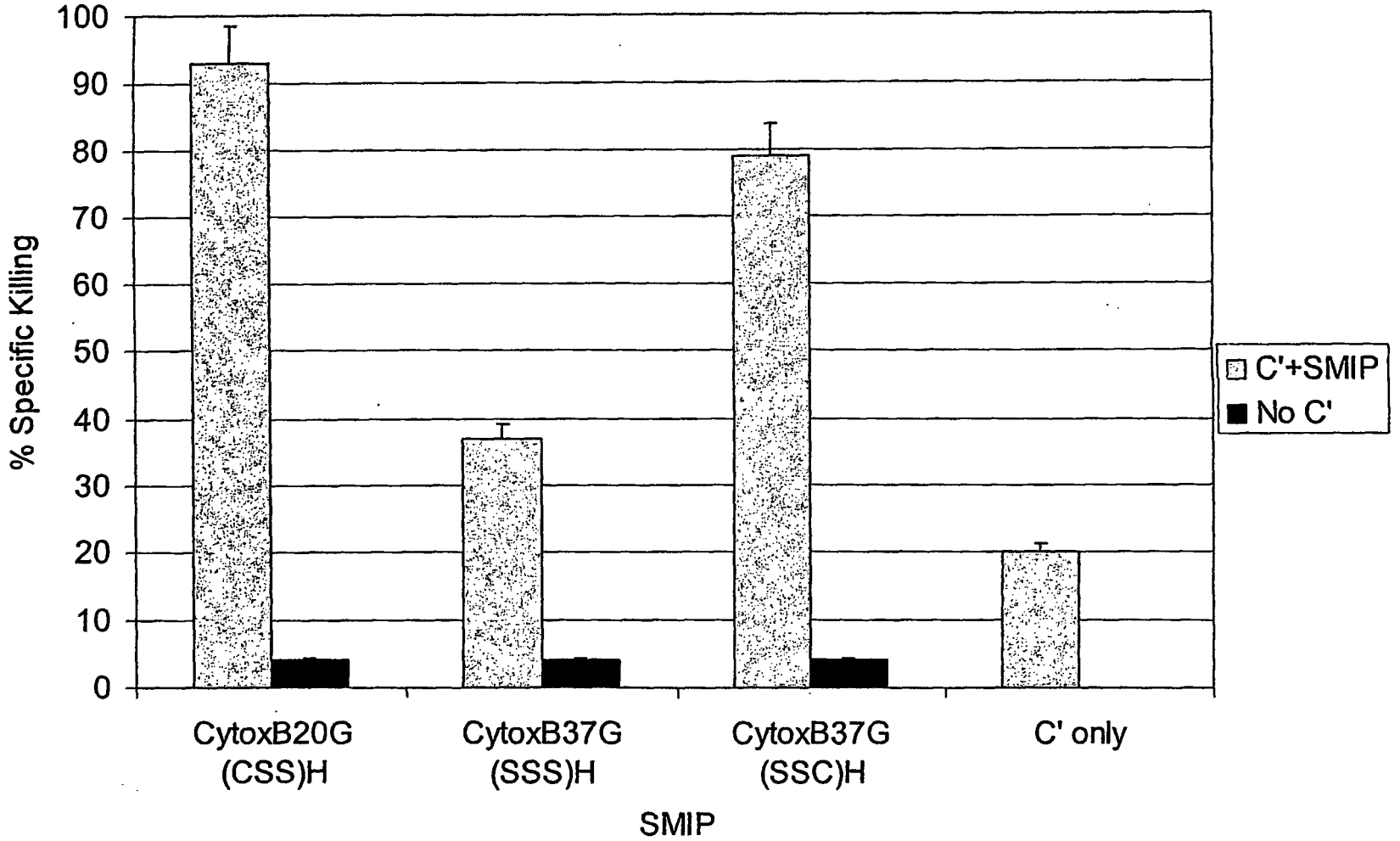

Fig. 83

Figure 86: CDC Activity of CytoxB37G SMIPS. CytoxB20G, CytoxB37 (SSS)H G, CytoxB37 (SCS)H, CytoxB37 (CSS)H, or CytoxB37 (SSC)H were incubated at 10 μg/ml with 10^4 Ramos Target Cells and a 1:10 dilution of rabbit complement (PelFreez) in a volume of 150 μl for 90 minutes. Aliquots were stained with trypan blue (Invitrogen), and counted using a hemacytometer to determine the percentage of the cell population killed during treatment. Negative controls with cells and only one reagent were also included.

WO 2005/017148

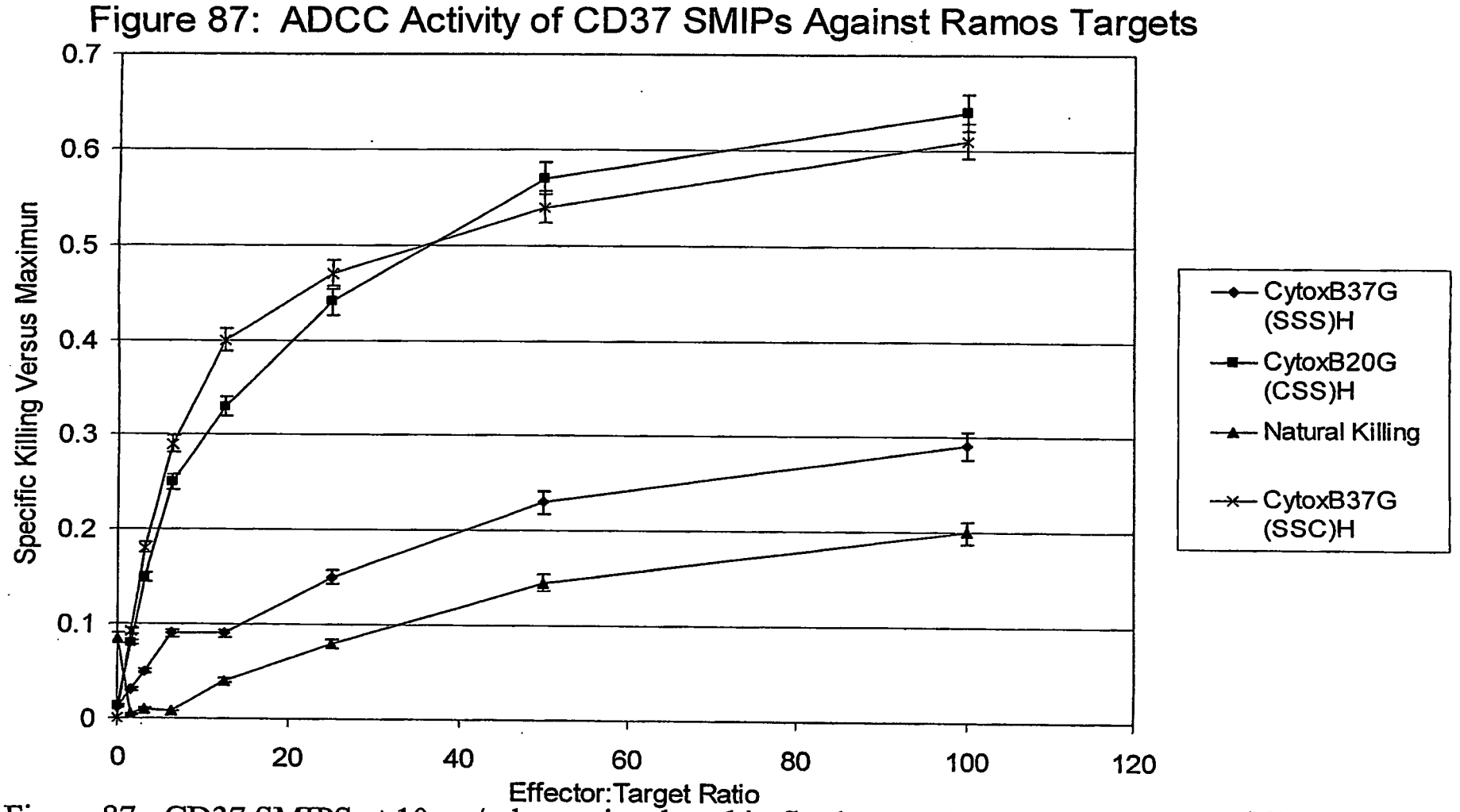

Fig. 84

Figure 87: CD37 SMIPS at 10 μg/ml were incubated in flat-bottom 96 well plates with 10^4 ^{51}Cr-labeled Ramos cells and resting human PBMCs at different effector:target ratios ranging from 0 to 100. All incubations were performed in triplicate at each effector:target ratio. Natural Killing was measured at each effector:target ratio by omission of SMIP. Spontaneous release was measured without addition of PBMC or fusion protein, and maximal release was measured by the addition of detergent (1% NP-40) to the appropriate wells. Reactions were incubated for 6 hours, and 100 ml culture supernatant harvested to a Lumaplate (Packard Instruments) and allowed to dry overnight prior to counting cpm released on a Packard Top Count NXT Microplate Scintillation Counter.